Thesis Paper

Estimating Spatial Cardiac Arrest Risk

Esmée M.L. Smellink

S2031124

University of Twente

Supervisors: D. Demirtas, R. Buter

02-07-24

Abstract

Out-of-hospital cardiac arrest (OHCA) is a significant public health problem, characterized by low survival rates. Early defibrillation is crucial for survival, highlighting the importance of nearby automated external defibrillators (AEDs). Current AED placement strategies often rely on historical OHCA data, which are limited in availability. Publicly available demographic/socioeconomic data are often easily available and shown to have correlations with OHCA risk. This study aims to 1) estimate spatial cardiac arrest risk using demographic/socioeconomic data alone 2) compare AED location models based solely on estimated risk with those incorporating historical OHCA data to inform demand. Machine learning techniques were applied to a comprehensive dataset spanning multiple municipalities. The Huber regression method emerged as the most effective, fine-tuned via cross-validation. Predicted OHCA incidence in each district was used to optimize AED locations, alongside AED optimization models that used smoothed out historical cardiac arrest data as demand.
Results were showcased using five municipalities as a test case, including Amsterdam, where the existing AED coverage was 43%. AED optimization based on the tuned model increased coverage to 55%, while historical OHCA-based models achieved 60% coverage. Similar trends were observed for the other municipalities. This 5% disparity underscores the value of an OHCA registry. Nonetheless, in its absence, machine learning models leveraging demographic and socioeconomic data offer a viable means to substantially enhance coverage.

Acknowledgements

This report is the final result of my Master thesis and completes my time as Master's student in Industrial Engineering and Management, with a specialization in Production and Logistics Management.

First, I would like to thank Robin Buter, my second supervisor, for guiding me through the research. In our many meeting he encouraged me to think critically and helped me improve my work. I could always ask for his help and advice. Thanks to my first supervisor, Derya Demirtas, for the valuable feedback and critical perspectives that significantly contributed to improving the research.

I would also like to thank the team at Amsterdam Resuscitation Studies for their expertise and fresh insights to the research.

Lastly, I would like to thank my family, boyfriend, and friends for their support during this thesis.

I hope you enjoy reading this thesis!

Esmée Smellink,

Oldenzaal, June 2024

Management summary

Objectives

This study aimed to:

1. Optimize spatial cardiac arrest risk estimation based on demographic and socioeconomic data.
2. Compare the efficiency of the optimized automated external defibrillator (AED) locations based on the estimated out-of-hospital cardiac arrest (OHCA) risk from the machine learning models with those based on Kernel Density Estimation (KDE) and historical cardiac arrest data.

Methods

This research used location data of OHCAs that occurred in North-Holland from 2010 to 2017. Demographic and socioeconomic data were obtained from public sources and linked to OHCA data at district level. Multiple machine learning methods were compared to predict OHCA incidence, with Huber regression turning out as the most effective method. The estimated OHCA risk was then used to optimize AED locations, and this optimization was compared to that based on KDE and historical OHCA data.

Key findings

The key findings of this study showed that the Huber regression model was able to accurately predict OHCA incidence at district level, with an R-squared of up to 0.96 for Amsterdam. The AED optimization based on the tuned Huber regression models increased coverage of OHCA locations compared to the current AED placement. However, KDE, which uses historical OHCA locations, outperformed the prediction models, particularly in the larger municipalities of Amsterdam and Zaanstad.

The AED optimization results showed no significant difference in coverage between models based on the feature selections and the model based on population-based strategy. Furthermore, no significant coverage difference was observed between the models based on the prediction methods

and those based on KDE for most years and municipalities. However, when considering the average coverage across all years, KDE performed significantly better than the prediction models for Amsterdam and Zaanstad.

This study demonstrates that machine learning models based on demographic and socioeconomic data can improve AED coverage when historical data is not available, although OHCA risk estimation based on KDE is more effective when historical data is obtainable.

1 Introduction

Out-of-hospital cardiac arrest (OHCA) is a significant public health problem with a low chance of survival. The average survival rate at hospital discharge in Europe is only 8% (Perkins et al., 2021). OHCA is a sudden cessation of the mechanical and electrical activity of the heart, occurring outside the hospital (Bolijn et al., 2021). After the first two minutes, the victim has a great risk of brain damage or death if no treatment has been initiated and this risk increases by the minute. Hence, a fast response is crucial (Cummins et al., 1985). Variations in OHCA rates and outcomes between the countries in Europe are high, suggesting that improvement of survival rates is possible by researching the causes of this variation (Gräsner et al., 2020; Scquizzato et al., 2022).

The chain of survival (Figure 1) describes the events that maximize the survival chance of the victim. The steps of this chain consist of early recognition and activation of the emergency system, early initiation of cardiopulmonary resuscitation (CPR), early defibrillation, advanced emergency medical services (EMS) care, and post resuscitation care (Thannhauser et al., 2021). Bystanders can play an important role by performing CPR and defibrillating the victim before EMS arrive. To start defibrillation early, an automated external defibrillator (AED) must be brought and connected to the victim as soon as possible (Holmberg et al., 2017). Therefore, it is vital to ensure adequate coverage of AEDs.

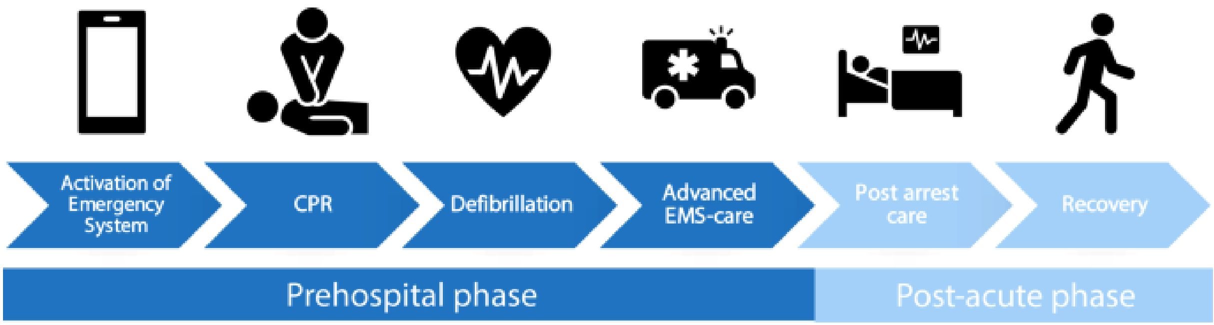

Figure 1. Chain of survival (Thannhauser et al., 2021)

To improve resuscitation attempts, volunteer responder systems (VRS) have been implemented in several countries, including the Netherlands (Folke et al., 2021). Adults who are trained in basic life support are allowed to register in this system. When the emergency dispatch centre receives a call, the dispatcher may decide to activate the alerting system. Afterwards, nearby registered volunteers receive a notification on their phone requesting to go to the victim to perform CPR, or retrieve an AED, of which the locations are given. Studies have shown that the system is effective in reducing the time until the first shock and increasing the chance of survival (Stieglis et al., 2022; Zijlstra et al., 2014).

Despite the importance of AEDs, the utilization of existing AEDs (not used by VRS) tends to be low for several reasons (Deakin et al., 2014). Bystanders may not know how or where to find an AED near the victim, which can be due to poor signage (Sidebottom et al., 2018). Also, the AED may be present but not accessible at that time (e.g., when a store is closed) (Hansen et al., 2013). Furthermore, bystanders may be unwilling to use an AED because they are not comfortable using the device, for example (Delhomme et al., 2019). Another reason for the low utilization of AEDs may be their inefficient placement (Deakin et al., 2018; Sondergaard et al., 2018). If AED locations are not near OHCA incidences, these AEDs would not be used.

The locations of AEDs can be optimized using mathematical models (Chan et al., 2016; Siddiq et al., 2013). These models need data on OHCA locations. However, historic OHCA data are generally only available for a select few regions since cardiac arrest registries are rare and labour intensive. On the contrary, demographic and socioeconomic data of all regions are often publicly available.

In the absence of cardiac arrest registries that provide locations of OHCA, demographic and socioeconomic data could be used to predict OHCA incidences and estimate their locations instead. Literature shows that low socioeconomic status (SES) correlates with an increased OHCA incidence (Lee et al., 2022; van Nieuwenhuizen et al., 2019). More generally, studies confirm the association of a higher risk of cardiac disease with low SES (Kanjilal et al., 2006; Kucharska-Newton et al., 2011). The influence of demographic features on OHCA risk is researched in literature by cluster analyses (Doan et al., 2021; Lerner et al., 2005). The studied correlation between demographic/socioeconomic factors and OHCA risk confirms the potential of estimating OHCA locations based on these publicly available data.

The aim of this paper is twofold. First, we will assess the performance of estimating spatial cardiac arrest risk based on demographic/socioeconomic data. We will optimize this performance by comparing the performances of different machine learning methods in estimating spatial cardiac arrest risk using historic cardiac arrest data and publicly available demographic/socioeconomic data. Second, we will assess the efficiency of the optimized AED locations based on the estimated risk from the machine learning model and demographic/socioeconomic data instead of KDE and historic data, to investigate whether AED location optimization is still beneficial without having historic cardiac arrest data.

The structure followed by the remainder of this paper is as follows: the next section presents a review of the literature on the effect of demographic/socioeconomic features on spatial cardiac arrest risk, machine learning methods that are able to estimate spatial cardiac arrest risk, and AED optimization (Section 2). Thereafter, we describe the data and experimental design (Section 3) and explain the models (Section 4). In Section 5, we explain the process of tuning the parameters of the OHCA risk estimation models, and present the performance of the optimized models. We discuss the results of the AED optimization based on historic cardiac locations and estimated locations (Section 6). Lastly, we present the discussion and conclusions (Section 7).

2 Literature review

This chapter reviews the literature that has been conducted in the field of OHCA risk estimation. Firstly, in Section 2.1, we discuss existing studies examining the relation between demographic/socioeconomic features and OHCA risk. Secondly, Section 2.2 provides an overview, summarizing the risk estimation methods found in literature that were either used for spatial OHCA risk estimation or are potentially useful in our study. Section 2.3 summarizes the literature on AED optimization. Finally, we discuss the gaps between our study and the existing literature in Section 2.4.

2.1 Features

2.1.1 Demographic factors

The literature shows a significant relation between OHCA risk and several demographic factors, like age. Age is a common feature in literature to be associated with the risk of cardiovascular disease and OHCA risk in particular. Increasing age correlates with a higher risk of OHCA and, for that reason, most studies adjust for age when researching the effect of other factors on OHCA incidence (Folke et al., 2010; Galea et al., 2007; Garcia et al., 2022). Straney et al. (2016) found the age of 65 or older as one of the significant factors in their multivariable model for predicting OHCA incidence. Ong et al. (2011) used the factor of 65 years or older as well, and also found a significant relation.

Ethnicity is another characteristic found to correlate with OHCA risk. Garcia et al. (2022) studied OHCA risk among Danish immigrants and found African, Arabic, and Eastern European immigrants to have a higher OHCA risk and Latin Americans to have a lower risk. Galea et al. (2007) researched disparities of OHCA incidence by race and found the incidence to be the highest for the African-American population and the lowest for the Caucasian population. Semple et al. (2013) and Sasson et al. (2012) found the African-American population to have higher OHCA risk, as well. Ong et al. (2011) examined cardiac arrests in Singapore and found a significantly lower OHCA risk in association with a higher proportion of Chinese.

Moreover, studies show an association between gender and cardiac arrest risk. Arunachalam et al. (2021) found gender as a significant factor of OHCA incidence, however, depending on the ethnicity of the population. In the Caucasian population, the incidence was higher among men, while women were more affected with OHCA in the African-American population. Bolijn et al. (2021) concluded that the OHCA incidence is higher among men than among women.

2.1.2 Socioeconomic status

Socioeconomic status (SES) is another important factor found in the literature to have a negative relation with OHCA incidence (Reinier et al., 2006; Straney et al., 2016). SES depends mainly on three factors: income, education, and occupation. It serves as an indicator of the place of a group or individual in society based on socioeconomic factors. The relation between sudden cardiac arrest risk and income, education or occupation as separate factors appeared in multiple studies, as well.

Studies generally found a lower income to correlate with higher OHCA risk. Folke et al. (2010) discussed that a lower household income is associated with higher OHCA incidence. Furthermore, a lower income corresponds to a higher risk of OHCA (van Nieuwenhuizen et al. (2023)). Additionally, a significant difference was found between high and low OHCA risk areas in terms of income and education level (Castra et al. (2019)).

Education was also individually found to have a positive relation with OHCA risk. Straney et al. (2016) found education level as a significant predictor in their model. Lastly, Sasson et al. (2010) identified a lower rate of high school graduates in high risk areas.

The last SES factor is occupation which is not included in many studies regarding OHCA risk. This may be due to lack of data and/or low expected significance. One study suggested that occupation and income are less associated with cardiovascular disease than education (Winkleby et al., 1992). Brown et al. (2019) divided ‘occupation’ into the categories: routine, intermediate, or professional/higher managerial. Their results show a higher proportion of routine occupations and a lower proportion of higher occupations in the high risk areas.

2.1.3 Health

Multiple factors influencing health negatively, like smoking or obesity, are associated with increased OHCA incidence. Straney et al. (2016) found smoking to be a significant factor influencing health negatively. More specifically, Thorgeirsson et al. (2005) found it to be a significant risk factor for men. Regarding overweight, Empana et al. (2004) found an increased cardiac arrest risk with higher waist circumference. In this light Margolis et al. (2022) found a significant positive trend of sudden cardiac arrest risk in relation to obesity.

2.1.4 Other features

Higher average residential property value in a district is often associated with a higher average income, which is often correlated to OHCA risk, as discussed in Section 2.1.2. Reinier et al. (2006) showed this relation between home value and OHCA risk. They found a significantly higher OHCA risk in areas with lower medium residential value (for patients <65 years old). Another feature with a significant correlation regarding OHCA risk is marital status. Empana et al. (2008) showed a higher OHCA risk for unmarried individuals. Lastly, household size in relation to the risk of OHCA was researched by Ong et al. (2011), but no significant relation was found.

Population density was found to be higher in the high risk areas (Fosbøl et al., 2014). Smith et al. (2022) described that the degree of rurality is generally defined by a classification made by the government or by the population density. Uber et al. (2017) represented population density in their study in terms of ‘urban’ and ‘rural’ and found OHCA risk to be higher in the urban centres, which are more populated. Certain locations such as casinos, airports, and underground networks were also found to be high risk, likely due to high population traffic (Lee et al., 2017; MacDonald et al., 2002; Valenzuela et al., 2000).

2.2 Risk estimation methods

2.2.1 Methods used for OHCA risk estimation

2.2.1.1 Spatial OHCA risk analysis methods

Methods to estimate spatial OHCA risk most found in literature are *Local or Global Moran's I* and *Getis-Ord Gi** (Anselin, 1995; Getis & Ord, 1992). Both are spatial autocorrelation statistical methods that determine clusters in a set of data. Often, the methods are used together in studies to combine their results and get a better solution (Nassel et al., 2014; Stassen et al., 2022; Wong et al., 2022). *Global Moran's Index* indicates whether clusters are present in the data, while the Local Moran's Index provides more information on the correlation between census tracts and their 'neighbours' (Kao et al., 2017). Getis-Ord Gi* identifies if a census tract is part of a cluster at a statistically significant level (Wong et al., 2022). These cluster analyses were used not only to analyze clusters of OHCA incidence, but also clusters of (no) bystander CPR (Fleming et al., 2021; Semple et al., 2013).

Kernel density estimation (KDE) and *Empirical Bayes* are approaches that smooth out data to create a risk surface. In the literature, KDE is used to find disease clusters, but also to compare the kernel-density map with AED locations (Chan et al., 2016; Chrisinger et al., 2016; Demirtas, 2016). To map the OHCA incidence, OHCA rates from locations and their neighbouring locations are required for this method (Lerner et al., 2005). Empirical Bayes modifies the values towards the average value of the data relative to the size of the population (Nassel et al., 2014). Sasson et al. (2012) and Semple et al. (2013) use Empirical Bayes smoothing to calculate spatial OHCA risk, after which cluster analysis methods are applied.

The *Integrated nested Laplace approximation* (INLA) method was introduced by Chopin (2009) as an alternative to Markov chain Monte Carlo. INLA is a more computationally efficient way to statistically analyze Gaussian models (Lin et al., 2016; Peluso et al., 2020). The method uses the Laplace approximation, which is an analytical expression to estimate the posterior probability distribution, in combination with numerical integration (Blangiardo & Cameletti, 2015). INLA can be used for risk estimation and forecasting (Auricchio et al., 2020).

Moon et al. (2022) used the *Dirichlet process mixture model* (DPMM) which is a Bayesian cluster method, to estimate OHCA risk. Instead of giving the number of clusters as input like for other clustering methods, the DPMM calculates this number in a way that maximizes the probability of the true distribution of the data.

Some of the methods described above are not suitable for use in this study. Local Moran's I, Global Moran's I, and Getis-Ord Gi*, show if clusters are present and the relation between areas and their neighbouring areas are determined. However, from this information, no estimation (prediction) of OHCA locations can be sampled. KDE and Empirical Bayes result in an OHCA risk surface from which OHCA locations can be sampled. However, historical locations are required to create this risk estimation. INLA can be used to predict OHCA incidence in future years, but not in other areas than those included in the training data. DPMM meets the criteria to be used in this study. As explained, the DPMM approach results in a distribution from which samples of OHCA locations can be obtained. This method does not necessitate input locations for risk estimation.

2.2.1.2 OHCA risk prediction methods

Extreme Gradient Boosting (XGBoost) is a machine-learning algorithm that creates predictive models. XGBoost fits decision trees to a training set of the data and validates them by the test set (Friedman, 2001; Nakashima et al., 2021). Decision tree-based models are suitable for classification and regression problems and can identify (OHCA risk) clusters in data. The clusters are defined by the rules that the decision tree analysis provides, which consist of the values of the independent variables that split the data in the best way (Kao et al., 2017; Moon et al., 2022). OHCA incidence can be predicted by applying the rules of the decision tree to the data.

Logistic regression is a machine learning method that estimates the coefficients of a logistic model in a linear combination to understand the relationship between the dependent and independent variables. Soo et al. (2001) used logistic regression to determine the influence of demographic factors on OHCA rates, and Warden et al. (2012) examined the effect of patient characteristics on being located in a cluster. After applying logistic regression, OHCA incidence can be predicted from the obtained coefficients of the logistic model.

Variational autoencoder (VAE) learns a compressed representation of the input data, also referred to as the latent space. The input data are encoded into the latent space, meaning that a probability distribution is estimated for each attribute of the data. The generator model creates samples from the probability distributions that can be decoded into results that will be similar to the input data (Kingma & Welling, 2013; Moon et al., 2022). Hence, from the latent space OHCA risk predictions can be created, from which estimated OHCA locations can be sampled. Moon et al. (2022) combined the VAE method with the DPMM.

As described and explained above, these methods are all appropriate for both estimating spatial cardiac arrest risk without requiring historic locations and sampling from this spatial risk to create estimated (predicted) OHCA locations.

2.2.2 Other risk estimation methods

2.2.2.1 Disease risk mapping models

In literature, more methods can be found to estimate the spatial risk that are potentially useful in this study but are not yet applied to OHCAs. The *Besag-York-Mollie* (BYM) model is a Bayesian method used for disease mapping by estimating the relative risk (Besag et al., 1991). Samat and Mey (2017) used the model to map the spatial risk of malaria in Malaysia and concluded that BYM is an appropriate tool to use in disease mapping. Alhdiri et al. (2017) used disease mapping based on the BYM model for stomach cancer in Libya. They compared the model to the Standardized Mortality Ratio Method and concluded that the results using the BYM model were better. BYM is compared with a finite *mixture model* by Green and Richardson (2002). Mixture models are used to discover clusters in data with their own distribution (McLachlan et al., 2019). Green and Richardson (2002) showed in their results a better performance of the mixture model in terms of adaptive smoothing and ignoring noise in the data. The BYM model is again compared by Knorr-Held and Raßer (2000) to a method based on the reversible jump Markov chain Monte Carlo (MCMC) approach, called the *KHR* method (Green, 1995). The reversible jump Markov chain Monte Carlo is a framework for Markov chain Monte Carlo simulation that allows for a varying number of dimensions. The KHR model shows promising results in their paper (Knorr-Held & Raßer, 2000). Best et al. (2005) compare the BYM, KHR and mixture model and conclude that BYM is a suitable method to map disease risk in small areas, with room for improvement.

The discussed methods, BYM, KHR and the mixture model, can all be used to estimate spatial OHCA risk based on historic and/or demographic/socioeconomic data.

2.2.2.2 Spatial crime risk estimation methods

Methods used outside the medical field of study might also be useful in estimating spatial risk, for example, methods estimating the risk of crime events. An example is *risk terrain modeling* (RTM) which is applied to predict the risk of shootings (Caplan et al. (2011)). The *rotational grid, Predictive Accuracy Index maximizing* (RGPAI) approach, introduced by Mohler and Porter (2018), is a crime forecasting method as well, that maximizes the evaluation metric 'Predictive Accuracy Index' directly. Moreover, *self-exciting point process modeling* is used in multiple fields of study, just as in crime forecasting (Mohler et al., 2011; Reinhart, 2018). Meijer and Wessels (2019) analyse the benefits and drawbacks of *predictive policing*, which is an adapted method from an algorithm to forecast earthquake aftershocks (Shapiro, 2017).

These crime forecasting methods all estimate spatial risk and, therefore, could be suitable for estimating OHCA risk. Most of these methods (except for RGPAI) have also shown applications in literature using demographic/socioeconomic factors (D'Angelo et al., 2022; Giménez-Santana et al., 2018; Hardyns & Rummens, 2018).

2.2.2.3 Other prediction methods

Many more machine learning methods could be useful for this study. An example is *Random Forest*, which is a classification and regression method. The method averages the estimations of multiple randomized decision trees (Biau & Scornet, 2016). Another set of supervised learning methods are the *support vector machine* (SVM) algorithms. This concept divides a hyperplane into classes by the maximization of the margin between the classes' closest points. The points located at the boundaries of the classes are called the support vectors (Hearst et al., 1998; Meyer & Wien, 2015). *Multilayer Perceptron* is a neural network methodology that uses multiple layers of nodes and non-linear activation functions for classification. The method is able to find approximate solutions to complex problems (Gardner & Dorling, 1998). Lastly, *k-Nearest-Neighbours* (KNN) is a simple, but effective, classification method that assigns an object to the class that included most of its *k* neighbours (Guo et al., 2003).

The four machine learning methods mentioned in this section are classification and regression methods that are applicable to the problem of this research.

2.2.3 Methods summarized

In this subchapter, we have discussed multiple methods found in the literature, of which some are more suitable for this research than others. INLA and DPMM are methods that are applied to spatial OHCA risk estimation in the literature. These methods seem to be appropriate to estimate spatial cardiac arrest risk and subsequently take samples from the results for the AED location optimization. XGBoost, logistic regression and VAE are other prediction methods that were used in the field of OHCA risk and are suitable for this study. BYM is already applied in the medical field of study to multiple diseases and could be an effective method to apply to OHCAs. Furthermore, the application of RTM to crime events shows potential for the method to be used in estimating OHCA risk. Two other methods that are likely to perform well in risk estimation are Random Forest and KNN.

2.3 AED optimization

AED placement was first researched based on identified high risk areas by type of public location, like airports, industrial sites and golf courses (Becker et al., 1998; Fedoruk et al., 2002; Gratton et al., 1999). The limitation to this methodology is that OHCAs that occur outside on the streets (outside public structures) cannot be used as input, which excludes a relatively large part of the data (Fedoruk et al., 2002; Rea et al., 2010). Therefore, researchers improved AED placement by basing it on OHCA clusters found by historical locations (Raun et al., 2013; Sasson et al., 2012; Semple et al., 2013).

The earliest research on AED placement using a Maximum Coverage Location Problem (MCLP) model was performed by Myers and Mohite (2009), who used this model to determine the optimal locations of AEDs in a university community. Chan et al. (2013) researched AED deployment in Toronto and showed that using a MCLP based on historic locations, outperformed the population-guided method. Sun et al. (2016) used the same approach and data, but they also implemented the operating hours of buildings in their model. Siddiq et al. (2013) optimized the AED locations in Toronto as well, but with the aim to research the relation between coverage and AED effective range. Chan (2016) and Dao et al. (2012) applied the MCLP to the vertical plane by taking into account the levels of a building. The MCLP model was extended by implementing probabilistic coverage to the multi-responder model, in three scenarios of bystander behaviour (Chan et al., 2016). Instead of using historic locations, Derevitskii et al. (2020) based the placement of AEDs on race and population, and found this approach to perform better when a large number of AEDs is deployed. Another input for AED optimization models could be mobile location data, which showed improvement in AED coverage (Zhang et al., 2023).

2.4 Contributions

This study makes several contribution to the literature. The main contribution is the comparison of a spatial risk estimation method based on demographic/socioeconomic data to KDE which is based on historical locations. Multiple methods were compared to find the best method for estimating OHCA locations and this method was compared to KDE by their performances on AED optimization.

In addition, this study is mainly performed on district-level in combination with the population density data on neighbourhood-level. Next to the main feature selection, a smaller set of features is used to make the model more generalizable. Also, the OHCA locations are estimated based solely on neighbourhood population density for comparison.

3 Methods

This section describes the methodology of this study. Section 3.1 describes the study settings, the acquisition and preparation of the demographic/socioeconomic data, the OHCA data and AED data, and how the classification of municipalities and districts is determined. We explain the approach of the study in Section 3.2 and finally define the experimental setup in Section 3.3.

3.1 Data acquisition and pre-processing

3.1.1 Study setting

This study used location data from EMS-treated OHCAs with presumed cardiac cause that occurred in regions of North-Holland from January 1, 2010 to December 31, 2017. Our dataset contained 62 municipalities and 481 districts. In the Netherlands, a municipality consists of multiple districts, each of which is subdivided into neighbourhoods. For each year, the number of OHCAs in each district was determined. The number of OHCAs was determined at district-level since districts are commonly homogeneous in socioeconomic structure, while large enough to contain a sufficient number of OHCAs to create a useful prediction model. Additionally, demographic and socioeconomic data for all districts within the study period were available per year.

3.1.2 OHCA and AED data

OHCA data were obtained from the cardiac arrest registry of the AmsteRdam REsuscitation STudies (ARREST). The data contained the coordinates and year of the OHCA occurrences. We used R (packages: maptools, sf, and raster) to determine the district code of each OHCA occurrence using the coordinates of the OHCAs and the borders of the districts in the same year. Subsequently, we counted the number of OHCAs in each district per year. We obtained a list of all AEDs in North-Holland that were registered in the database of HartslagNu at November 2022.

3.1.3 Demographic and socioeconomic data

Publicly available demographic and socioeconomic data were obtained from the Central Bureau of Statistics (CBS) and health data were obtained from the National Institute for Public Health and the Environment (RIVM). The CBS data were available per year, per district, and per neighbourhood. The RIVM data, which concerned only the health data, were available per four years, per district and per neighbourhood. All data, as well as the OHCA counts, were linked to a year and district code. The CBS data were also linked to a neighbourhood code.

Table 1 lists the data features that we considered based on the literature and the possible correlation with OHCA risk based on experts' opinions. Univariate analysis showed all these features to be significant (see Section 9.3). In the remainder of this paper, we will refer to this selection of features as the full selection. Studies have shown that income, ethnicity, age, health, and gender are associated with OHCA risk (Anderson et al., 1991; Bolijn et al., 2021; Galea et al., 2007; Straney et al., 2016; van Nieuwenhuizen et al., 2023). Most OHCAs occur at home (Folke et al., 2010). Therefore, in the case of larger households and households with children, the chance of an OHCA being witnessed is greater than in smaller or one-person households. The household characteristics were interesting for this study since our dataset only contained EMS-treated and therefore witnessed OHCAs.

The literature has shown that socioeconomic status is associated with health, which is associated with OHCA risk (Winkleby et al., 1992). Socioeconomic status was included in this study taking into account the average property in a district and the number of inhabitants with unemployment benefits (Reinier et al., 2006; Soo et al., 2001). Public locations that are busy during the day have a higher OHCA risk (Sun et al., 2017), and we used the number of businesses in a district to project this. The address density indicates the urbanity of the districts (Dulk et al., 1992), which could correlate with higher OHCA risk (Mirowsky et al., 2017).

Table 1. List of included features (full selection)

Category	**Feature**	**Description**
Income	Income	Average income per income receiver
Ethnicity	Western	Number of inhabitants with a migration background whose origin group is Indonesia, Japan, or one of the countries in the continents of Europe (excl. Turkey), North America and Oceania.
	Moroccan	Number of inhabitants with a migration background whose country of birth is Morocco
	Antillean or Aruban	Number of inhabitants with a migration background whose country of birth is the Antilles or Aruba

	Surinamese	Number of inhabitants with a migration background whose country of birth is Suriname
	Turkish	Number of inhabitants with a migration background whose country of birth is Turkey
	Other non-western	Number of inhabitants with a migration background that are not included in the other categories
Age	15-24y	Number of inhabitants with an age between 15 and 24 years old
	25-44y	Number of inhabitants with an age between 25 and 44 years old
	45-64y	Number of inhabitants with an age between 45 and 64 years old
	65y+	Number of inhabitants with an age of 65+ years old
Health	Health	Number of inhabitants that experiences good health
	Overweight	Number of inhabitants that is overweight
	Smoking	Number of inhabitants smoking
Gender	Male	Number of male inhabitants
Households	One-person households	Number of one-person households
	Households with children	Number of households with children
	Household size	Average household size
Residences	Residence value	Average residence value
Benefits	Unemployment benefits	Number of inhabitants receiving unemployment benefits
Businesses	Businesses	Number of businesses
Address density	District address density	The average address density for every address in the district, which is the number of addresses per square meter within a circle with a radius of 1 km from every address.

RIVM's data were only published for 2012, 2016, and 2020. Therefore, we decided to use the data of 2012 for 2010 to 2013, and the data of 2016 for 2014 to 2017 as a proxy.

In the second input dataset, a smaller selection of the features was made, which reduces the amount of required data and the chance of overfitting. In the rest of the paper, this feature selection will be called the small selection. A model was created with multivariate linear regression using the full feature selection. The small selection was made based on the significant features in this model (see Section 9.1), and on the relevance of the features in literature.

The small feature selection is listed in the following table (Table 2):

Table 2. Small feature selection

Features included in the small feature selection
Number of male inhabitants
Inhabitants aged 15-24 years old
Inhabitants aged 25-44 years old
Inhabitants aged 65+ years old
Address density

In Section 9.2, an explanation is given of how we obtained the full and small feature selections.

3.1.4 Municipality and district classification

The coordinates of the borders of municipalities and districts were retrieved from CBS (Kadaster / Central Bureau of Statistics, 2017). Since the data are coupled to a district code, changes in municipality or district borders during the study period, and thus changes in district codes, had to be considered. Therefore, for each year, we used the border of the districts of that year.

3.1.5 Data cleaning

The dataset initially contained 7,517 OHCAs across 2,711 unique pairs of year and district. We excluded nine municipalities with a total of zero OHCAs over eight years, suggesting that no data were collected for those areas. Furthermore, we excluded 53 districts that had an average of 0.25 or fewer OHCAs per year in the same eight-year period. The yearly OHCA data of these districts contain a lot of zeros which can cause bias in the model. As a result, the dataset was reduced to 7,481 OHCAs across 2,128 different combinations of year and district. After removing rows with missing values in any of the features, the final dataset consisted of 6,869 OHCAs across 1,941 different pairs of year and district.

3.2 Approach

Figure 2 illustrates the approach of this study and the data used in the process. The demographic/socioeconomic data, health data and cardiac arrest locations were combined into a dataset to serve as input for the model selection.

In the next step, the models were trained on the training set (see Section 3.3) with the full feature selection, to predict the incidence of cardiac arrests within the districts based on demographic and socioeconomic factors. These models were then evaluated on the test set (see Section 3.3) and the most effective method was selected based on performance metrics (Table 3).

Applying this method, we fine-tuned the models using two input datasets: one incorporating 22 features (full selection) and the other including 5 features (small selection). These models were tuned via cross-validation on the training set. The optimal parameter settings for each model were determined based on the weighted average performance metrics.

Predictions of OHCA counts per year per district were made using these tuned models. Subsequently, estimated locations were generated based on these predictions and the neighbourhood populations (see Section 4.4), which, along with the current AED locations, were input for the AED location optimization (see Section 4.6).

Another input dataset explored was a population-based strategy, where OHCA locations were estimated solely based on the neighbourhood population densities (see Section 4.4). AED locations were then optimized according to these estimated locations. Additionally, historic cardiac arrest locations were used as input for KDE to obtain estimated cardiac arrest locations. The locations constituted a fourth input dataset for AED location optimization.

The test sets that we used to evaluate the optimized AED locations each include one year of historical OHCA locations. The test set of a selected year was used to evaluate the optimized locations that were based on the predictions of that selected year, and for the optimized locations that were based on KDE using the other years (excluding the selected year) of historical OHCA locations.

These steps resulted in several outcomes that were compared: we obtained coverage values from the AED optimization based on prediction models using demographic/socioeconomic data with two different feature selections, based solely on population density, and based on historical cardiac arrest locations smoothed out by KDE.

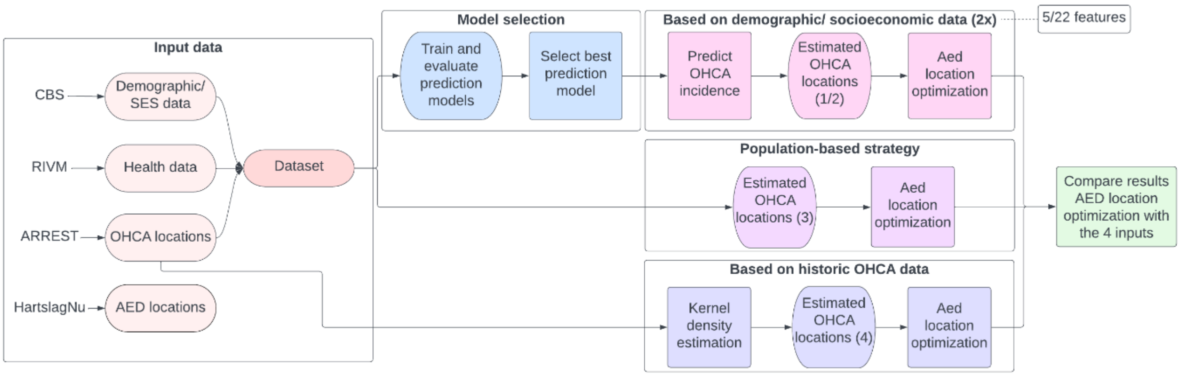

Figure 2. Flowchart of the study approach

3.3 Experimental design

3.3.1 Training, validation, and test sets

The data for the predictions models were divided into a training set and test set. In this study, the test set consisted of one municipality, and each municipality takes its turn as test set. This way, the data was not correlated by having data of a municipality in both the training and test set. The rest of the data were part of the training set. The tuning of the prediction model for a municipality was performed on the training set using cross-validation.

The training set for the AED optimization contained estimated locations derived from predictions of a specific year, while the test set consisted of real historical OHCA locations from the same year. Furthermore, when the training set contained estimated locations derived via KDE using seven years of data, the test set included OHCA location data from the year omitted in KDE input. This approach ensured evaluation on unseen data.

3.3.2 Performance measures

The Mean Absolute Error (MAE) is a common metric for assessing regression models and is useful for comparing methods. The Mean Absolute Percentage Error (MAPE) gives the average error relative to the observed values. Observed zero values cause this metric to be infinitive, which makes it unsuitable for this study.

The Mean Squared Error (MSE) penalizes large errors more than small errors. Taking the square root of this metric results in the Root Mean Squared Error (RMSE), which is the standard deviation of the prediction errors. Since it is more important in this study to have predictions close to the real value than getting predictions exactly right, the MSE or RMSE serve as appropriate performance metrics. Using the Root Mean Squared Logarithmic Error (RMSLE), outliers have less effect on the value since the errors are scaled. This property makes it relevant for evaluating model performance with a focus on non-outliers. Moreover, RMSLE penalizes underestimates more severely than overestimates, which aligns well with this study. Overestimating OHCA risk, and consequently placing more AEDs, is preferable to underestimating OHCA risk since placing too few AEDs could reduce the survival rate.

Another performance measurement used for regression is R-squared (R^2). The value of this metric shows what percentage of the fitted data can be explained by the model using the residual sum of squares. The Adjusted R-Squared metric is a modified version of R-squared that calculates how much a new feature improves the model more (or less) than expected. Both performance measures are invalid for non-linear models.

The explained variance (ExpVar) is comparable to R^2 as it shows the extent to which the variance can be explained by the model. However, unlike R^2, ExpVar is considering the mean error. Lastly, the maximum error (MaxError) offers a straightforward, interpretable metric by highlighting the largest error.

In the evaluation of the experiments, we used the MAE, MSE, MSLE, R^2, ExpVar and MaxError metrics. By comparing the values of these metrics in the experiments, we had a good analysis of their performances. The formulas of the these performance metrics can be found in Table 3.

Table 3. Performance metric formulas

Performance metric	**Formula** (with A_t = actual value, F_t = forecasted value, μ = mean actual value, and N = number of datapoints)
MAE	$\frac{1}{N}\sum_{t=1}^{N}\lvert A_t - F_t\rvert$
MSE	$\frac{1}{N}\sum_{t=1}^{N}(A_t - F_t)^2$
MSLE	$\frac{1}{N}\sum_{t=1}^{N}(\log(A_t + 1) - \log(F_t + 1))^2$
R^2	$1 - \frac{\sum_{t=1}^{N}(A_t - F_t)^2}{\sum_{t=1}^{N}(A_t - \mu)^2}$
ExpVar	$1 - \frac{Var(A_t - F_t)}{Var(A_t)}$
MaxError	$Max(\lvert A_t - F_t\rvert)$

4 Models

In this chapter, we elaborate on the models and methods used in this study. Section 4.1 summarizes the spatial OHCA risk methods that we compared. In the next sections, we describe the method selection process (Section 4.2), we explain our approach to creating predictions from the input data (Section 4.3), and to creating estimated OHCA locations from the predictions (Section 4.4). Section 4.5 describes the KDE model, and, lastly, we formulate the AED location optimization method (Section 4.6).

4.1 Machine learning methods

PyCaret is a machine-learning library package in Python that we used to train and evaluate multiple regression methods. PyCaret includes 24 methods that are listed and categorized in Table 4.

Table 4. PyCaret regression methods (Tsai et al., 2022)

Name	Category
Linear Regression	Linear (Classic Linear)
Lasso Regression	Linear (Feature selection)
Elastic Net	Linear (Feature selection)
Least Angle Regression	Linear (Feature selection)
Lasso Least Angle Regression	Linear (Feature selection)
Orthogonal Matching Pursuit	Linear (Feature selection)
Bayesian Ridge	Linear (Bayesian)
Automatic Relevance Determination	Linear (Bayesian)
Ridge Regression	Linear (Miscellaneous)
Passive Aggressive Regressor	Linear (Miscellaneous)
Random Sample Consensus	Linear (Outlier robust)
TheilSen Regressor	Linear (Outlier robust)
Huber Regressor	Linear (Outlier robust)
Kernel Ridge	Kernel Ridge
Support Vector Regression	Support vector
K Neighbors Regressor	Nearest Neighbours
Decision Tree Regressor	Decision Trees
Random Forest Regressor	Ensemble
Extra Trees Regressor	Ensemble
AdaBoost Regressor	Ensemble
Gradient Boosting Regressor	Ensemble
MLP Regressor	Neural Network (Supervised)
Extreme Gradient Boosting	Gradient Boosting Extension
Light Gradient Boosting Machine	Gradient Boosting Extension

The linear regression methods result in a linear combination of the independent variables with the aim of minimizing the residual (Shalev-Shwartz & Ben-David, 2014). Kernel ridge is a regression model that estimates the distribution by kernel smoothing, while a penalty is used to decrease the coefficients and in that way handle correlation between independent variables (Murphy, 2022). In addition to minimizing the residual, Support Vector models try to maximize the margins between the training set and the hyperplane. Nearest neighbours estimates values based on the average value of the closest points (Shalev-Shwartz & Ben-David, 2014). Decision tree regression models break the dataset down into subsets that result in a tree with decision nodes. Ensemble methods use the predicted values of multiple regression models to improve their predictions (Murphy, 2022). A Neural Network uses weights to input data in order to create output, similar to linear regression. The difference is that the neural network algorithm learns more complex relations between variables by creating multiple hidden layers of nodes (Shalev-Shwartz & Ben-David, 2014). Gradient boosting is an ensemble method that combines base models. The base models are created by predicting the negative gradient of the loss function based on the errors of the previous iterations (Murphy, 2022).

4.2 Method selection

The performance of the machine learning methods was assessed using PyCaret. The input data included the full feature selection. The procedure is detailed in Algorithm 1 and further described below.

Initially, a loop iterates over the municipalities, with each municipality serving as the test set in turn. In each iteration, the input data was split into training and test sets, with the dependent variable set as the number of OHCAs. Next, we looped over each PyCaret method, where in each loop a model was created based on the training data. This model was then used to predict the OHCA counts for the respective test set. In cases where negative predictions were encountered, they were adjusted to zero.

Prediction errors were then computed and weighted based on the real number of OHCAs in each district. Subsequently, performance metrics (Table 3) were calculated for each model. The tuning process that followed after we selected the best performing method is described in Section 5.

Algorithm 1. Determining the performances of the machine learning methods using PyCaret.

Input: Dataset with feature and OHCA data, including the full feature selection.

1. For each municipality *m*:
    a. Split training and test set. The test set contains the feature data specific to municipality *m*, while the training set comprises the feature data and OHCA amounts of all municipalities except for *m*.
    b. For each method *j*:
        i. Create a model *i* using the training set.
        ii. Predict OHCA values $\hat{y}$ for the test set based on model *i*.
        iii. If negative predicted values $\hat{y}$ are present, set them to zero.
        iv. Calculate and weigh the performance metric values using the true values y and predicted values $\hat{y}$.
2. Determine the weighted average metric values per method.

4.3 Input data to predictions

Following the selection of the best method and the subsequent tuning of the models (as detailed in Section 5), predictions were derived from the input data. A summary of the process can be found below (Algorithm 2). The predictions were generated for both input datasets, encompassing either the full or small feature selection. For each municipality, the training and test sets were defined, as well as the dependent variable, i.e., the number of OHCAs. A model was then created from the training data, using the parameter values determined through tuning. Subsequently, the OHCA counts of the test set were predicted using the model. Performance metrics (Table 3) were computed and weighted based on the actual number of OHCAs in each district. The process was repeated for each municipality and feature selection.

Algorithm 2. Deriving predicted OHCA counts from feature data.

Input: The best performing method determined in previous steps (Section 4.2), a selected municipality m, and a dataset containing both OHCA data and feature data of a chosen feature selection.

1. Split training and test set. The test set contains the feature data specific to municipality m, while the training set comprises the feature data and OHCA amounts of all municipalities except for m.
2. Create a model *i* based on the training set using the selected prediction method and the parameter settings determined through tuning.
3. Predict OHCAs values $\hat{y}$ for the test set based on model *i*.
4. Calculate the weighted performance metric values using the true values y and predicted values $\hat{y}$.

4.4 Predictions to estimated OHCA locations

From the predictions, we derived estimated OHCA locations that will serve as input for AED optimization (see Algorithm 3). For a chosen municipality and year, we selected a district within this municipality through sampling, with the probabilities determined by the predicted number of OHCAs in each district. Subsequently, a neighbourhood was sampled within the selected district, with probabilities based on neighbourhood populations. A location within this neighbourhood was then uniformly sampled.

These steps were repeated until a total of 10,000 estimated OHCA locations were generated for the chosen municipality. This number was chosen to strike a balance between creating a sufficient model and maintaining a manageable computational time.

Algorithm 3. Estimation of OHCA locations based on the predicted OHCA counts.

Input: Dataset including the true OHCA counts y and predictions $\hat{y}$ of the districts in a selected municipality *m*, year and feature selection. As well as, the populations *p* of the neighbourhoods in the selected municipality *m* and year.

1. Sample one district d_m within municipality *m* where the probability of a district d_m being sampled is: $\frac{y_{d_m}}{\sum_{d_m \in D_m} y_{d_m}}$, with D_m being the set of districts in municipality *m*.
2. Sample one neighbourhood n_d within district *d* where the probability of a neighbourhood n_d being sampled is: $\frac{p_{n_d}}{\sum_{n_d \in N_d} p_{n_d}}$, with N_d being the set of neighbourhoods in district *d*.
3. Uniformly sample a location within neighbourhood n_d.

For the population-based strategy (Algorithm 4), the 10,000 locations were distributed across the neighbourhoods within a municipality by sampling based on neighbourhood populations. The resulting number of points was uniformly distributed across the neighbourhoods.

Algorithm 4. Estimation of OHCA locations based on neighbourhood population density.

Input: Dataset including the populations *p* of the neighbourhoods in the selected municipality *m* and year.

1. Sample one neighbourhood n_m within municipality *m* where the probability of a neighbourhood n_m being sampled is: $\frac{p_{n_m}}{\sum_{n_m \in N_m} p_{n_m}}$, with N_m being the set of neighbourhoods in municipality *m*.
2. Uniformly sample a location within neighbourhood n_m.

4.5 Kernel Density Estimation

Kernel Density estimation is a statistical smoothing technique. This method smooths data by putting a Kernel function on each datapoint. The kernel density is estimated by taking the sum of these Kernel functions on each point in space. OHCA locations are estimated by sampling a location using the kernel density as weights. The degree of smoothing is determined by the bandwidth (Murphy, 2022). In this study, the bandwidth is selected and compared using three methods: bootstrap, likelihood, and least-squares cross validation. Bootstrap resamples a dataset multiple times, calculating the bandwidth for each resample to estimate its distribution. Likelihood evaluates the probability of the observed data given a bandwidth, selecting the bandwidth that maximizes this likelihood. Least-squares cross validation involves dividing the data, iteratively training models and evaluating their performance using a loss function. It selects the bandwidth by minimizing the average loss across the iterations.

4.6 AED location optimization

4.6.1 Optimization model

The general maximum coverage location problem (GMCLP) is a suitable model to optimize AED locations (Berman & Krass, 2002; Chan et al., 2016). The GMCLP is defined as follows.

Let I be the set of demand locations that represent the OHCA locations. Let J^e be the set of locations of the existing facilities, representing the existing AED locations, and J^c the set of candidate locations for the facilities, representing candidate locations for the AEDs. The set J includes the elements of both the sets J^e and J^c (which do not share a common element). The level of coverage is denoted by c_{ij}, which depends on the distance between the demand location i and the facility location j.

We define the parameter N as the number of facilities to be deployed. The decision variable Y_j is 1 if a facility is located at j, and 0 otherwise. Moreover, X_{ij} has value 1 if demand location i is covered by facility location j, and 0 otherwise.

The mathematical model is formulated as follows:

maximize	$\sum_{i\in I}\sum_{j\in J} c_{ij}X_{ij}$		(1)
subject to	$\sum_{j\in J^c} Y_j \leq N,$		(2)
	$Y_j = 1,$	$\forall j \in J^e$	(3)
	$X_{ij} \leq Y_j,$	$\forall i \in I, \forall j \in J^c$	(4)

$$\sum_{j \in J} X_{ij} \leq 1, \qquad \forall i \in I \qquad (5)$$

$$X_{ij} \in \{0,1\}, \qquad \forall i \in I, \forall j \in J^c \qquad (6)$$

$$Y_j \in \{0,1\}, \qquad \forall j \in J \qquad (7)$$

The objective function (1) maximizes the total coverage of the demand locations in *I*. The first constraint (2) ensures the number of facilities located at candidate locations to be at most *N*. At the existing location, facilities have already been placed, which is defined in constraint (3). In constraint (4) it is ensured that a demand location can only be covered by an open facility. Constraint (5) guarantees that each demand location is covered by at most one facility.

The GMCLP is solved using binary integer programming to find the exact solution. The problem instance should be as large as possible, but the computational time to solve the problem should not exceed one hour. The optimized AED locations are evaluated on a test set. The performances are measured by total coverage (objective value).

5 Prediction model selection and tuning

In this chapter, we first explain how we selected the best prediction model (Section 5.1). Then, we discuss the selected prediction model and its parameters (Section 5.2). Finally, we focus on the tuning process (Section 5.3) and present the results of this process (Section 5.4).

5.1 Selected method

The best performing method was Huber regression. The PyCaret models for the method selection (Section 4.2) were compared based on the performance metrics (Table 3). Since districts with more OHCAs have more influence on AED placement and coverage, we weighted the values per metric based on the (real) number of OHCAs in each district. Subsequently, the average value of the metrics was calculated per method. The results can be found in Table 5.

Table 5. Summary of the performance of the machine learning methods by the metrics: Mean Average Error (MAE), Mean Squared Error (MSE), Mean Squared Logarithmic Error (MSLE), R Squared (R^2), Explained Variance (ExpVar), and Maximum Error (MaxError). The results of the best performing method are in bold.

	MAE	**MSE**	**MSLE**	**R^2**	**ExpVar**	**MaxError**
Linear Regression	0.23	1.51	0.26	0.95	0.95	27.44
Lasso Regression	0.21	1.13	0.26	0.96	0.97	18.32
Ridge Regression	0.23	1.50	0.26	0.95	0.95	27.24
Elastic Net	0.22	1.22	0.26	0.96	0.96	19.49
Least Angle Regression	0.81	12.98	1.85	0.59	0.61	52.82
Lasso Least Angle Regr.	0.22	1.15	0.26	0.96	0.97	18.97
Orthogonal Matching Purs.	0.24	1.46	0.30	0.95	0.96	21.47
Bayesian Ridge	0.22	1.13	0.26	0.96	0.97	20.55
Automatic Relevance Det.	0.61	13.72	0.64	0.57	0.58	52.87
Passive Aggressive Regr.	0.63	13.54	0.92	0.57	0.58	56.00
Random Sample Cons.	1.02	54.61	0.89	-0.73	-0.69	140.79
TheilSen Regressor	0.31	2.97	0.27	0.91	0.91	27.07
Huber Regressor	**0.20**	**0.92**	**0.24**	**0.97**	**0.97**	**21.49**
Kernel Ridge	0.24	1.64	0.26	0.95	0.95	22.77
Support Vector Regressor	0.52	11.22	0.31	0.65	0.65	48.94
K Neighbors Regressor	0.41	6.20	0.32	0.80	0.81	38.30
Decision Tree Regressor	0.35	3.72	0.51	0.88	0.89	36.00
Random Forest Regressor	0.33	4.23	0.27	0.87	0.87	32.99
Extra Trees Regressor	0.34	4.62	0.27	0.85	0.86	33.84
AdaBoost Regressor	0.33	4.24	0.49	0.87	0.87	33.00
Gradient Boosting Regr.	0.34	4.53	0.27	0.86	0.86	34.22
MLP Regressor	21.18	27201.56	3.93	-859.01	-844.83	2844.57
Light G.B. Machine	0.39	5.87	0.29	0.81	0.82	38.10

5.2 Huber Regression

Huber regression is a robust linear regression algorithm that applies a regularization penalty. The algorithm combines two loss functions:

$$l_\epsilon(r,\epsilon) = \begin{cases} r^2/2 & if\ |r| \le \epsilon, \\ \epsilon|r| - \epsilon^2/2, & otherwise. \end{cases}$$

The least square function is used for residuals (r) less than or equal to epsilon, and absolute deviation is used for residuals larger than epsilon (Huber, 1964).

Huber regression has two main parameters in PyCaret: epsilon and alpha. The value of epsilon defines the threshold of switching between the two loss functions. A larger epsilon makes Huber more robust to outliers. Alpha determines the strength of the regularization penalty. The grids we used for the parameters were based on literature and trials (Brisbois & Dziedzic, 2023; Nevendra & Singh, 2022; Xie & Wang, 2018). For epsilon we used the grid [1, 1.5, 2, 2.5] and for alpha the grid [0.0001, 0.001, 0.01, 0.1, 1]. The other parameters were kept at their default values.

5.3 Approach to tuning

The model performances with several parameter settings were examined by cross validation. The best parameter values were determined for each training set, excluding one of the municipalities, and for each of the two feature selections. For the cross validation, 10 folds were created, each containing 4 municipalities, after which the municipality from the test set was excluded. A model was created from the data excluding the municipalities of one fold and by using one of the parameter value combinations. The number of OHCAs was predicted for the excluded municipalities using the created model and the performance metrics were calculated (Table 3). These steps were repeated for each of the ten folds and every parameter value combination.

5.4 Tuning results

The results with Amsterdam, Zaanstad, Haarlem, Haarlemmermeer or Alkmaar in the test set (so excluded from the cross validation) can be found in Section 9.7. These municipalities were chosen as examples since their OHCA count is the highest within our study period. Table 6 shows the best parameter settings for each municipality and feature selection based on the value of R^2, as this metric shows best how well the data fits the model. The values in the table are the weighted average metric values of the cross validation on the training set, based on the number of district-year combinations in each fold.

Table 6. Parameter tuning results.

Performance of parameter settings evaluated by the average cross validation metric values on the training set. The results of the best performing parameter value combinations (based on R^2) are shown for ten training sets with a certain feature selection and excluding a certain municipality.

Excluded municipality	**Feature selection**	**Epsilon**	**Alpha**	**MAE**	**MSE**	**MSLE**	**R^2**	**ExpVar**	**MaxError**
Amsterdam	Full	1.5	0.001	1.324	3.288	0.251	0.503	0.512	7.510
	Small	2	0.1	1.307	3.170	0.248	0.514	0.522	7.312
Zaanstad	Full	1	0.001	1.455	5.343	0.236	0.603	0.613	10.063
	Small	1.5	0.1	1.554	6.962	0.245	0.584	0.589	11.064
Haarlem	Full	1	0.01	1.566	8.750	0.247	0.536	0.544	12.933
	Small	1	0.1	1.540	6.559	0.250	0.545	0.556	10.514
Haarlemmermeer	Full	1	0.01	1.506	5.960	0.243	0.530	0.544	11.814
	Small	1	0.01	1.571	7.058	0.251	0.519	0.530	11.283
Alkmaar	Full	1	0.1	1.471	5.270	0.249	0.556	0.565	10.056
	Small	1	0.01	1.538	6.168	0.254	0.540	0.551	11.142

6 Results

In this chapter, we present the results of this study. First, we present the performance of the tuned model on the test set for the different feature selections (Section 6.1). Secondly, we visualize the results by heatmaps for both the feature selections, the population-based strategy, and KDE (Section 6.2). Lastly, we report the results of the AED optimization based on Huber and KDE (Section 6.3).

6.1 Tuned model predictions

After tuning the parameters of the Huber models, we trained the models on the training sets and predicted the OHCA incidence for the test sets using the two selections of features. The quality of the predictions was measured by the performance metrics (Table 3).

Table 7 shows the results for the test sets of the five municipalities. These results are based on input data with either the full or the small feature selection. For Amsterdam the model seems to perform better using the full feature selection. On the other hand, for Zaanstad, Haarlem and Haarlemmermeer the small feature selection seems to have a better performance. In the case of Alkmaar, the results from both feature selection were very similar.

Table 7. Performance metric values of the predictions created by the Huber model with tuned parameters. The input data contains either the full or the small feature selection.

	Amsterdam		Zaanstad		Haarlem		Haarlemmer-meer		Alkmaar	
	Full	**Small**	**Full**	**Small**	**Full**	**Small**	**Full**	**Small**	**Full**	**Small**
MAE	0.95	1.31	0.67	0.62	0.68	0.60	0.35	0.32	0.65	0.65
MSE	6.16	12.22	1.74	1.36	2.71	2.01	0.78	0.66	1.50	1.50
MSLE	0.22	0.25	0.32	0.33	0.26	0.29	0.24	0.22	0.15	0.16
R^2	0.96	0.93	0.72	0.78	0.81	0.86	0.97	0.98	0.67	0.67
ExpVar	0.97	0.94	0.79	0.84	0.85	0.89	0.98	0.98	0.76	0.76
MaxError	18.63	23.45	6.52	5.35	12.22	10.70	4.60	4.98	5.28	5.87

6.2 Heatmaps OHCA incidence

To visualize the quality of the estimated OHCA locations, we created heatmaps of the five municipalities for both feature selections and for the population-based strategy of the estimations for 2017 (Figure 3-7). The heatmaps are based on the density of the OHCAs per neighbourhood. We scaled the number of estimated locations per neighbourhood to a total amount per municipality that is equal to the average number of OHCAs in that municipality. Then, we divided this number by the surface area of the neighbourhood. We also created heatmaps of the OHCA risk estimated by KDE.

The KDE heatmap of Amsterdam clearly indicates a hotspot in the centre of the municipality, which is absent in the heatmaps based on estimated locations. The KDE heatmap of Zaanstad shows a large hotspot in the bottom-right, consistent with the other heatmaps, although the hotspot appears in the same district but not in the same neighbourhoods. Additionally, the small hotspot on the left side of the KDE heatmap is missing from the heatmaps based on estimated locations. Also, the population-based heatmap of Zaanstad reveals a hotspot at the top, which is absent in the other heatmaps.

For Haarlem, the KDE heatmap displays two main hotspots, one at the bottom and another in the centre. These hotspots are not clear in the other heatmaps, except for a single neighbourhood in the centre of the full selection heatmap. For Haarlemmermeer, all heatmaps show a few high-risk areas surrounded by many low-risk neighbourhoods. In the full and small selection heatmaps, the higher risk areas are located in the top-right, whereas in the KDE heatmap, the highest risk is in the centre. Finally, all heatmaps of Alkmaar consistently show the highest risk on the northern part of the municipality. While the hotspots are in the correct districts, they are not precisely in the correct neighbourhoods.

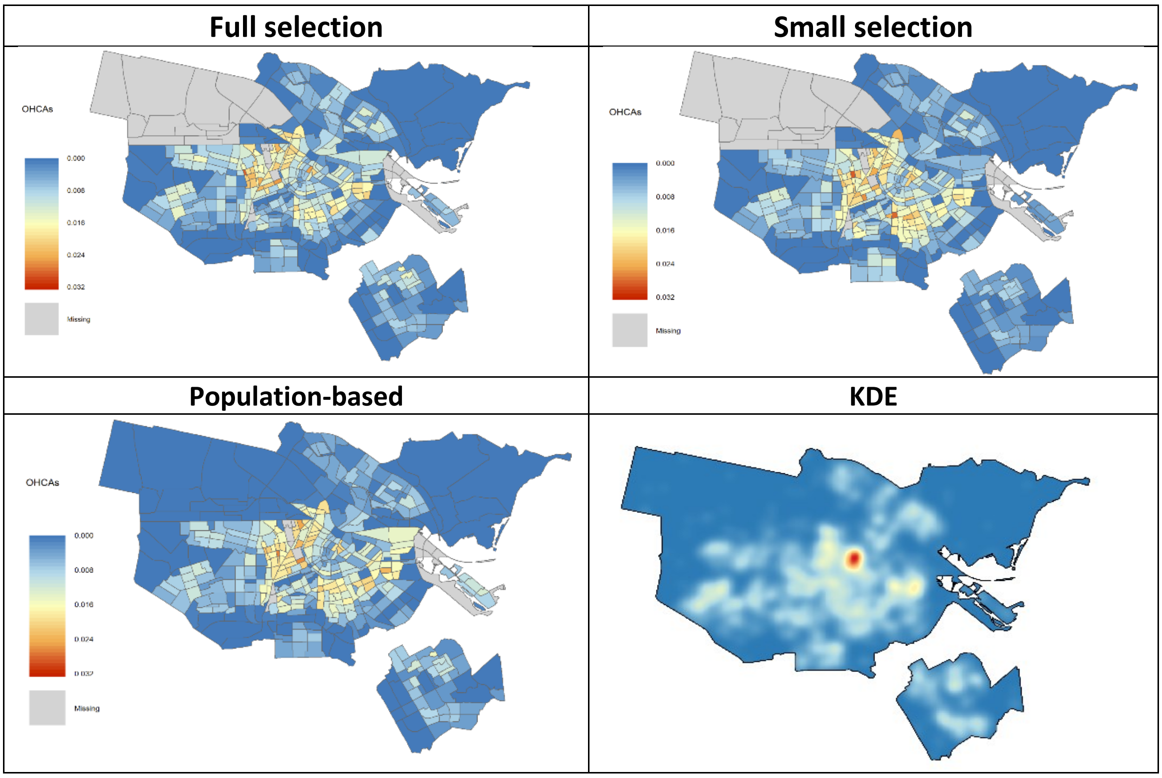

Figure 3. Heatmaps of the OHCA risk in Amsterdam (2017).

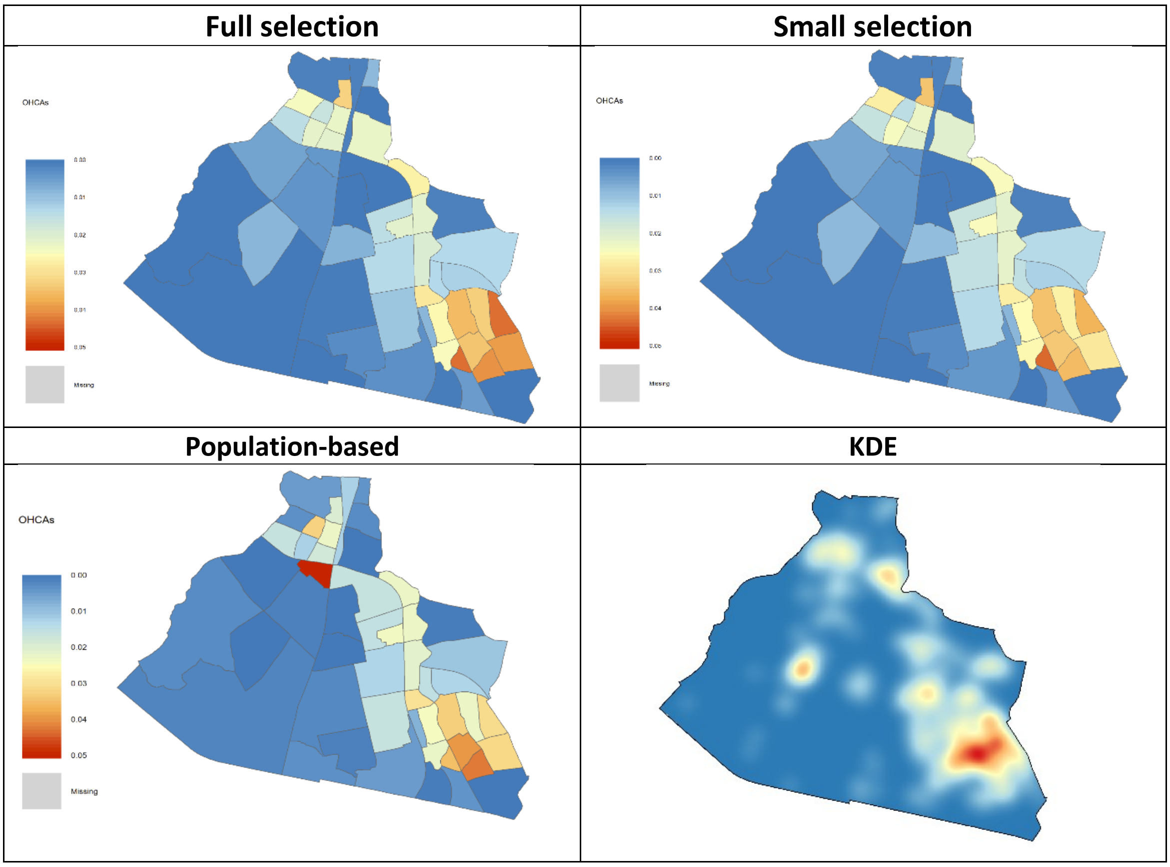

Figure 4. Heatmaps of the OHCA risk in Zaanstad (2017).

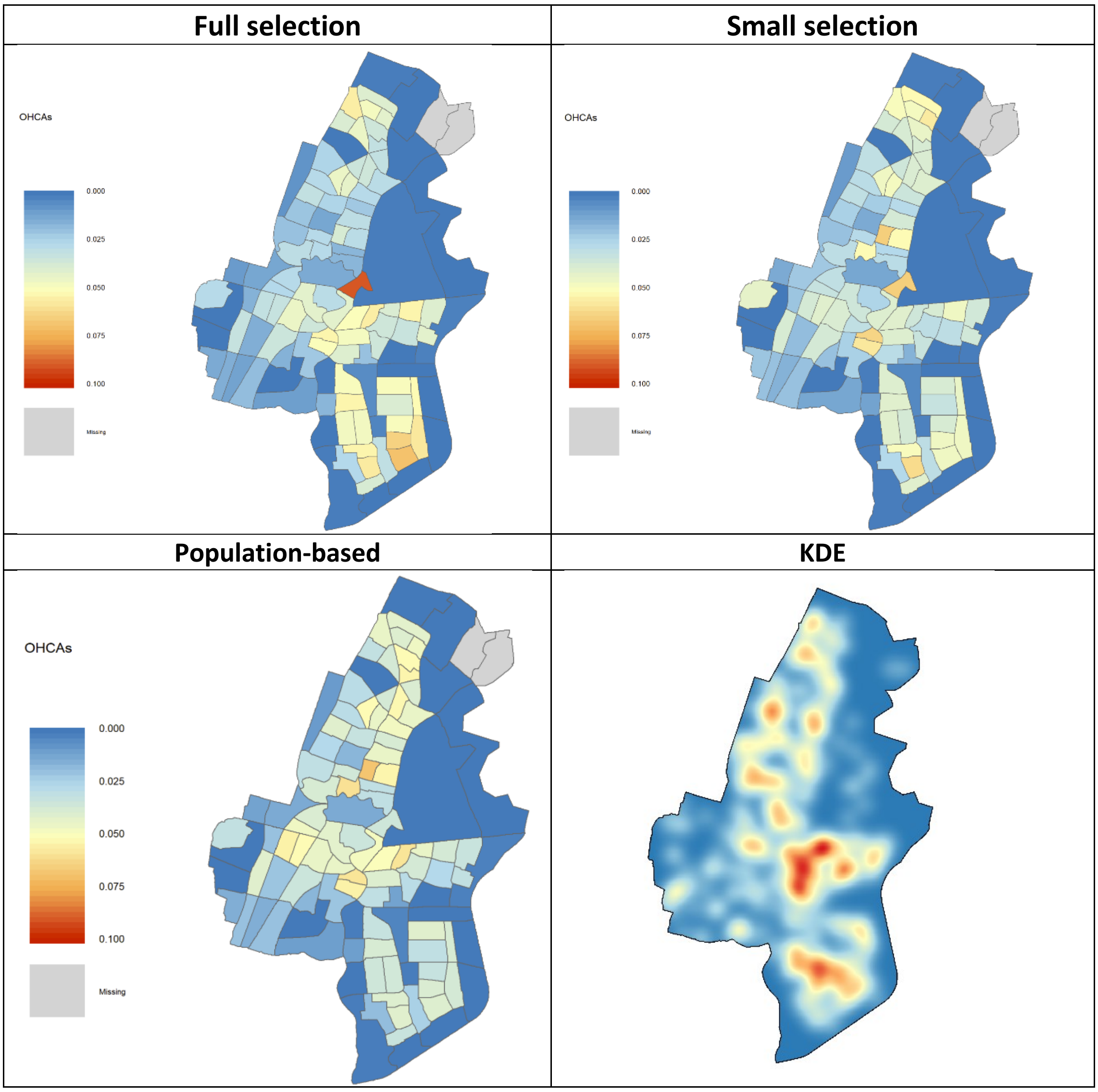

Figure 5. Heatmaps of the OHCA risk in Haarlem (2017).

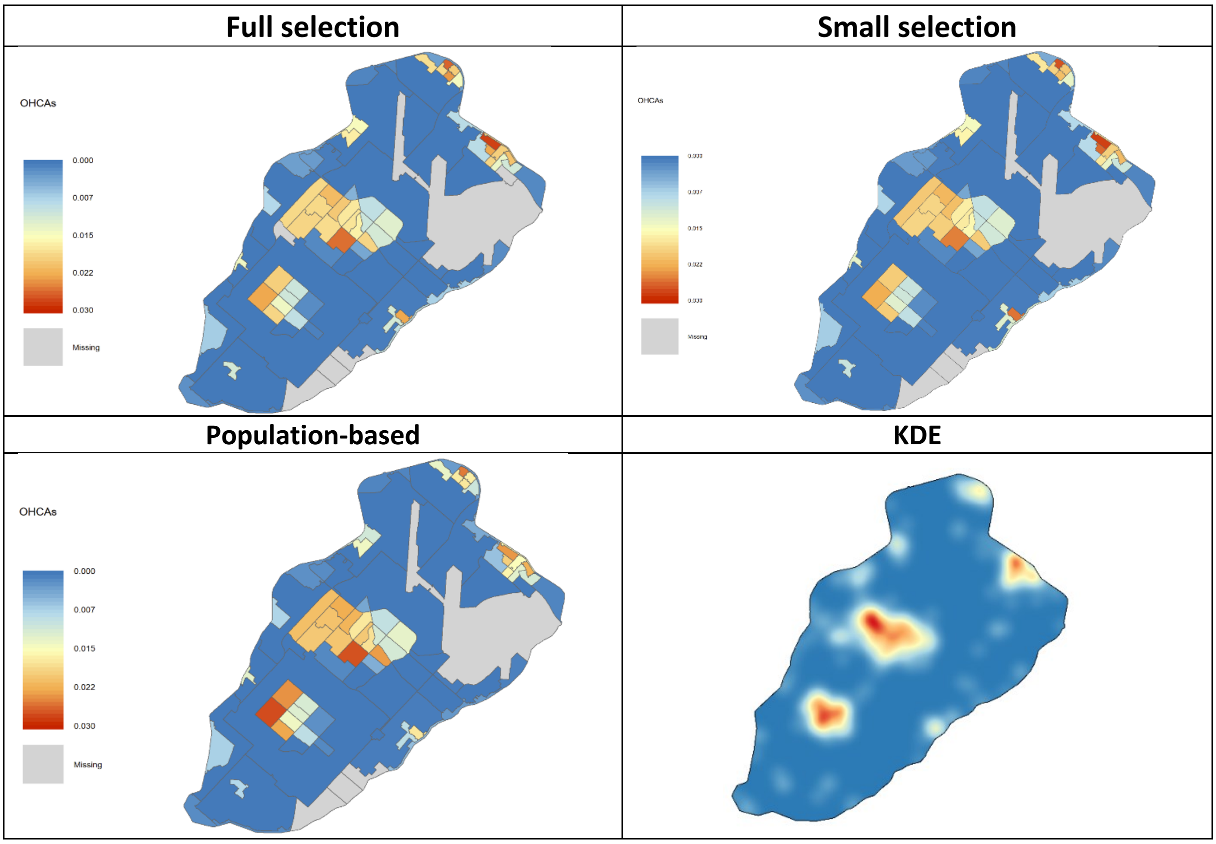

Figure 6. Heatmaps of the OHCA risk in Haarlemmermeer (2017).

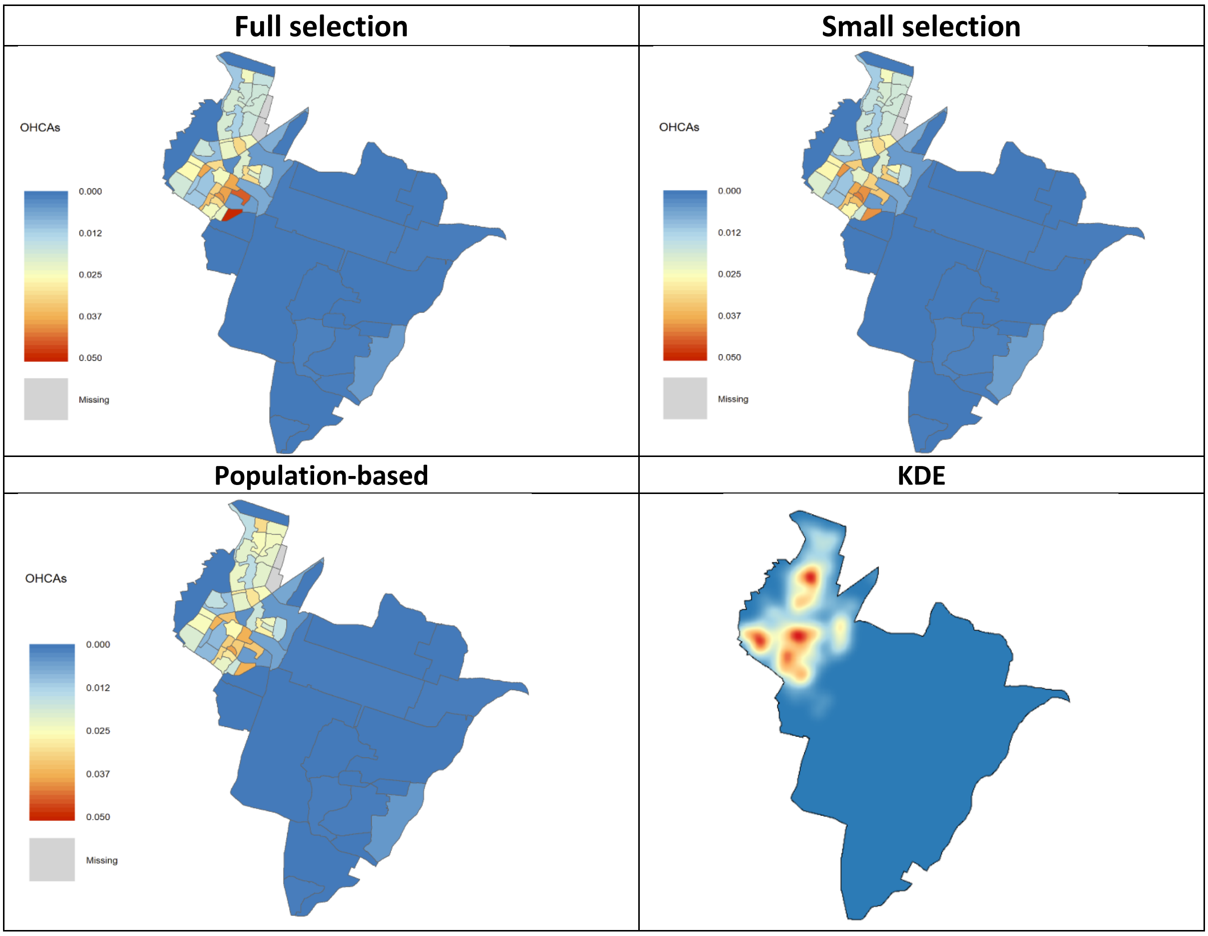

Figure 7. Heatmaps of the OHCA risk in Alkmaar (2017).

6.3 AED optimization

This section presents the results of the AED optimization for Amsterdam, Zaanstad, Haarlem, Haarlemmermeer and Alkmaar based on the full and small feature selection, the population-based strategy, and KDE.

6.3.1 Results real data test set

Tables 8-12 display the average coverage for each year and method across the municipalities after relocation of the AEDs. The coverage values of the current AED locations are in the tables, as well. The number of AEDs used for each year and municipality can be found in Section 9.4. The bandwidths used for the KDE approaches are detailed in Section 9.8.

For Amsterdam, the coverage values are significantly better compared to the current AED locations across all methods. For the other municipalities, the results are not consistently significant when considering individual years. However, when examining the average coverage across all years, the AED placements using the predictions models are significantly better than the current AED placement in each municipality.

Overall, KDE seems to outperform the predictions methods, although the prediction models have a higher coverage value in 2016 and 2017 for Haarlem, 2017 for Haarlemmermeer, and 2010, 2011, 2014 and 2016 for Alkmaar. For Amsterdam, KDE shows significantly better results in the years 2010 and 2012.

Table 13 provides the average results per municipality, which are calculated by taking the average coverage of all test points across all years. These results indicate that KDE is significantly more effective for Amsterdam and Zaanstad.

No significant differences were observed between the full selection, small selection and population-based strategy in each of the municipalities.

Table 8. Average coverage of current AED locations and AED relocation per year per method for Amsterdam. The best performing method based on estimated locations and the best performing KDE method are highlighted.

Amsterdam

	Average coverage (95% CI)						
	Current selection	Full selection	Small selection	Population -based	KDE Bootstrap	KDE Likelihood	KDE Least Squares
2010	46.2 (42.6 - 49.8)	54.3 (51.6 - 57.1)	54.4 (51.9 - 56.9)	53.8 (51.1 - 56.4)	54.2 (51.8 - 56.6)	57.8 (55.3 - 60.3)	59.5 (57.0 - 62.0)
2011	41.7 (38.1 - 45.2)	54.6 (51.5 - 57.7)	52.1 (49.1 - 55.0)	54.0 (51.2 - 56.8)	53.9 (51.0 - 56.7)	56.1 (53.3 - 58.9)	60.2 (57.5 - 63.0)
2012	42.2 (38.6 - 45.8)	53.6 (50.8 - 56.3)	52.3 (49.4 - 55.2)	55.4 (52.5 - 58.2)	53.8 (51.2 - 56.5)	57.2 (54.3 - 60.0)	62.0 (59.0 - 65.0)
2013	40.7 (37.1 - 44.2)	51.5 (48.4 - 54.5)	54.4 (51.4 - 57.5)	52.7 (49.7 - 55.8)	53.2 (50.5 - 55.9)	56.1 (53.3 - 58.9)	58.0 (55.2 - 60.9)
2014	44.6 (41.5 - 47.8)	54.1 (51.6 - 56.6)	52.4 (49.8 - 55.0)	54.7 (52.1 - 57.2)	53.0 (50.7 - 55.4)	58.0 (55.6 - 60.3)	57.8 (55.3 - 60.3)
2015	43.1 (40.1 - 46.0)	55.5 (53.0 - 57.9)	55.0 (52.6 - 57.4)	53.3 (51.0 - 55.5)	54.1 (51.8 - 56.4)	58.1 (55.9 - 60.2)	59.8 (57.3 - 62.2)
2016	44.3 (41.6 - 47.1)	59.5 (57.2 - 61.7)	59.7 (57.4 - 62.0)	59.6 (57.3 - 61.9)	54.6 (52.3 - 56.9)	57.8 (55.7 - 59.8)	60.8 (58.5 - 63.2)
2017	41.9 (39.0 - 44.8)	57.8 (55.6 - 60.1)	59.1 (56.9 - 61.3)	56.9 (54.6 - 59.2)	53.2 (51.1 - 55.2)	57.3 (55.2 - 59.5)	61.1 (58.9 - 63.4)

Table 9. Average coverage of current AED locations and AED relocation per year per method for Zaanstad. The best performing method based on estimated locations and the best performing KDE method are highlighted.

Zaanstad

	Average coverage (95% CI)						
	Current selection	Full selection	Small selection	Population -based	KDE Bootstrap	KDE Likelihood	KDE Least Squares
2010	38.8 (31.5 - 46.2)	47.9 (41.7 - 54.2)	50.4 (44.6 - 56.2)	52.8 (46.4 - 59.1)	47.4 (41.3 - 53.5)	53.3 (46.9 - 59.6)	55.8 (49.9 - 61.8)
2011	40.9 (33.2 - 48.6)	47.1 (40.9 - 53.4)	54.5 (48.3 - 60.7)	52.7 (46.3 - 59.2)	53.7 (46.4 - 61)	57.4 (51.0 - 63.8)	58.3 (51.6 - 65.0)
2012	38.9 (30.9 - 46.9)	49.7 (43.2 - 56.1)	52.5 (44.9 0 60.0)	49.7 (43.7 - 55.8)	48.9 (42.9 - 54.9)	58.1 (51.4 - 64.8)	57.1 (49.9 - 64.3)
2013	45.2 (38.1 - 52.4)	54.1 (47.8 - 60.5)	51.9 (46.3 - 57.5)	49 (43.6 - 54.3)	48.9 (43.3 - 54.6)	55.4 (50.2 - 60.7)	56.9 (51.5 - 62.4)
2014	39.4 (32.1 - 46.8)	55.9 (50.1 - 61.7)	53.9 (49.0 - 58.9)	50.7 (45.6 - 55.7)	50.1 (45.0 - 55.2)	55.5 (49.6 - 61.3)	59.6 (53.5 - 65.6)
2015	44.9 (38.6 - 51.3)	48.6 (43.0 - 54.2)	46.6 (41.2 0 52.0)	50.4 (45.1 - 55.7)	46.5 (41.6 - 51.3)	53.5 (48.8 - 58.1)	55.5 (50.8 - 60.2)
2016	34.2 (28.5 - 40.0)	51.6 (45.9 - 57.3)	51.5 (46.2 - 56.8)	49.8 (44.4 - 55.2)	50.1 (44.4 - 55.7)	54.1 (49.2 - 59.1)	57.4 (52.8 - 62.1)
2017	39.5 (32.5 - 46.4)	50.7 (44.4 - 57.0)	46.8 (41.2 - 52.5)	47.4 (41.7 - 53.1)	52.9 (46.7 - 59.0)	49.4 (44.4 - 54.4)	54.6 (48.4 - 60.8)

Table 10. Average coverage of current AED locations and AED relocation per year per method for Haarlem. The best performing method based on estimated locations and the best performing KDE method are highlighted.

Haarlem

	Average coverage (95% CI)						
	Current selection	Full selection	Small selection	Population -based	KDE Bootstrap	KDE Likelihood	KDE Least Squares
2010	50.3 (44.3 - 56.2)	58.8 (51.6 - 66.0)	53.7 (48.4 - 59.0)	57.3 (51.3 - 63.2)	61.3 (56.2 - 66.4)	61.9 (56.0 - 67.8)	59.3 (52.5 - 66.1)
2011	55.1 (49.7 - 60.5)	55.9 (50.0 - 61.9)	56.3 (50.1 - 62.4)	54.2 (48.8 - 59.7)	58.3 (53.8 - 62.9)	64.1 (58.8 - 69.5)	62.7 (57.6 - 67.9)
2012	51.8 (46.3 - 57.3)	57.8 (52.1 - 63.6)	61.4 (56.3 - 66.5)	57.9 (52.9 - 62.9)	53.9 (48.1 - 59.8)	62.4 (57.1 - 67.7)	58.1 (52.6 - 63.5)
2013	52.8 (47.2 - 58.4)	57.5 (52.0 - 63.0)	57.5 (52.3 - 62.7)	56.1 (51.3 - 60.8)	60.8 (56.2 - 65.3)	60.4 (55.2 - 65.5)	62.6 (57.9 - 67.2)
2014	54.7 (47.6 - 61.9)	59.8 (54.1 - 65.4)	59.9 (54.6 - 65.2)	62.5 (56.0 - 69.0)	58.4 (53.2 - 63.7)	61.2 (54.9 - 67.5)	61.7 (55.4 - 68.0)
2015	54.1 (48.7 - 59.5)	58.1 (53.1 - 63.2)	55.3 (49.7 - 60.8)	54.5 (50.5 - 58.6)	62.0 (58.1 - 66.0)	62.9 (58.6 - 67.1)	64.0 (59.8 - 68.2)
2016	52.4 (48.0 - 56.8)	63.7 (59.4 - 68.0)	63.3 (59.3 - 67.4)	68.6 (64.7 - 72.6)	59.7 (55.1 - 64.2)	61.5 (57.0 - 66.0)	62.7 (57.3 - 68)
2017	57.3 (51.8 - 62.9)	62.6 (57.7 - 67.4)	62.9 (58.2 - 67.6)	65.1 (60.8 - 69.4)	59.9 (55.4 - 64.5)	60.5 (56.3 - 64.7)	63.5 (59.3 - 67.8)

Table 11. Average coverage of current AED locations and AED relocation per year per method for Haarlemmermeer. The best performing method based on estimated locations and the best performing KDE method are highlighted.

Haarlemmermeer

	Average coverage (95% CI)						
	Current selection	Full selection	Small selection	Population -based	KDE Bootstrap	KDE Likelihood	KDE Least Squares
2010	49.8 (42.1 - 57.4)	58.5 (50.8 - 66.3)	57.7 (50.1 - 65.4)	60.9 (53.0 - 68.9)	52.2 (44.8 - 59.6)	59.1 (51.7 - 66.4)	61.7 (54.7 - 68.7)
2011	47.8 (39.8 - 55.7)	48.5 (40.2 - 56.8)	48.8 (40.3 - 57.3)	52.1 (43.1 - 61.1)	46.2 (38.5 - 54.0)	55.3 (50.0 - 60.6)	55.6 (49.0 - 62.2)
2012	40.0 (32.3 - 47.6)	51.1 (43.8 - 58.4)	51.8 (44.4 - 59.2)	50.8 (42.7 - 58.9)	46.7 (39.3 - 54.0)	48.0 (40.4 - 55.5)	52.4 (44.6 - 60.3)
2013	40.3 (31.1 - 49.6)	39.2 (30.2 - 48.2)	40.9 (31.1 - 50.7)	40.6 (30.8 - 50.5)	36.3 (27.8 - 44.8)	41.8 (31.9 - 51.7)	47.4 (38.7 - 56.1)
2014	53.4 (47.3 - 59.6)	54.8 (48.5 - 61.1)	53.8 (46.7 - 61.0)	54.9 (47.7 - 62.0)	45.3 (38.7 - 52.0)	51.6 (44.8 - 58.5)	56.4 (49.6 - 63.2)
2015	44.7 (38.1 - 51.3)	55.2 (48.6 - 61.7)	56.1 (49.2 - 63.0)	54.7 (48.1 - 61.2)	43.6 (37.5 - 49.6)	57.4 (51.2 - 63.5)	57.1 (50.9 - 63.4)
2016	40.8 (34.0 - 47.5)	50.4 (43.5 - 57.4)	49.2 (42.6 - 55.9)	48.3 (41.3 - 55.4)	40.6 (33.9 - 47.3)	48.1 (40.9 - 55.3)	51.8 (45.0 - 58.5)
2017	47.9 (40.9 - 55.0)	49.7 (42.7 - 56.7)	52.3 (44.9 - 59.6)	47.4 (40.6 - 54.2)	43.6 (37.0 - 50.2)	51.8 (45.1 - 58.4)	50.0 (43.0 - 57.1)

Table 12. Average coverage of current AED locations and AED relocation per year per method for Alkmaar. The best performing method based on estimated locations and the best performing KDE method are highlighted.

Alkmaar

	Average coverage (95% CI)						
	Current selection	**Full selection**	**Small selection**	**Population -based**	**KDE Bootstrap**	**KDE Likelihood**	**KDE Least Squares**
2010	67.0 (61.2 - 72.9)	70.4 (65.5 - 75.2)	72.5 (67.8 - 77.2)	68.4 (63.5 - 73.3)	69.0 (64.6 - 73.5)	70.3 (66.1 - 74.5)	68.6 (64.3 - 72.9)
2011	55.4 (48.9 - 62.0)	66.7 (59.9 - 73.5)	68.2 (61.5 - 74.9)	67.0 (60.1 - 73.8)	63.4 (57.6 - 69.3)	63.7 (57.7 - 69.8)	64.7 (57.8 - 71.6)
2012	52.0 (44.3 - 59.7)	65.5 (59.5 - 71.5)	67.9 (61.7 - 74.0)	66.2 (60.1 - 72.4)	65.9 (60.1 - 71.6)	72.3 (66.7 - 77.9)	66.8 (59.3 - 74.3)
2013	63.1 (57.0 - 69.2)	68.7 (63.9 - 73.5)	70.5 (66.4 - 74.7)	71.1 (66.7 - 75.5)	68.1 (63.6 - 72.5)	68.3 (64.7 - 71.9)	73.4 (68.6 - 78.2)
2014	57.8 (49.0 - 66.6)	65.8 (58.5 - 73.1)	62.1 (54.7 - 69.5)	58.5 (51.8 - 65.2)	62.1 (55.7 - 68.4)	64.8 (57.9 - 71.6)	61.4 (53.8 - 68.9)
2015	54.2 (44.9 - 63.6)	61.7 (53.2 - 70.3)	62.3 (52.7 - 71.9)	59.2 (50.5 - 68.0)	58.3 (51.9 - 64.7)	62.1 (54.6 - 69.7)	63.1 (55.0 - 71.1)
2016	60.0 (52.7 - 67.4)	61.2 (55.7 - 66.7)	64.4 (58.2 - 70.6)	69.6 (63.6 - 75.5)	68.4 (63.8 - 73.0)	68.4 (64.1 - 72.8)	65.3 (58.7 - 72.0)
2017	59.5 (47.2 - 71.7)	55.4 (45.8 - 65.0)	55.3 (46.5 - 64.1)	61.6 (51.9 - 71.2)	63.2 (56.9 - 69.6)	62.5 (55.1 - 69.9)	61.0 (50.6 - 71.4)

Table 13. Average coverage of current AED locations and AED relocation per method across all years for each municipality. The best performing method based on estimated locations and the best performing KDE method are highlighted.

All years

	Average coverage (95% CI)						
	Current selection	**Full selection**	**Small selection**	**Population -based**	**KDE Bootstrap**	**KDE Likelihood**	**KDE Least Squares**
AMS	43.2 (42.0 - 44.3)	55.4 (54.5 - 56.4)	55.3 (54.4 - 56.2)	55.3 (54.4 - 56.2)	53.8 (52.9 - 54.6)	57.4 (56.5 - 58.2)	59.9 (59.0 - 60.8)
ZAA	40.3 (37.8 - 42.7)	50.8 (48.6 - 53.0)	50.7 (48.6 - 52.7)	50.2 (48.2 - 52.2)	49.6 (47.5 - 51.6)	54.4 (52.4 - 56.3)	56.8 (54.8 - 58.8)
HAA	53.6 (51.6 - 55.5)	59.4 (57.4 - 61.3)	58.8 (57.0 - 60.7)	59.5 (57.7 - 61.3)	59.4 (57.7 - 61.1)	61.9 (60.1 - 63.7)	62.0 (60.1 - 63.8)
HLM	45.5 (42.9 - 48.1)	51.1 (48.5 - 53.8)	51.5 (48.7 - 54.2)	51.1 (48.3 - 53.9)	44.1 (41.5 - 46.6)	51.5 (48.9 - 54.1)	53.9 (51.3 - 56.4)
ALK	58.9 (56.1 - 61.6)	65.1 (62.7 - 67.4)	66.3 (63.9 - 68.7)	65.8 (63.5 - 68.2)	65.2 (63.2 - 67.1)	66.9 (64.9 - 68.9)	66.0 (63.5 - 68.5)

6.3.2 Histograms coverage

Figures 8-12 visualise the coverage per year and per method, for each municipality. These histograms of the AED coverage reveal several key findings.

For Amsterdam, the prediction methods demonstrated improved performance in 2016 and 2017 compared to previous years (Figure 8). For Zaanstad, the full feature selection results in relatively high coverage in 2013 and 2014, but the small selection resulted in notably low coverage in 2015 and 2017 (Figure 9). For Haarlem, the average coverage improved in 2016 and 2017, particularly with the population-based strategy (Figure 10). The coverage values for Haarlemmermeer using the prediction and KDE methods were quite consistent, with the largest difference observed in 2013, where the small selection prediction method had a coverage of 41, compared to the best KDE method with a coverage of 47 (Figure 11). For Alkmaar, there was a noticeable decrease in coverage in the last years for most prediction methods, except for the population-based strategy, which showed improved coverage in 2016 (Figure 12).

In Figure 13, the final histogram shows the average coverage across all years, for each method and municipality. There is no substantial difference in performance among prediction methods. However, it appears that the KDE methods have a somewhat better performance, particularly in the larger municipalities Amsterdam and Zaanstad. Notably, the histogram highlights that the KDE bootstrap method performs worse than the other methods for Haarlemmermeer.

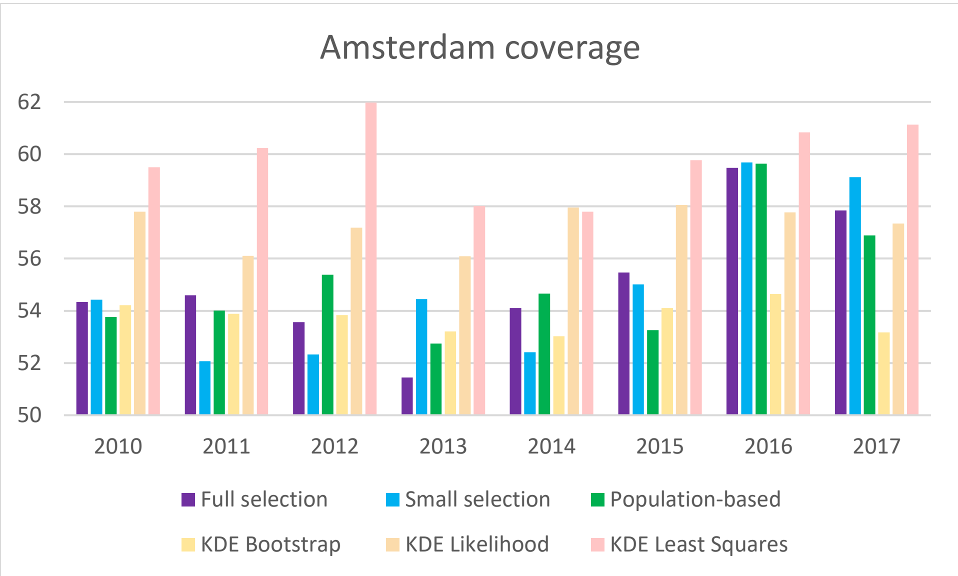

Figure 8. Histogram of the coverage per year per method in Amsterdam.

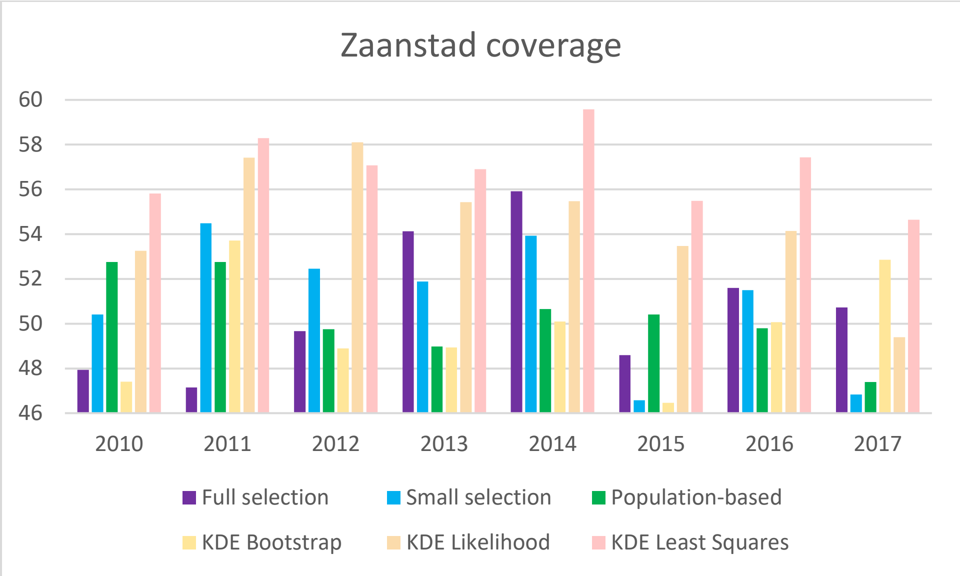

Figure 9. Histogram of the coverage per year per method in Zaanstad.

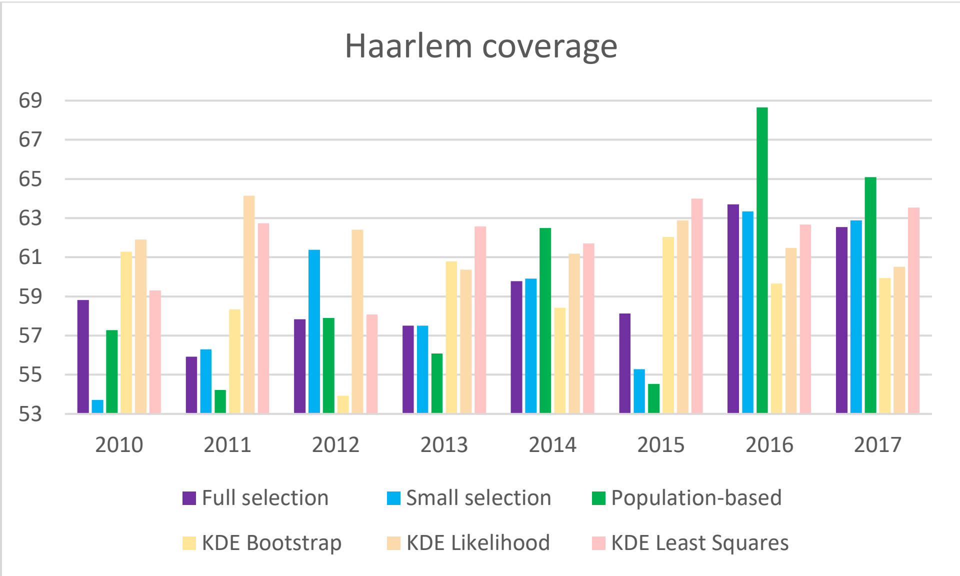

Figure 10. Histogram of the coverage per year per method in Haarlem.

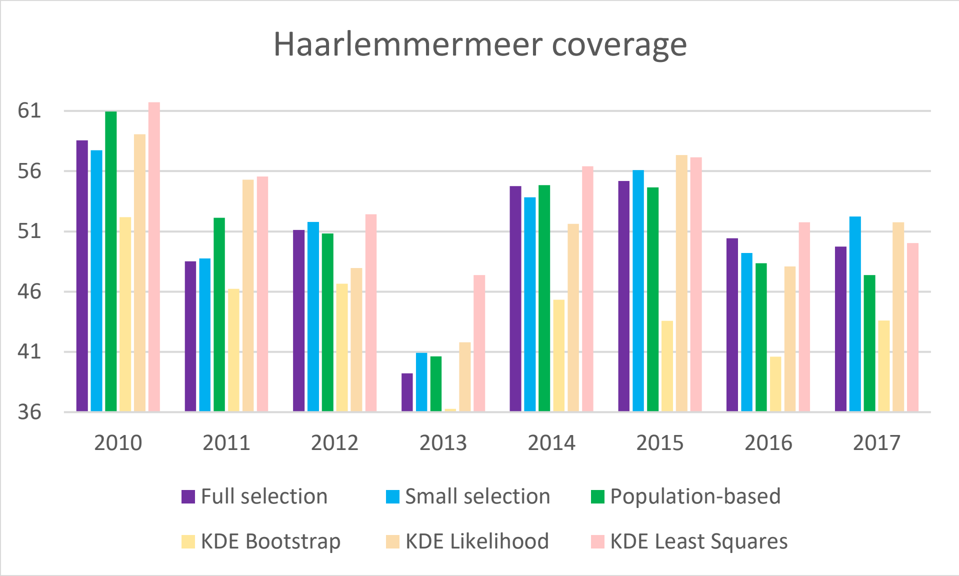

Figure 11. Histogram of the coverage per year per method in Haarlemmermeer.

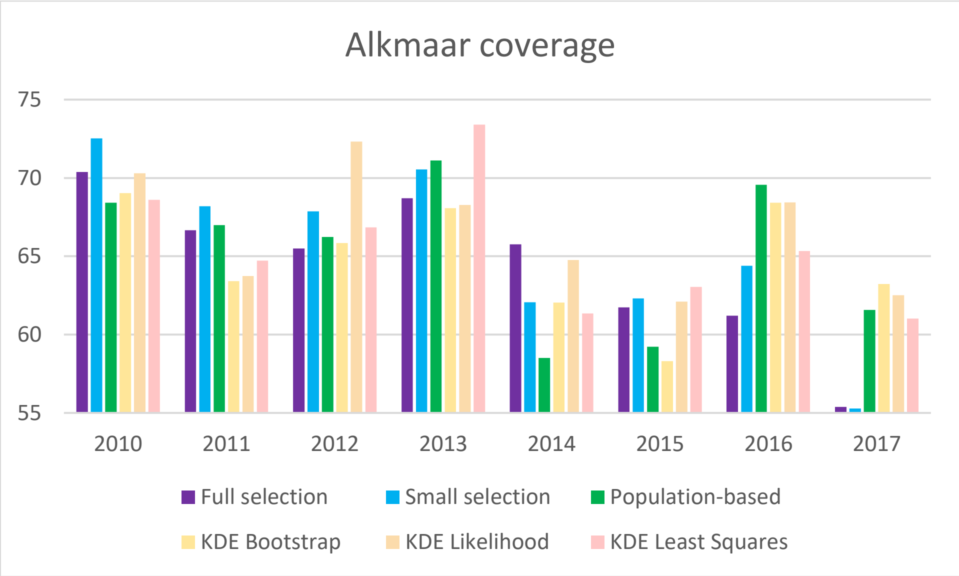

Figure 12. Histogram of the coverage per year per method in Alkmaar.

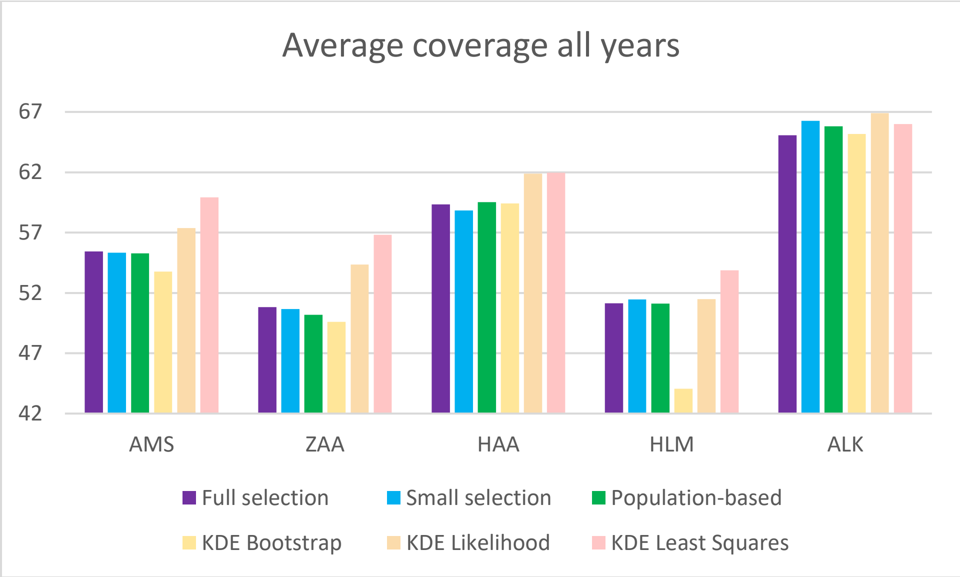

Figure 13. Histogram of the average coverage across all years per method.

7 Discussion and conclusion

7.1 Discussion

In this study, we presented prediction models that can accurately (R^2 of 0.96 for Amsterdam) estimate the OHCA incidence in districts of municipalities in North Holland, using demographic and socioeconomic data. The coverage of current AED locations in Amsterdam improved from 43% to 55% with the use of these prediction models, compared to a 60% coverage when KDE and historical data were used.

The Huber regression method emerged as the most effective for predicting OHCA incidence, compared to other machine learning methods considered. Huber regression, along with the other methods that performed well, incorporates regularization to handle multicollinearity and prevent overfitting. Tuning the Huber model parameters via cross-validation resulted in strong predictive performance, with the full feature selection (22 variables) performing best for Amsterdam, while the small feature selection (5 variables) was preferred for Zaanstad, Haarlem and Haarlemmermeer (Table 7). This difference may be due to overfitting when using a larger feature set in smaller municipalities, whereas Amsterdam, being the largest part of the dataset, may benefit from the full feature selection because of its greater data complexity.

Visualizing the predicted OHCA risk by heatmaps revealed some insights. For Amsterdam, the model did not capture the hotspot in the centre, which might be due to the lack of tourist-related data in the features. Additionally, in the heatmaps with the full selection of Haarlem and Alkmaar, hotspots are in the wrong spot because of the 'number of businesses' feature. Industrial areas, characterized by a high number of businesses, were predicted by the model to have high OHCA incidence. When this incidence was distributed across the neighbourhoods in the district based on population density, the neighbourhoods with higher population densities (and lower amount of businesses) were predicted to have overly high OHCA risk relative to their surface area.

The results of the AED optimization show that the coverage of the AED placement using the prediction models is significantly better than the coverage of current AED placement considering average values across all years. Additionally, for Amsterdam, the coverage using the prediction models is higher than current situation even when considering individual years.

The AED optimization results indicate no significant difference between the feature selections and population-based strategy. However, our study demonstrates that predictions based on demographic and socioeconomic data are quite accurate, achieving the study’s first aim. These predictions can be effectively used on their own, such as in prioritizing areas for improving CPR performance. Furthermore, no significant difference is observed between the prediction methods and KDE for most years and municipalities. This lack of difference may be caused by the small test set used for evaluation, as it consists of real historical data. However, when considering the average coverage across all years, KDE performs significantly better than the prediction models for Amsterdam and Zaanstad.

The histograms visualizing the coverage results showed that for both Amsterdam and Haarlem, the prediction models perform better in 2016 and 2017. In these years, the number of districts was increased compared to previous years, potentially leading to improved performance as locations were estimated on a smaller scale. The low performance of the KDE bootstrap method for Haarlemmermeer across all years can be explained by the methods’ relatively large bandwidth. Given that Haarlemmermeer has a few concentrated hotspots (see Figure 6), this extensive smoothing results in AEDs being placed in the low-risk areas around the hotspots. The histograms in Section 9.9 show a consistent pattern over the years for each municipality in terms of the predicted OHCA incidence proportion per district. This indicates that most of the variation in the coverage over the years is due to variations in actual OHCA data, rather than variations in demographic and socioeconomic data or predictions.

In addition to the contributions of this research to the literature, there are substantial social implications. The study shows the potential of optimizing AED placement even in the absence of historical OHCA data. This is particularly valuable for underdeveloped regions where such historical data may be lacking but demographic and socioeconomic data are often available. The results of this study show the potential of applying the approach not only in the Netherlands but also in other regions around the world. By strategically placing AEDs based on predictive models and demographic and socioeconomic data, quicker response times to OHCA can be ensured, potentially increasing the chances of survival. The OHCA estimates obtained using the models in this paper can also be used to guide other public health resource allocations, not only the AEDs. There are many studies which looked into identifying high risk areas within a city or municipality for this purpose but they often use actual OHCA data (Buter et al., 2023; Demirtas et al., 2015; Nassel et al., 2014; Wong et al., 2022). The novelty of our models is that they can examine OHCA risk levels and differences between districts, even if the OHCA data is not available.

The study has several limitations. Firstly, the OHCA data used was on district level rather than on individual level, which may impact the level of detail and accuracy of the predictions. Additionally, absolute values of the demographic and socioeconomic data were used instead of percentages to incorporate population, which could influence the results because of correlation of the data (analysis in Section 9.5). However, the Huber regressor of PyCaret includes L2-regularization to address multicollinearity and overfitting. As education data, which has been shown to have a relation with OHCA risk, was not available per year per district, it was excluded from the feature selections.

Another limitation is that since district and neighbourhood codes and borders change frequently, the data was not aggregated. Aggregation of the data could have potentially increased performance by reducing zero values in the dataset. The prediction methods rely on borders because of the input data, rather than using a smooth risk map like KDE, which could provide a more continuous representation of OHCA risk.

Furthermore, the prediction models do not perform as well for large districts or neighbourhoods with a less homogeneous population, which could affect their generalizability. Finally, the real data test set had a relatively small number of datapoints, resulting in large confidence intervals for the results and therefore few significant results. However, using actual historical locations in the test set provides a real presentation of the performances of the methods.

One suggestion for further exploration of this research is the testing of other prediction methods. While this study focused on the methods included in the PyCaret package, other machine learning methods could be explored and compared. Additionally, other methods based on historical data could be investigated. Next to KDE used in this study, there might be methods that estimate spatial OHCA risk even more accurate. Another possibility for further research is the testing of other AED optimization methods, instead of the GMCLP model used in this study. Furthermore, focusing on only shockable OHCAs may provide more valuable results, as these are the cases where AEDs are most effective. Future research could improve the estimation of the OHCA locations by not using population densities on neighbourhood-level, but on a more detailed scale. Lastly, developing a more generalized prediction model that can be applied to other regions, besides the municipalities of North-Holland, would increase the applicability of the approach.

7.2 Conclusion

This study compares a spatial risk estimation method based on demographic and socioeconomic data to KDE, which is based on historical locations. Huber regression was found to be the most effective for predicting OHCA incidence. The results of the AED optimization showed no significant difference between the feature selections and population-based strategy, and no significant difference was observed between the prediction methods and KDE for most years and municipalities. This study demonstrates that machine learning models based on demographic and socioeconomic data can improve AED coverage in the absence of historical data, although KDE based on historical data remains the more effective approach when such data is available.

8 References

Alhdiri, M. A. S., Samat, N. A., & Mohamed, Z. (2017). Disease mapping for stomach cancer in libya based on Besag–York–Mollié (BYM) Model. *Asian Pacific Journal of Cancer Prevention: APJCP, 18*(6), 1479.

Anderson, K. M., Odell, P. M., Wilson, P. W., & Kannel, W. B. (1991). Cardiovascular disease risk profiles. *American heart journal, 121*(1), 293-298.

Anselin, L. (1995). Local indicators of spatial association—LISA. *Geographical analysis, 27*(2), 93-115.

Arunachalam, K., Zhang, Z., Chu, A., & Maan, A. (2021). Impact of racial and gender variations in patients with out-of-hospital cardiac arrest: A nation-wide study. *Critical Pathways in Cardiology, 20*(1), 25-30.

Auricchio, A., Peluso, S., Caputo, M. L., Reinhold, J., Benvenuti, C., Burkart, R., Cianella, R., Klersy, C., Baldi, E., & Mira, A. (2020). Spatio-temporal prediction model of out-of-hospital cardiac arrest: Designation of medical priorities and estimation of human resources requirement. *PloS one, 15*(8), e0238067.

Becker, L., Eisenberg, M., Fahrenbruch, C., & Cobb, L. (1998). Public locations of cardiac arrest: implications for public access defibrillation. *Circulation, 97*(21), 2106-2109.

Berman, O., & Krass, D. (2002). The generalized maximal covering location problem. *Computers & Operations Research, 29*(6), 563-581.

Besag, J., York, J., & Mollié, A. (1991). Bayesian image restoration, with two applications in spatial statistics. *Annals of the institute of statistical mathematics, 43*(1), 1-20.

Best, N., Richardson, S., & Thomson, A. (2005). A comparison of Bayesian spatial models for disease mapping. *Statistical methods in medical research, 14*(1), 35-59.

Biau, G., & Scornet, E. (2016). A random forest guided tour. *Test, 25*(2), 197-227.

Blangiardo, M., & Cameletti, M. (2015). *Spatial and spatio-temporal Bayesian models with R-INLA*. John Wiley & Sons.

Bolijn, R., Sieben, C. H., Kunst, A. E., Blom, M., Tan, H. L., & van Valkengoed, I. G. (2021). Sex differences in incidence of out-of-hospital cardiac arrest across ethnic and socioeconomic groups: A population-based cohort study in the Netherlands. *International Journal of Cardiology, 343*, 156-161.

Brisbois, A., & Dziedzic, R. (2023). Multivariate Regression Models for Predicting Pump-as-Turbine Characteristics. *Water, 15*(18), 3290.

Brown, T. P., Booth, S., Hawkes, C. A., Soar, J., Mark, J., Mapstone, J., Fothergill, R. T., Black, S., Pocock, H., & Bichmann, A. (2019). Characteristics of neighbourhoods with high incidence of out-of-hospital cardiac arrest and low bystander cardiopulmonary resuscitation rates in England. *European Heart Journal-Quality of Care and Clinical Outcomes, 5*(1), 51-62.

Buter, R., van Schuppen, H., Koffijberg, H., Hans, E. W., Stieglis, R., & Demirtas, D. (2023). Where do we need to improve resuscitation? Spatial analysis of out-of-hospital cardiac arrest incidence and mortality. *Scandinavian Journal of Trauma, Resuscitation and Emergency Medicine, 31*(1), 63.

Caplan, J. M., Kennedy, L. W., & Miller, J. (2011). Risk terrain modeling: Brokering criminological theory and GIS methods for crime forecasting. *Justice quarterly, 28*(2), 360-381.

Castra, L., Genin, M., Escutnaire, J., Baert, V., Agostinucci, J.-M., Revaux, F., Ursat, C., Tazarourte, K., Adnet, F., & Hubert, H. (2019). Socioeconomic status and incidence of cardiac arrest: a spatial approach to social and territorial disparities. *European Journal of Emergency Medicine, 26*(3), 180-187.

Chan, T. C. (2016). Optimal Defibrillator Placement in a High-rise Building. *Circulation, 134*(suppl_1), A16773-A16773.

Chan, T. C., Demirtas, D., & Kwon, R. H. (2016). Optimizing the deployment of public access defibrillators. *Management science, 62*(12), 3617-3635.

Chan, T. C., Li, H., Lebovic, G., Tang, S. K., Chan, J. Y., Cheng, H. C., Morrison, L. J., & Brooks, S. C. (2013). Identifying locations for public access defibrillators using mathematical optimization. *Circulation, 127*(17), 1801-1809.

Chopin, N. (2009). Approximate Bayesian inference for latent Gaussian models by using integrated nested Laplace. *Journal of the Royal Statistical Society. Series B (Statistical Methodology), 71*(2), 319-392.

Chrisinger, B. W., Grossestreuer, A. V., Laguna, M. C., Griffis, H. M., Branas, C. C., Wiebe, D. J., & Merchant, R. M. (2016). Characteristics of automated external defibrillator coverage in Philadelphia, PA, based on land use and estimated risk. *Resuscitation, 109*, 9-15.

Cummins, R. O., Eisenberg, M. S., Hallstrom, A. P., & Litwin, P. E. (1985). Survival of out-of-hospital cardiac arrest with early initiation of cardiopulmonary resuscitation. *The American Journal of Emergency Medicine, 3*(2), 114-119.

D’Angelo, N., Payares, D., Adelfio, G., & Mateu, J. (2022). Self-exciting point process modelling of crimes on linear networks. *Statistical Modelling*, 1471082X221094146.

Dao, T. H. D., Zhou, Y., Thill, J.-C., & Delmelle, E. (2012). Spatio-temporal location modeling in a 3D indoor environment: the case of AEDs as emergency medical devices. *International Journal of Geographical Information Science, 26*(3), 469-494.

Deakin, C. D., Anfield, S., & Hodgetts, G. A. (2018). Underutilisation of public access defibrillation is related to retrieval distance and time-dependent availability. *Heart, 104*(16), 1339-1343.

Deakin, C. D., Shewry, E., & Gray, H. H. (2014). Public access defibrillation remains out of reach for most victims of out-of-hospital sudden cardiac arrest. *Heart, 100*(8), 619-623.

Delhomme, C., Njeim, M., Varlet, E., Pechmajou, L., Benameur, N., Cassan, P., Derkenne, C., Jost, D., Lamhaut, L., & Marijon, E. (2019). Automated external defibrillator use in out-of-hospital cardiac arrest: Current limitations and solutions. *Archives of cardiovascular diseases, 112*(3), 217-222.

Demirtas, D. (2016). *Facility location under uncertainty and spatial data analytics in healthcare*. University of Toronto (Canada).

Demirtas, D., Brooks, S. C., Morrison, L. J., & Chan, T. C. (2015). Spatiotemporal stability of public cardiac arrests. *Circulation, 132*(suppl_3), A15003-A15003.

Derevitskii, I., Kogtikov, N., Lees, M. H., Cai, W., & Ong, M. E. (2020). Risk-based AED placement-Singapore case. Computational Science–ICCS 2020: 20th International Conference, Amsterdam, The Netherlands, June 3–5, 2020, Proceedings, Part IV 20,

Doan, T. N., Wilson, D., Rashford, S., Ball, S., & Bosley, E. (2021). Spatiotemporal variation in the risk of out-of-hospital cardiac arrests in Queensland, Australia. *Resuscitation plus, 8*, 100166.

Dulk, C. d., Van de Stadt, H., & Vliegen, J. (1992). Een nieuwe maatstaf voor stedelijkheid: de omgevingsadressendichtheid. *Maandstatistiek van de bevolking, 92*(7), 14-27.

Empana, J.-P., Jouven, X., Lemaitre, R., Sotoodehnia, N., Rea, T., Raghunathan, T., Simon, G., & Siscovick, D. (2008). Marital status and risk of out-of-hospital sudden cardiac arrest in the population. *European Journal of Preventive Cardiology, 15*(5), 577-582.

Empana, J., Ducimetiere, P., Charles, M., & Jouven, X. (2004). Sagittal abdominal diameter and risk of sudden death in asymptomatic middle-aged men: the Paris Prospective Study I. *Circulation, 110*(18), 2781-2785.

Fedoruk, J., Currie, W. L., & Gobet, M. (2002). Locations of cardiac arrest: affirmation for community Public Access Defibrillation (PAD) Program. *Prehospital and Disaster Medicine, 17*(4), 202-205.

Fleming, D., Owens, A., Eckstein, M., & Sanko, S. (2021). Spatiotemporal analysis of out-of-hospital cardiac arrest in the City of Los Angeles, 2011–2019. *Resuscitation, 165*, 110-118.

Folke, F., Andelius, L., Gregers, M. T., & Hansen, C. M. (2021). Activation of citizen responders to out-of-hospital cardiac arrest. *Current Opinion in Critical Care, 27*(3), 209-215.

Folke, F., Gislason, G. H., Lippert, F. K., Nielsen, S. L., Weeke, P., Hansen, M. L., Fosbøl, E. L., Andersen, S. S., Rasmussen, S., & Schramm, T. K. (2010). Differences between out-of-hospital cardiac arrest in residential and public locations and implications for public-access defibrillation. *Circulation, 122*(6), 623-630.

Fosbøl, E. L., Dupre, M. E., Strauss, B., Swanson, D. R., Myers, B., McNally, B. F., Anderson, M. L., Bagai, A., Monk, L., & Garvey, J. L. (2014). Association of neighborhood characteristics with incidence of out-of-hospital cardiac arrest and rates of bystander-initiated CPR: implications for community-based education intervention. *Resuscitation, 85*(11), 1512-1517.

Friedman, J. H. (2001). Greedy function approximation: a gradient boosting machine. *Annals of statistics*, 1189-1232.

Galea, S., Blaney, S., Nandi, A., Silverman, R., Vlahov, D., Foltin, G., Kusick, M., Tunik, M., & Richmond, N. (2007). Explaining racial disparities in incidence of and survival from out-of-hospital cardiac arrest. *American journal of epidemiology, 166*(5), 534-543.

Garcia, R., Rajan, D., Warming, P. E., Svane, J., Vissing, C., Weeke, P., Barcella, C. A., Jabbari, R., Gislason, G. H., & Torp-Pedersen, C. (2022). Ethnic disparities in out-of-hospital cardiac arrest: A population-based cohort study among adult Danish immigrants. *The Lancet Regional Health-Europe, 22*, 100477.

Gardner, M. W., & Dorling, S. (1998). Artificial neural networks (the multilayer perceptron)—a review of applications in the atmospheric sciences. *Atmospheric environment, 32*(14-15), 2627-2636.

Getis, A., & Ord, J. K. (1992). The analysis of spatial association by use of distance statistics. *Geographical analysis, 24*(3), 189-206.

Giménez-Santana, A., Caplan, J. M., & Drawve, G. (2018). Risk terrain modeling and socio-economic stratification: Identifying risky places for violent crime victimization in Bogotá, Colombia. *European Journal on Criminal Policy and Research, 24*(4), 417-431.

Gräsner, J.-T., Wnent, J., Herlitz, J., Perkins, G. D., Lefering, R., Tjelmeland, I., Koster, R. W., Masterson, S., Rossell-Ortiz, F., & Maurer, H. (2020). Survival after out-of-hospital cardiac arrest in Europe-Results of the EuReCa TWO study. *Resuscitation, 148*, 218-226.

Gratton, M., Lindholm, D. J., & Campbell, J. P. (1999). Public-access defibrillation: where do we place the AEDs? *Prehospital Emergency Care, 3*(4), 303-305.

Green, P. J. (1995). Reversible jump Markov chain Monte Carlo computation and Bayesian model determination. *Biometrika, 82*(4), 711-732.

Green, P. J., & Richardson, S. (2002). Hidden Markov models and disease mapping. *Journal of the American statistical association, 97*(460), 1055-1070.

Guo, G., Wang, H., Bell, D., Bi, Y., & Greer, K. (2003). KNN model-based approach in classification. OTM Confederated International Conferences" On the Move to Meaningful Internet Systems",

Hansen, C. M., Wissenberg, M., Weeke, P., Ruwald, M. H., Lamberts, M., Lippert, F. K., Gislason, G. H., Nielsen, S. L., Køber, L., & Torp-Pedersen, C. (2013). Automated external defibrillators inaccessible to more than half of nearby cardiac arrests in public locations during evening, nighttime, and weekends. *Circulation, 128*(20), 2224-2231.

Hardyns, W., & Rummens, A. (2018). Predictive policing as a new tool for law enforcement? Recent developments and challenges. *European Journal on Criminal Policy and Research, 24*(3), 201-218.

Hearst, M. A., Dumais, S. T., Osuna, E., Platt, J., & Scholkopf, B. (1998). Support vector machines. *IEEE Intelligent Systems and their applications, 13*(4), 18-28.

Holmberg, M. J., Vognsen, M., Andersen, M. S., Donnino, M. W., & Andersen, L. W. (2017). Bystander automated external defibrillator use and clinical outcomes after out-of-hospital cardiac arrest: A systematic review and meta-analysis. *Resuscitation, 120*, 77-87.

Huber, P. J. (1964). Robust Estimation of a Location Parameter. *The Annals of Mathematical Statistics, 35*(1), 73-101, 129. https://doi.org/10.1214/aoms/1177703732

Kadaster / Central Bureau of Statistics. (2017). *Wijk- en Buurtkaart 2016*. https://www.cbs.nl/nl-nl/dossier/nederland-regionaal/geografische-data/wijk-en-buurtkaart-2017

Kanjilal, S., Gregg, E. W., Cheng, Y. J., Zhang, P., Nelson, D. E., Mensah, G., & Beckles, G. L. (2006). Socioeconomic status and trends in disparities in 4 major risk factors for cardiovascular disease among US adults, 1971-2002. *Archives of internal medicine, 166*(21), 2348-2355.

Kao, J.-H., Chan, T.-C., Lai, F., Lin, B.-C., Sun, W.-Z., Chang, K.-W., Leu, F.-Y., & Lin, J.-W. (2017). Spatial analysis and data mining techniques for identifying risk factors of Out-of-Hospital Cardiac Arrest. *International Journal of Information Management, 37*(1), 1528-1538.

Kingma, D. P., & Welling, M. (2013). Auto-encoding variational bayes. *arXiv preprint arXiv:1312.6114*.

Knorr-Held, L., & Raßer, G. (2000). Bayesian detection of clusters and discontinuities in disease maps. *Biometrics, 56*(1), 13-21.

Kucharska-Newton, A. M., Harald, K., Rosamond, W. D., Rose, K. M., Rea, T. D., & Salomaa, V. (2011). Socioeconomic indicators and the risk of acute coronary heart disease events: comparison of population-based data from the United States and Finland. *Annals of epidemiology, 21*(8), 572-579.

Lee, M., Demirtas, D., Buick, J. E., Feldman, M. J., Cheskes, S., Morrison, L. J., Chan, T. C., & Investigators, R. E. (2017). Increased cardiac arrest survival and bystander intervention in enclosed pedestrian walkway systems. *Resuscitation, 118*, 1-7.

Lee, S. Y., Park, J. H., Choi, Y. H., Lee, J., Ro, Y. S., Hong, K. J., Song, K. J., & Shin, S. D. (2022). Individual socioeconomic status and risk of out-of-hospital cardiac arrest: A nationwide case–control analysis. *Academic Emergency Medicine*.

Lerner, E. B., Fairbanks, R. J., & Shah, M. N. (2005). Identification of out-of-hospital cardiac arrest clusters using a geographic information system. *Academic Emergency Medicine, 12*(1), 81-84.

Lin, B.-C., Chen, C.-W., Chen, C.-C., Kuo, C.-L., Fan, I. c., Ho, C.-K., Liu, I., & Chan, T.-C. (2016). Spatial decision on allocating automated external defibrillators (AED) in communities by multi-criterion two-step floating catchment area (MC2SFCA). *International Journal of Health Geographics, 15*(1), 1-14.

MacDonald, R. D., Mottley, J. L., & Weinstein, C. (2002). Impact of prompt defibrillation on cardiac arrest at a major international airport. *Prehospital Emergency Care, 6*(1), 1-5.

Margolis, G., Elbaz-Greener, G., Ruskin, J. N., Roguin, A., Amir, O., & Rozen, G. (2022). The impact of obesity on sudden cardiac death risk. *Current Cardiology Reports, 24*(5), 497-504.

McLachlan, G. J., Lee, S. X., & Rathnayake, S. I. (2019). Finite mixture models. *Annual review of statistics and its application, 6*, 355-378.

Meijer, A., & Wessels, M. (2019). Predictive policing: Review of benefits and drawbacks. *International Journal of Public Administration, 42*(12), 1031-1039.

Meyer, D., & Wien, F. (2015). Support vector machines. *The Interface to libsvm in package e1071, 28*, 20.

Mirowsky, J. E., Devlin, R. B., Diaz-Sanchez, D., Cascio, W., Grabich, S. C., Haynes, C., Blach, C., Hauser, E. R., Shah, S., & Kraus, W. (2017). A novel approach for measuring residential socioeconomic factors associated with cardiovascular and metabolic health. *Journal of exposure science & environmental epidemiology, 27*(3), 281-289.

Mohler, G., & Porter, M. D. (2018). Rotational grid, PAI-maximizing crime forecasts. *Statistical Analysis and Data Mining: The ASA Data Science Journal, 11*(5), 227-236.

Mohler, G. O., Short, M. B., Brantingham, P. J., Schoenberg, F. P., & Tita, G. E. (2011). Self-exciting point process modeling of crime. *Journal of the American statistical association, 106*(493), 100-108.

Moon, H. J., Shin, Y. J., & Cho, Y. S. (2022). Identification of out-of-hospital cardiac arrest clusters using unsupervised learning. *The American Journal of Emergency Medicine, 62*, 41-48.

Murphy, K. P. (2022). *Probabilistic machine learning: an introduction*. MIT press.

[Record #159 is using a reference type undefined in this output style.]

Nakashima, T., Ogata, S., Noguchi, T., Tahara, Y., Onozuka, D., Kato, S., Yamagata, Y., Kojima, S., Iwami, T., & Sakamoto, T. (2021). Machine learning model for predicting out-of-hospital cardiac arrests using meteorological and chronological data. *Heart, 107*(13), 1084-1091.

Nassel, A. F., Root, E. D., Haukoos, J. S., McVaney, K., Colwell, C., Robinson, J., Eigel, B., Magid, D. J., & Sasson, C. (2014). Multiple cluster analysis for the identification of high-risk census tracts for out-of-hospital cardiac arrest (OHCA) in Denver, Colorado. *Resuscitation, 85*(12), 1667-1673.

Nevendra, M., & Singh, P. (2022). Empirical investigation of hyperparameter optimization for software defect count prediction. *Expert Systems with Applications, 191*, 116217.

Ong, M. E. H., Earnest, A., Shahidah, N., Ng, W. M., Foo, C., & Nott, D. J. (2011). Spatial variation and geographic-demographic determinants of out-of-hospital cardiac arrests in the city-state of Singapore. *Annals of emergency medicine, 58*(4), 343-351.

Peluso, S., Mira, A., Rue, H., Tierney, N. J., Benvenuti, C., Cianella, R., Caputo, M. L., & Auricchio, A. (2020). A Bayesian spatiotemporal statistical analysis of out-of-hospital cardiac arrests. *Biometrical Journal, 62*(4), 1105-1119.

Perkins, G. D., Gräsner, J.-T., Semeraro, F., Olasveengen, T., Soar, J., Lott, C., Van de Voorde, P., Madar, J., Zideman, D., & Mentzelopoulos, S. (2021). European resuscitation council guidelines 2021: executive summary. *Resuscitation, 161*, 1-60.

Raun, L. H., Jefferson, L. S., Persse, D., & Ensor, K. B. (2013). Geospatial analysis for targeting out-of-hospital cardiac arrest intervention. *American Journal of Preventive Medicine, 45*(2), 137-142.

Rea, T. D., Olsufka, M., Bemis, B., White, L., Yin, L., Becker, L., Copass, M., Eisenberg, M., & Cobb, L. (2010). A population-based investigation of public access defibrillation: role of emergency medical services care. *Resuscitation, 81*(2), 163-167.

Reinhart, A. (2018). A review of self-exciting spatio-temporal point processes and their applications. *Statistical Science, 33*(3), 299-318.

Reinier, K., Stecker, E. C., Vickers, C., Gunson, K., Jui, J., & Chugh, S. S. (2006). Incidence of sudden cardiac arrest is higher in areas of low socioeconomic status: a prospective two year study in a large United States community. *Resuscitation, 70*(2), 186-192.

Samat, N. A., & Mey, L. W. (2017). Malaria disease mapping in malaysia based on Besag-York-Mollie (BYM) model. Journal of physics: Conference series,

Sasson, C., Cudnik, M. T., Nassel, A., Semple, H., Magid, D. J., Sayre, M., Keseg, D., Haukoos, J. S., Warden, C. R., & Group), C. S. (2012). Identifying high-risk geographic areas for cardiac arrest using three methods for cluster analysis. *Academic Emergency Medicine, 19*(2), 139-146.

Sasson, C., Keirns, C. C., Smith, D., Sayre, M., Macy, M., Meurer, W., McNally, B. F., Kellermann, A. L., Iwashyna, T. J., & Group, C. S. (2010). Small area variations in out-of-hospital cardiac arrest: does the neighborhood matter? *Annals of internal medicine, 153*(1), 19-22.

Scquizzato, T., Gamberini, L., D'Arrigo, S., Galazzi, A., Babini, G., Losiggio, R., Imbriaco, G., Fumagalli, F., Cucino, A., & Landoni, G. (2022). Incidence, characteristics, and outcome of out-of-hospital cardiac arrest in Italy: A systematic review and meta-analysis. *Resuscitation plus, 12*, 100329.

Semple, H. M., Cudnik, M. T., Sayre, M., Keseg, D., Warden, C. R., & Sasson, C. (2013). Identification of high-risk communities for unattended out-of-hospital cardiac arrests using GIS. *Journal of community health, 38*(2), 277-284.

Shalev-Shwartz, S., & Ben-David, S. (2014). *Understanding machine learning: From theory to algorithms*. Cambridge university press.

Shapiro, A. (2017). Reform predictive policing. *Nature, 541*(7638), 458-460.

Siddiq, A. A., Brooks, S. C., & Chan, T. C. (2013). Modeling the impact of public access defibrillator range on public location cardiac arrest coverage. *Resuscitation, 84*(7), 904-909.

Sidebottom, D. B., Potter, R., Newitt, L. K., Hodgetts, G. A., & Deakin, C. D. (2018). Saving lives with public access defibrillation: a deadly game of hide and seek. *Resuscitation, 128*, 93-96.

Smith, A., Masters, S., Ball, S., & Finn, J. (2022). The incidence and outcomes of out-of-hospital cardiac arrest in metropolitan versus rural locations: A systematic review and meta-analysis. *Resuscitation*.

Sondergaard, K. B., Hansen, S. M., Pallisgaard, J. L., Gerds, T. A., Wissenberg, M., Karlsson, L., Lippert, F. K., Gislason, G. H., Torp-Pedersen, C., & Folke, F. (2018). Out-of-hospital cardiac arrest:

Probability of bystander defibrillation relative to distance to nearest automated external defibrillator. *Resuscitation, 124*, 138-144.

Soo, L., Huff, N., Gray, D., & Hampton, J. R. (2001). Geographical distribution of cardiac arrest in Nottinghamshire. *Resuscitation, 48*(2), 137-147.

Stassen, W., Theron, E., Slingsby, T., & Wylie, C. (2022). Out-of-hospital cardiac arrests in the city of Cape Town metropole of the Western Cape province of South Africa: a spatio-temporal analysis. *Cardiovascular Journal of Africa, 33*(5), 260-266.

Stieglis, R., Zijlstra, J. A., Riedijk, F., Smeekes, M., van der Worp, W. E., Tijssen, J. G., Zwinderman, A. H., Blom, M. T., & Koster, R. W. (2022). Alert system-supported lay defibrillation and basic life-support for cardiac arrest at home. *European heart journal, 43*(15), 1465-1474.

Straney, L. D., Bray, J. E., Beck, B., Bernard, S., Lijovic, M., & Smith, K. (2016). Are sociodemographic characteristics associated with spatial variation in the incidence of OHCA and bystander CPR rates? A population-based observational study in Victoria, Australia. *BMJ open, 6*(11), e012434.

Sun, C. L., Brooks, S. C., Morrison, L. J., & Chan, T. C. (2017). Ranking businesses and municipal locations by spatiotemporal cardiac arrest risk to guide public defibrillator placement. *Circulation, 135*(12), 1104-1119.

Sun, C. L., Demirtas, D., Brooks, S. C., Morrison, L. J., & Chan, T. C. (2016). Overcoming spatial and temporal barriers to public access defibrillators via optimization. *Journal of the American College of Cardiology, 68*(8), 836-845.

Thannhauser, J., Nas, J., Waalewijn, R., van Royen, N., Bonnes, J. L., Brouwer, M. A., & de Boer, M.-J. (2021). Towards individualised treatment of out-of-hospital cardiac arrest patients: an update on technical innovations in the prehospital chain of survival. *Netherlands Heart Journal*, 1-5.

Thorgeirsson, G., Thorgeirsson, G., Sigvaldason, H., & Witteman, J. (2005). Risk factors for out-of-hospital cardiac arrest: the Reykjavik Study. *European heart journal, 26*(15), 1499-1505.

Tsai, E. R., Demirtas, D., Hoogendijk, N., Tintu, A. N., & Boucherie, R. J. (2022). Turnaround time prediction for clinical chemistry samples using machine learning. *Clinical Chemistry and Laboratory Medicine (CCLM), 60*(12), 1902-1910.

Uber, A., Sadler, R. C., Chassee, T., & Reynolds, J. C. (2017). Bystander cardiopulmonary resuscitation is clustered and associated with neighborhood socioeconomic characteristics: a geospatial analysis of Kent County, Michigan. *Academic Emergency Medicine, 24*(8), 930-939.

Valenzuela, T. D., Roe, D. J., Nichol, G., Clark, L. L., Spaite, D. W., & Hardman, R. G. (2000). Outcomes of rapid defibrillation by security officers after cardiac arrest in casinos. *New England journal of medicine, 343*(17), 1206-1209.

van Nieuwenhuizen, B. P., Oving, I., Kunst, A. E., Daams, J., Blom, M. T., Tan, H. L., & van Valkengoed, I. G. (2019). Socio-economic differences in incidence, bystander cardiopulmonary resuscitation and survival from out-of-hospital cardiac arrest: a systematic review. *Resuscitation, 141*, 44-62.

van Nieuwenhuizen, B. P., Tan, H. L., Blom, M. T., Kunst, A. E., & van Valkengoed, I. G. (2023). Association Between Income and Risk of Out-of-Hospital Cardiac Arrest: A Retrospective Cohort Study. *Circulation: Cardiovascular Quality and Outcomes, 16*(2), e009080.

Warden, C., Cudnik, M. T., Sasson, C., Schwartz, G., & Semple, H. (2012). Poisson cluster analysis of cardiac arrest incidence in Columbus, Ohio. *Prehospital Emergency Care, 16*(3), 338-346.

Winkleby, M. A., Jatulis, D. E., Frank, E., & Fortmann, S. P. (1992). Socioeconomic status and health: how education, income, and occupation contribute to risk factors for cardiovascular disease. *American journal of public health, 82*(6), 816-820.

Wong, P. P.-y., Low, C.-T., Cai, W., Leung, K. T.-y., & Lai, P.-C. (2022). A spatiotemporal data mining study to identify high-risk neighborhoods for out-of-hospital cardiac arrest (OHCA) incidents. *Scientific Reports, 12*(1), 1-9.

Xie, J., & Wang, Q. (2018). Benchmark Machine Learning Approaches with Classical Time Series Approaches on the Blood Glucose Level Prediction Challenge. *Khd@ ijcai, 10*.

Zhang, J., Mu, L., Zhang, D., Rajbhandari-Thapa, J., Chen, Z., Pagán, J. A., Li, Y., Son, H., & Liu, J. (2023). Spatiotemporal Optimization for the Placement of Automated External Defibrillators Using Mobile Phone Data. *ISPRS International Journal of Geo-Information, 12*(3), 91.

Zijlstra, J. A., Stieglis, R., Riedijk, F., Smeekes, M., Van der Worp, W. E., & Koster, R. W. (2014). Local lay rescuers with AEDs, alerted by text messages, contribute to early defibrillation in a Dutch out-of-hospital cardiac arrest dispatch system. *Resuscitation, 85*(11), 1444-1449.

9 Appendix

9.1 List with significant features

Table 14. List of significant features

Categories	Significant features
Gender	Male
Age	15-24y
	25-44y
	65y+
Address density	Address density
Ethnicity	Turkish
	Moroccan
Residences	Residence value
Benefits	Unemployment benefits
Businesses	Businesses
Health	Health
	Overweight
	Smoking
Income	Income per income receiver
Households	1-person household
	Household with children

9.2 Feature selections

Table 15. A list of all features, the full and small feature selections used in this research, and a subset of features.

All features (1)	Full selection (2)	Subset (3)	Small selection (4)
Male	Male	Male	Male
15-24y	15-24y	15-24y	15-24y
25-44y	25-44y	25-44y	25-44y
65y+	65y+	65y+	65y+
Address density	Address density	Address density	Address density
Turkish	Turkish	Turkish	
Antillean or Aruban	Antillean or Aruban	Moroccan	
Residence value	Residence value	Residence value	
Unemployment benefits	Unemployment benefits	Unemployment benefits	
Businesses	Businesses	Businesses	
Health	Health	Health	
Overweight	Overweight	Overweight	
Smoking	Smoking	Smoking	
Income per income receiver	Income per income receiver	Income per income receiver	
1-person household	1-person household	1-person household	
Household with children	Household with children	Household with children	
Household size	Household size		
Western	Western		
Moroccan	Moroccan		

Surinamese	Surinamese		
Other non-western	Other non-western		
45-64y	45-64y		
Disability benefits			
Population			
Female			
0-14y			
Unmarried			
Married			
Divorced			
Widowed			
Non-western			
Births			
Deaths			
Households			
Household without children			
Population density			
Residences			
Owner-occupied residences			
Rental residences			
Social residences			
Other rental residences			
Unknown owner residences			
Residences build before 2000			
Residences build from 2000			
Electricity usage			
Electricity usage in apartments			
Electricity usage in terrace houses			
Electricity usage in corner houses			
Electricity usage in semi-detached houses			
Electricity usage in detached houses			
Gas usage			
Gas usage in apartments			
Gas usage in terrace houses			
Gas usage in corner houses			

Gas usage in semi-detached houses			
Gas usage in detached houses			
District heating			
Income receivers			
Income per inhabitant			
Low income			
High income			
Non-active			
Households with low income			
Households with high income			
Households with income below a limit			
Household with income below social minimum			
Passenger cars			
Passenger cars per household			
Passenger cars by area			
Motorcycles			
Area			
Land area			
Disability			
Anxiety			
Loneliness			

Table 16 shows different sets of features. These sets are made based on different criteria:

All features (1): The first set includes the features obtained from CBS data that have a value for each year from 2010 to 2017. It also includes the features from RIVM data that are available for the years 2012 and 2016.

Full selection (2): Features from the first selection are included if they could have a correlation with OHCA risk based on literature and/or experts' opinions. Features are excluded if they could correlate with other features. All the features of this selection were significant in the model created by univariate linear regression (see Section 9.3).

Subset (3): This list contains the features of the full feature selection that were significant in the model created by multivariate linear regression.

Small selection (4): This selection contains a limited amount of features to reduce the chance of overfitting and the amount of required data, and consists of features from subset (3) that were found to be correlated with OHCA risk in the literature.

9.3 Results univariate regression

Table 16. List of features included in the univariate regression model and whether they were significant (p < 0.05).

Feature	Significant
Male	TRUE
15-24y	TRUE
25-44y	TRUE
45-64y	TRUE
65y+	TRUE
Western	TRUE
Moroccan	TRUE
Antillean or Aruban	TRUE
Surinamese	TRUE
Turkish	TRUE
Other non-western	TRUE
One-person households	TRUE
Households with children	TRUE
Household size	TRUE
Income	TRUE
Unemployment benefits	TRUE
Businesses	TRUE
District address density	TRUE
Residence value	TRUE
Health	TRUE
Overweight	TRUE
Smoker	TRUE

9.4 Number of AEDs per year per municipality

This section presents the number of AEDs used in the AED optimization model per year and municipality.

Table 17. Number of AEDs used in the AED optimization model per year per municipality.

Number of AEDs	Alkmaar	Amsterdam	Haarlem	Haarlemmer meer	Zaanstad
2010	40	241	47	35	55
2011	41	225	51	42	44
2012	34	221	56	49	52
2013	38	232	57	38	62
2014	31	297	40	56	59
2015	31	316	71	54	82
2016	40	342	63	66	78
2017	20	339	58	53	63

9.5 Analysis of using percentages or absolute values

This section presents an analysis of using either percentages or absolute values as input data.

The results can be found in Tables 18-23.

Table 18. Performance of the Bayesian ridge regression, linear regression, and decision tree using either absolute values or percentages in the input data.

	Bayesian ridge regression		**Linear regression**		**Decision tree**	
	Absolute values	**Percentages**	**Absolute values**	**Percentages**	**Absolute values**	**Percentages**
MAE	0.283935	0.45107	0.441247	0.460484	0.419683	0.434048
MSE	2.334842	6.245369	7.451612	6.542251	5.358398	4.772795
R^2	0.938632	0.830046	0.804145	0.821967	0.859162	0.870119

Table 19. The coefficient values of the features in the Bayesian ridge and linear regression models using either absolute values or percentages as input.

Model coefficients				
	Bayesian ridge		**Linear regression**	
Feature	**Absolute values**	**Percentages**	**Absolute values**	**Percentages**
Male	9.56E-04	-6.24E-02	1.70E-03	-5.22E-02
15-24y	-2.16E-04	-5.52E-02	-7.55E-04	-1.71E-01
25-44y	-9.83E-05	-6.64E-02	-1.14E-04	-1.90E-01
45-64y	3.11E-04	-1.23E-02	3.23E-04	-7.71E-02
65y+	1.19E-03	5.93E-02	1.10E-03	-8.08E-05
Western	-8.28E-05	-2.40E-02	9.25E-05	-4.76E-02
Moroccan	-1.47E-04	2.26E-02	-2.11E-04	5.19E-02
Antillean or Aruban	3.42E-04	4.39E-02	1.80E-03	2.46E-01
Surinamese	2.74E-04	1.38E-01	-8.18E-05	1.16E-01
Turkish	3.93E-04	2.90E-02	5.08E-04	4.66E-02
Other non-western	1.87E-04	1.17E-01	1.13E-04	1.42E-01

One-person households	1.60E-04	-1.27E-02	5.94E-05	-2.30E-02
Households with children	4.93E-06	1.54E-03	1.02E-04	9.97E-03
Household size	-4.89E-06	-3.27E-03	-1.05E+00	-1.90E+00
Income	-5.27E-05	-4.65E-02	-1.76E-02	-5.98E-02
Unemployment benefits	-2.87E-04	4.52E-04	-2.63E-04	4.15E-04
Businesses	8.02E-04	1.99E-03	7.26E-04	2.08E-03
District address density	2.67E-05	7.94E-05	2.73E-05	7.30E-05
Residence value	-8.35E-07	-1.01E-02	3.31E-01	-2.58E-01
Health	-6.37E-04	3.78E-02	-8.72E-04	1.17E-01
Overweight	-2.24E-04	-3.08E-02	-6.16E-04	-2.98E-02
Smoker	1.24E-04	9.57E-02	-1.91E-04	1.45E-01

Table 10. Correlation matrix of the full feature selection using percentages (first part).

Correlation matrices											
Correlation matrix percentages											
	Male	**15-24y**	**25-44y**	**45-64y**	**65y+**	**Western**	**Moroccan**	**Antillean or Aruban**	**Surinamese**	**Turkish**	**Other non-western**
Male	1	0.283	0.282	0.140	-0.461	0.135	-0.029	-0.002	0.002	-0.040	-0.026
15-24y	0.283	1	0.094	-0.056	-0.367	0.018	0.188	0.252	0.226	0.123	0.242
25-44y	0.282	0.094	1	-0.681	-0.682	0.548	0.416	0.296	0.338	0.352	0.518
45-64y	0.140	-0.056	-0.681	1	0.188	-0.303	-0.426	-0.292	-0.253	-0.412	-0.498
65y+	-0.461	-0.367	-0.682	0.188	1	-0.201	-0.251	-0.186	-0.287	-0.212	-0.282
Western	0.135	0.018	0.548	-0.303	-0.201	1	0.251	0.236	0.234	0.135	0.498
Moroccan	-0.029	0.188	0.416	-0.426	-0.251	0.251	1	0.250	0.422	0.614	0.530
Antillean or Aruban	-0.002	0.252	0.296	-0.292	-0.186	0.236	0.250	1	0.672	0.200	0.641
Surinamese	0.002	0.226	0.338	-0.253	-0.287	0.234	0.422	0.672	1	0.284	0.749
Turkish	-0.040	0.123	0.352	-0.412	-0.212	0.135	0.614	0.200	0.284	1	0.463
Other non-western	-0.026	0.242	0.518	-0.498	-0.282	0.498	0.530	0.641	0.749	0.463	1
One-person households	0.021	0.043	0.245	-0.197	-0.044	0.165	0.078	0.149	0.103	0.106	0.117
Households with children	0.074	0.012	-0.116	0.131	-0.298	-0.440	-0.226	-0.186	-0.155	-0.092	-0.323
Household size	0.060	-0.018	-0.408	0.316	-0.186	-0.653	-0.276	-0.309	-0.261	-0.153	-0.467
Income	-0.148	-0.217	-0.076	0.067	0.057	0.410	-0.210	-0.152	-0.158	-0.277	-0.096
Unemployment benefits	-0.056	0.056	0.198	-0.127	-0.157	0.117	0.203	0.169	0.280	0.103	0.196
Businesses	0.012	0.053	0.319	-0.182	-0.182	0.340	0.230	0.107	0.217	0.067	0.225
District address density	-0.014	0.057	0.139	-0.101	-0.114	0.130	0.212	0.088	0.224	0.054	0.178
Residence value	0.021	-0.091	-0.148	0.269	-0.082	-0.059	-0.245	-0.227	-0.167	-0.234	-0.340
Health	0.281	0.066	-0.052	0.232	-0.259	-0.002	-0.398	-0.337	-0.278	-0.513	-0.424
Overweight	-0.143	-0.033	-0.021	-0.085	0.110	-0.188	0.214	0.240	0.177	0.449	0.255
Smoker	0.167	0.181	0.673	-0.388	-0.410	0.451	0.431	0.437	0.417	0.463	0.555

Table 21. Correlation matrix of the full feature selection using percentages (second part).

	One-person households	Households with children	Household size	Income	Unemployment benefits	Businesses	District address density	Residence value	Health	Overweight	Smoker
Male	0.021	0.074	0.060	-0.148	-0.056	0.012	-0.014	0.021	0.281	-0.143	0.167
15-24y	0.043	0.012	-0.018	-0.217	0.056	0.053	0.057	-0.091	0.066	-0.033	0.181
25-44y	0.245	-0.116	-0.408	-0.076	0.198	0.319	0.139	-0.148	-0.052	-0.021	0.673
45-64y	-0.197	0.131	0.316	0.067	-0.127	-0.182	-0.101	0.269	0.232	-0.085	-0.388
65y+	-0.044	-0.298	-0.186	0.057	-0.157	-0.182	-0.114	-0.082	-0.259	0.110	-0.410
Western	0.165	-0.440	-0.653	0.410	0.117	0.340	0.130	-0.059	-0.002	-0.188	0.451
Moroccan	0.078	-0.226	-0.276	-0.210	0.203	0.230	0.212	-0.245	-0.398	0.214	0.431
Antillean or Aruban	0.149	-0.186	-0.309	-0.152	0.169	0.107	0.088	-0.227	-0.337	0.240	0.437
Surinamese	0.103	-0.155	-0.261	-0.158	0.280	0.217	0.224	-0.167	-0.278	0.177	0.417
Turkish	0.106	-0.092	-0.153	-0.277	0.103	0.067	0.054	-0.234	-0.513	0.449	0.463
Other non-western	0.117	-0.323	-0.467	-0.096	0.196	0.225	0.178	-0.340	-0.424	0.255	0.555
One-person households	1	0.338	-0.371	-0.144	0.311	0.218	0.176	0.005	-0.114	-0.111	0.444
Households with children	0.338	1	0.667	-0.045	0.037	-0.151	-0.038	0.347	0.318	-0.156	-0.183
Household size	-0.371	0.667	1	0.050	-0.146	-0.294	-0.120	0.319	0.408	-0.082	-0.577
Income	-0.144	-0.045	0.050	1	-0.044	0.086	-0.005	0.440	0.524	-0.554	-0.339
Unemployment benefits	0.311	0.037	-0.146	-0.044	1	0.563	0.586	-0.026	0.071	-0.169	0.290
Businesses	0.218	-0.151	-0.294	0.086	0.563	1	0.734	-0.057	0.125	-0.255	0.306
District address density	0.176	-0.038	-0.120	-0.005	0.586	0.734	1	-0.088	0.130	-0.204	0.196
Residence value	0.005	0.347	0.319	0.440	-0.026	-0.057	-0.088	1	0.426	-0.342	-0.249
Health	-0.114	0.318	0.408	0.524	0.071	0.125	0.130	0.426	1	-0.813	-0.490
Overweight	-0.111	-0.156	-0.082	-0.554	-0.169	-0.255	-0.204	-0.342	-0.813	1	0.352
Smoker	0.444	-0.183	-0.577	-0.339	0.290	0.306	0.196	-0.249	-0.490	0.352	1

Table 22. Correlation matrix of the full feature selection using absolute values (first part).

Correlation matrix absolute values											
	Male	15-24y	25-44y	45-64y	65y+	Western	Moroccan	Antillean or Aruban	Surinamese	Turkish	Other non-western
Male	1	0.991	0.981	0.992	0.936	0.943	0.779	0.707	0.690	0.741	0.895
15-24y	0.991	1	0.965	0.983	0.916	0.915	0.815	0.742	0.736	0.776	0.919
25-44y	0.981	0.965	1	0.957	0.885	0.971	0.761	0.674	0.648	0.717	0.868
45-64y	0.992	0.983	0.957	1	0.943	0.924	0.731	0.722	0.700	0.694	0.893
65y+	0.936	0.916	0.885	0.943	1	0.878	0.703	0.614	0.589	0.686	0.808
Western	0.943	0.915	0.971	0.924	0.878	1	0.679	0.605	0.558	0.634	0.805
Moroccan	0.779	0.815	0.761	0.731	0.703	0.679	1	0.457	0.513	0.965	0.695
Antillean or Aruban	0.707	0.742	0.674	0.722	0.614	0.605	0.457	1	0.973	0.428	0.921
Surinamese	0.690	0.736	0.648	0.700	0.589	0.558	0.513	0.973	1	0.476	0.922
Turkish	0.741	0.776	0.717	0.694	0.686	0.634	0.965	0.428	0.476	1	0.660
Other non-western	0.895	0.919	0.868	0.893	0.808	0.805	0.695	0.921	0.922	0.660	1
One-person households	0.945	0.931	0.965	0.924	0.864	0.950	0.723	0.675	0.652	0.682	0.850
Households with children	0.907	0.911	0.851	0.910	0.848	0.766	0.739	0.672	0.684	0.716	0.823
Household size	-0.193	-0.186	-0.233	-0.177	-0.220	-0.279	-0.148	-0.188	-0.149	-0.137	-0.224

Income	-0.028	-0.050	-0.016	-0.025	-0.021	0.058	-0.080	-0.083	-0.083	-0.123	-0.066
Unemployment benefits	0.687	0.685	0.687	0.686	0.604	0.646	0.507	0.570	0.551	0.486	0.639
Businesses	0.858	0.820	0.894	0.845	0.784	0.940	0.553	0.517	0.470	0.501	0.708
District address density	0.856	0.842	0.816	0.860	0.846	0.786	0.641	0.558	0.554	0.599	0.738
Residence value	-0.116	-0.123	-0.106	-0.111	-0.146	-0.089	-0.118	-0.133	-0.112	-0.138	-0.151
Health	0.999	0.991	0.981	0.990	0.934	0.941	0.786	0.706	0.690	0.746	0.894
Overweight	0.950	0.933	0.914	0.956	0.919	0.874	0.673	0.674	0.642	0.658	0.844
Smoker	0.990	0.983	0.982	0.978	0.921	0.954	0.777	0.723	0.706	0.739	0.905

Table 23. Correlation matrix of the full feature selection using absolute values (second part).

	One-person households	**Households with children**	**Household size**	**Income**	**Unemployment benefits**	**Businesses**	**District address density**	**Residence value**	**Health**	**Overweight**	**Smoker**
Male	0.945	0.907	-0.193	-0.028	0.687	0.858	0.856	-0.116	0.999	0.950	0.990
15-24y	0.931	0.911	-0.186	-0.050	0.685	0.820	0.842	-0.123	0.991	0.933	0.983
25-44y	0.965	0.851	-0.233	-0.016	0.687	0.894	0.816	-0.106	0.981	0.914	0.982
45-64y	0.924	0.910	-0.177	-0.025	0.686	0.845	0.860	-0.111	0.990	0.956	0.978
65y+	0.864	0.848	-0.220	-0.021	0.604	0.784	0.846	-0.146	0.934	0.919	0.921
Western	0.950	0.766	-0.279	0.058	0.646	0.940	0.786	-0.089	0.941	0.874	0.954
Moroccan	0.723	0.739	-0.148	-0.080	0.507	0.553	0.641	-0.118	0.786	0.673	0.777
Antillean or Aruban	0.675	0.672	-0.188	-0.083	0.570	0.517	0.558	-0.133	0.706	0.674	0.723
Surinamese	0.652	0.684	-0.149	-0.083	0.551	0.470	0.554	-0.112	0.690	0.642	0.706
Turkish	0.682	0.716	-0.137	-0.123	0.486	0.501	0.599	-0.138	0.746	0.658	0.739
Other non-western	0.850	0.823	-0.224	-0.066	0.639	0.708	0.738	-0.151	0.894	0.844	0.905
One-person households	1	0.851	-0.261	-0.019	0.745	0.877	0.789	-0.093	0.946	0.854	0.966
Households with children	0.851	1	-0.039	-0.060	0.698	0.660	0.804	-0.050	0.908	0.874	0.886
Household size	-0.261	-0.039	1	0.050	-0.146	-0.294	-0.120	0.319	-0.184	-0.187	-0.231
Income	-0.019	-0.060	0.050	1	-0.044	0.086	-0.005	0.440	-0.015	-0.097	-0.039
Unemployment benefits	0.745	0.698	-0.146	-0.044	1	0.563	0.586	-0.026	0.689	0.620	0.717
Businesses	0.877	0.660	-0.294	0.086	0.563	1	0.734	-0.057	0.855	0.781	0.872
District address density	0.789	0.804	-0.120	-0.005	0.586	0.734	1	-0.088	0.855	0.825	0.840
Residence value	-0.093	-0.050	0.319	0.440	-0.026	-0.057	-0.088	1	-0.105	-0.167	-0.119
Health	0.946	0.908	-0.184	-0.015	0.689	0.855	0.855	-0.105	1	0.937	0.987
Overweight	0.854	0.874	-0.187	-0.097	0.620	0.781	0.825	-0.167	0.937	1	0.930
Smoker	0.966	0.886	-0.231	-0.039	0.717	0.872	0.840	-0.119	0.987	0.930	1

9.6 Analysis prediction per neighbourhood versus divided by population

This second presents the results of the analysis between predicting per neighbourhood and dividing the predictions per district across the neighbourhoods by population (Tables 24-29).

Results Zaanstad

Table 24. Average (Avg) coverage and standard deviation (Std) on the test set and coverage on the training set are presented for the current AED locations, relocation or addition of AEDs, when predicting per neighbourhood in Zaanstad.

Prediction (NBH)			
	Avg coverage	*Std coverage*	**Training coverage**
Current coverage	37.90	27.46	
Relocation	48.55	24.74	53.95
Add 20	47.91	24.00	46.63
Add 40	51.94	23.21	52.55
Add 80	57.24	21.90	59.73
Add 160	63.49	20.26	67.15
Add 320	69.96	18.23	74.44

Table 25. Average (Avg) coverage and standard deviation (Std) on the test set and coverage on the training set are presented for the current AED locations, relocation or addition of AEDs, when predicting per district and subsequently divide the predictions across the neighbourhoods based on population in Zaanstad.

Prediction (NBH population)			
	Avg coverage	*Std coverage*	**Training coverage**
Current coverage	37.90	27.46	
Relocation	48.71	24.43	54.18
Add 20	47.30	24.30	46.49
Add 40	51.53	23.16	52.68
Add 80	57.07	21.80	59.81
Add 160	63.46	20.09	67.34
Add 320	70.15	18.16	74.49

Table 26. Average (Avg) coverage and standard deviation (Std) on the test set and coverage on the training set are presented for the current AED locations, relocation or addition of AEDs, when predicting per district in Zaanstad.

Prediction (district)			
	Avg coverage	*Std coverage*	**Training coverage**
Current coverage	37.90	27.46	27.50
Relocation	43.85	25.66	48.91
Add 20	46.28	24.49	41.75
Add 40	49.62	23.87	47.49
Add 80	54.75	22.23	54.71
Add 160	60.67	20.50	62.77

Add 320	67.54	17.85	71.16

Results Amsterdam

Table 27. Average (Avg) coverage and standard deviation (Std) on the test set and coverage on the training set are presented for the current AED locations, relocation or addition of AEDs, when predicting per neighbourhood in Amsterdam.

Prediction (NBH)			
	Avg coverage	*Std coverage*	**Training coverage**
Current coverage	38.68	*26.83*	
Relocation	48.94	*26.31*	65.09
Add 20	41.62	*26.39*	50.18
Add 40	43.72	*26.36*	53.45
Add 80	47.14	*25.87*	58.00
Add 160	51.89	*25.14*	63.83
Add 320	57.57	*24.58*	70.27

Table 28. Average (Avg) coverage and standard deviation (Std) on the test set and coverage on the training set are presented for the current AED locations, relocation or addition of AEDs, when predicting per district and subsequently divide the predictions across the neighbourhoods based on population in Amsterdam.

Prediction (NBH population)			
	Avg coverage	*Std coverage*	**Training coverage**
Current coverage	38.68	*26.83*	
Relocation	47.71	*27.01*	70.04
Add 20	41.15	*26.75*	55.79
Add 40	43.17	*26.56*	58.85
Add 80	46.33	*26.16*	62.99
Add 160	50.86	*25.83*	68.34
Add 320	56.82	*25.00*	73.86

Table 29. Average (Avg) coverage and standard deviation (Std) on the test set and coverage on the training set are presented for the current AED locations, relocation or addition of AEDs, when predicting per district in Amsterdam.

Prediction (district)			
	Avg coverage	*Std coverage*	**Training coverage**
Current coverage	38.68	*26.83*	44.86
Relocation	45.82	*27.17*	70.47
Add 20	40.88	*27.12*	54.81
Add 40	42.53	*27.03*	58.16
Add 80	45.63	*26.54*	62.45
Add 160	49.88	*25.94*	67.85
Add 320	56.03	*24.66*	73.92

9.7 Parameter tuning

9.7.1 Amsterdam

Table 30. Model parameter tuning results for Amsterdam using the full feature selection. Best values for the parameters, Epsilon and Alpha, are in bold.

	Average metric values per coefficient value							
	MAE	**MSE**	**MSLE**	**R^2**	**ExpVar**	**MaxError**	**Epsilon**	**Alpha**
Mean	1.327	3.313	0.252	0.499	0.510	7.473	1	0.0001
Mean	1.326	3.292	0.252	0.501	0.512	7.448	1	0.001
Mean	1.325	3.295	0.251	0.501	0.512	7.452	1	0.01
Mean	1.325	3.300	0.252	0.501	0.512	7.470	1	0.1
Mean	1.328	3.314	0.252	0.499	0.510	7.478	1	1
Mean	1.330	3.317	0.252	0.500	0.510	7.509	1.5	0.0001
Mean	1.324	3.288	0.251	0.503	0.512	7.510	**1.5**	**0.001**
Mean	1.327	3.298	0.251	0.501	0.511	7.478	1.5	0.01
Mean	1.329	3.315	0.251	0.499	0.509	7.539	1.5	0.1
Mean	1.327	3.302	0.251	0.501	0.510	7.533	1.5	1
Mean	1.330	3.310	0.251	0.499	0.508	7.559	2	0.0001
Mean	1.328	3.310	0.251	0.500	0.509	7.595	2	0.001
Mean	1.331	3.315	0.251	0.498	0.506	7.578	2	0.01
Mean	1.329	3.306	0.251	0.500	0.509	7.632	2	0.1
Mean	1.326	3.294	0.251	0.501	0.509	7.576	2	1
Mean	1.331	3.327	0.252	0.498	0.505	7.585	2.5	0.0001
Mean	1.330	3.316	0.252	0.499	0.507	7.569	2.5	0.001
Mean	1.330	3.313	0.252	0.499	0.507	7.532	2.5	0.01
Mean	1.328	3.307	0.252	0.499	0.507	7.599	2.5	0.1
Mean	1.327	3.301	0.252	0.500	0.508	7.585	2.5	1

Table 31. Model parameter tuning results for Amsterdam using the small feature selection. Best values for the parameters, Epsilon and Alpha, are in bold.

	Average metric values per coefficient value							
	MAE	**MSE**	**MSLE**	**R^2**	**ExpVar**	**MaxError**	**Epsilon**	**Alpha**
Mean	1.306	3.222	0.247	0.508	0.520	7.486	1	0.0001
Mean	1.307	3.221	0.247	0.508	0.520	7.475	1	0.001
Mean	1.306	3.218	0.247	0.508	0.521	7.472	1	0.01
Mean	1.308	3.224	0.247	0.507	0.519	7.474	1	0.1
Mean	1.308	3.226	0.248	0.507	0.520	7.497	1	1
Mean	1.309	3.205	0.249	0.510	0.521	7.322	1.5	0.0001
Mean	1.309	3.205	0.249	0.510	0.521	7.322	1.5	0.001
Mean	1.309	3.205	0.249	0.510	0.521	7.322	1.5	0.01
Mean	1.309	3.205	0.249	0.510	0.521	7.322	1.5	0.1
Mean	1.309	3.205	0.249	0.510	0.521	7.322	1.5	1
Mean	1.308	3.172	0.248	0.513	0.522	7.317	2	0.0001
Mean	1.308	3.173	0.248	0.513	0.522	7.318	2	0.001
Mean	1.308	3.173	0.249	0.513	0.522	7.317	2	0.01

Mean	1.307	3.170	0.248	0.514	0.522	7.312	**2**	**0.1**
Mean	1.307	3.170	0.248	0.514	0.522	7.312	2	1
Mean	1.309	3.176	0.248	0.512	0.521	7.304	2.5	0.0001
Mean	1.309	3.176	0.248	0.512	0.521	7.304	2.5	0.001
Mean	1.309	3.176	0.248	0.512	0.521	7.304	2.5	0.01
Mean	1.309	3.176	0.248	0.512	0.521	7.304	2.5	0.1
Mean	1.309	3.176	0.248	0.512	0.521	7.304	2.5	1

9.7.2 Zaanstad

Table 32. Model parameter tuning results for Zaanstad using the full feature selection. Best values for the parameters, Epsilon and Alpha, are in bold.

	Average metric values per coefficient value							
	MAE	**MSE**	**MSLE**	**R^2**	**ExpVar**	**MaxError**	**Epsilon**	**Alpha**
Mean	1.460	5.392	0.236	0.602	0.611	9.997	1	0.0001
Mean	1.455	5.343	0.236	0.603	0.613	10.063	**1**	**0.001**
Mean	1.463	5.438	0.237	0.602	0.610	10.633	1	0.01
Mean	1.468	5.623	0.236	0.602	0.611	10.648	1	0.1
Mean	1.457	5.329	0.237	0.602	0.611	10.028	1	1
Mean	1.458	5.493	0.238	0.602	0.611	10.101	1.5	0.0001
Mean	1.464	5.593	0.238	0.603	0.611	9.982	1.5	0.001
Mean	1.468	5.741	0.238	0.600	0.609	10.146	1.5	0.01
Mean	1.467	5.687	0.238	0.600	0.609	10.180	1.5	0.1
Mean	1.467	5.722	0.237	0.599	0.608	10.269	1.5	1
Mean	1.469	5.682	0.239	0.598	0.606	10.220	2	0.0001
Mean	1.465	5.591	0.239	0.599	0.608	10.173	2	0.001
Mean	1.465	5.588	0.238	0.599	0.608	10.074	2	0.01
Mean	1.464	5.540	0.238	0.599	0.608	10.257	2	0.1
Mean	1.480	5.933	0.239	0.595	0.604	10.986	2	1
Mean	1.486	5.968	0.239	0.595	0.603	11.063	2.5	0.0001
Mean	1.485	5.918	0.238	0.595	0.604	10.796	2.5	0.001
Mean	1.478	5.703	0.237	0.598	0.606	10.598	2.5	0.01
Mean	1.467	5.421	0.238	0.598	0.606	9.764	2.5	0.1
Mean	1.479	5.754	0.238	0.595	0.604	10.587	2.5	1

Table 33. Model parameter tuning results for Zaanstad using the small feature selection. Best values for the parameters, Epsilon and Alpha, are in bold.

	Average metric values per coefficient value							
	MAE	**MSE**	**MSLE**	**R^2**	**ExpVar**	**MaxError**	**Epsilon**	**Alpha**
Mean	1.569	7.328	0.246	0.582	0.588	11.362	1	0.0001
Mean	1.569	7.369	0.245	0.582	0.588	11.357	1	0.001
Mean	1.570	7.351	0.244	0.582	0.588	11.343	1	0.01
Mean	1.571	7.345	0.246	0.581	0.588	11.343	1	0.1
Mean	1.568	7.324	0.245	0.583	0.589	11.365	1	1
Mean	1.554	6.962	0.245	0.584	0.589	11.064	1.5	0.0001
Mean	1.554	6.962	0.245	0.584	0.589	11.064	1.5	0.001

Mean	1.554	6.962	0.245	0.584	0.589	11.064	1.5	0.01
Mean	1.554	6.962	0.245	0.584	0.589	11.064	**1.5**	**0.1**
Mean	1.554	6.962	0.245	0.584	0.589	11.064	1.5	1
Mean	1.553	6.868	0.247	0.583	0.588	10.830	2	0.0001
Mean	1.553	6.868	0.247	0.583	0.588	10.830	2	0.001
Mean	1.553	6.868	0.247	0.583	0.588	10.830	2	0.01
Mean	1.553	6.868	0.247	0.583	0.588	10.830	2	0.1
Mean	1.553	6.868	0.247	0.583	0.588	10.830	2	1
Mean	1.553	6.832	0.248	0.581	0.586	10.777	2.5	0.0001
Mean	1.553	6.832	0.248	0.581	0.586	10.777	2.5	0.001
Mean	1.553	6.832	0.248	0.581	0.586	10.777	2.5	0.01
Mean	1.553	6.832	0.248	0.581	0.586	10.777	2.5	0.1
Mean	1.553	6.832	0.248	0.581	0.586	10.777	2.5	1

9.7.3 Haarlem

Table 34. Model parameter tuning results for Haarlem using the full feature selection. Best values for the parameters, Epsilon and Alpha, are in bold.

	Average metric values per coefficient value							
	MAE	MSE	MSLE	R^2	ExpVar	MaxError	Epsilon	Alpha
Mean	1.595	10.047	0.258	0.525	0.535	14.146	1	0.0001
Mean	1.585	9.790	0.253	0.528	0.537	13.740	1	0.001
Mean	1.566	8.750	0.247	0.536	0.544	12.933	**1**	**0.01**
Mean	1.577	9.447	0.251	0.529	0.539	13.611	1	0.1
Mean	1.570	8.897	0.247	0.535	0.544	12.933	1	1
Mean	1.572	9.089	0.247	0.534	0.543	12.859	1.5	0.0001
Mean	1.570	9.092	0.248	0.532	0.541	12.884	1.5	0.001
Mean	1.582	9.381	0.249	0.531	0.540	13.247	1.5	0.01
Mean	1.590	9.605	0.250	0.528	0.538	13.411	1.5	0.1
Mean	1.570	9.104	0.247	0.534	0.543	13.151	1.5	1
Mean	1.573	8.888	0.246	0.535	0.544	12.415	2	0.0001
Mean	1.571	9.005	0.246	0.532	0.542	12.822	2	0.001
Mean	1.568	9.064	0.247	0.532	0.542	12.698	2	0.01
Mean	1.567	9.006	0.247	0.532	0.543	12.985	2	0.1
Mean	1.578	9.321	0.248	0.530	0.539	12.869	2	1
Mean	1.596	9.976	0.251	0.525	0.534	13.339	2.5	0.0001
Mean	1.613	10.481	0.255	0.521	0.530	13.782	2.5	0.001
Mean	1.622	10.780	0.256	0.520	0.528	13.768	2.5	0.01
Mean	1.580	9.619	0.249	0.531	0.538	12.974	2.5	0.1
Mean	1.577	9.593	0.249	0.530	0.538	13.047	2.5	1

Table 35. Model parameter tuning results for Haarlem using the small feature selection. Best values for the parameters, Epsilon and Alpha, are in bold.

	Average metric values per coefficient value							
	MAE	MSE	MSLE	R^2	ExpVar	MaxError	Epsilon	Alpha
Mean	1.542	6.581	0.251	0.544	0.555	10.515	1	0.0001

	MAE	MSE	MSLE	R^2	ExpVar	MaxError	Epsilon	Alpha
Mean	1.540	6.561	0.250	0.545	0.556	10.551	1	0.001
Mean	1.541	6.570	0.250	0.544	0.555	10.526	1	0.01
Mean	1.540	6.559	0.250	0.545	0.556	10.514	**1**	**0.1**
Mean	1.541	6.577	0.250	0.545	0.555	10.550	1	1
Mean	1.561	7.377	0.250	0.538	0.546	10.987	1.5	0.0001
Mean	1.561	7.377	0.250	0.538	0.546	10.987	1.5	0.001
Mean	1.561	7.377	0.250	0.538	0.546	10.987	1.5	0.01
Mean	1.561	7.377	0.250	0.538	0.546	10.987	1.5	0.1
Mean	1.561	7.373	0.252	0.539	0.546	10.981	1.5	1
Mean	1.565	7.452	0.252	0.537	0.545	11.069	2	0.0001
Mean	1.565	7.452	0.252	0.537	0.545	11.069	2	0.001
Mean	1.565	7.452	0.252	0.537	0.545	11.069	2	0.01
Mean	1.565	7.452	0.252	0.537	0.545	11.069	2	0.1
Mean	1.563	7.336	0.252	0.538	0.546	10.913	2	1
Mean	1.574	7.535	0.255	0.532	0.541	11.191	2.5	0.0001
Mean	1.574	7.535	0.255	0.532	0.541	11.191	2.5	0.001
Mean	1.574	7.535	0.255	0.532	0.541	11.191	2.5	0.01
Mean	1.574	7.535	0.255	0.532	0.541	11.191	2.5	0.1
Mean	1.574	7.535	0.255	0.532	0.541	11.191	2.5	1

9.7.4 Haarlemmermeer

Table 36. Model parameter tuning results for Haarlemmermeer using the full feature selection. Best values for the parameters, Epsilon and Alpha, are in bold.

	Average metric values per coefficient value							
	MAE	**MSE**	**MSLE**	**R^2**	**ExpVar**	**MaxError**	**Epsilon**	**Alpha**
Mean	1.509	6.106	0.243	0.528	0.543	12.149	1	0.0001
Mean	1.507	5.988	0.244	0.529	0.543	12.025	1	0.001
Mean	1.506	5.960	0.243	0.530	0.544	11.814	**1**	**0.01**
Mean	1.513	6.214	0.244	0.527	0.542	12.401	1	0.1
Mean	1.512	6.170	0.243	0.528	0.542	12.135	1	1
Mean	1.520	6.447	0.244	0.525	0.539	11.359	1.5	0.0001
Mean	1.526	6.649	0.245	0.522	0.536	11.679	1.5	0.001
Mean	1.524	6.595	0.244	0.522	0.536	11.749	1.5	0.01
Mean	1.514	6.336	0.244	0.525	0.539	11.481	1.5	0.1
Mean	1.524	6.593	0.244	0.523	0.538	11.731	1.5	1
Mean	1.567	7.387	0.246	0.515	0.529	11.938	2	0.0001
Mean	1.567	7.400	0.246	0.514	0.528	11.957	2	0.001
Mean	1.568	7.421	0.245	0.515	0.530	11.955	2	0.01
Mean	1.571	7.504	0.246	0.514	0.529	12.121	2	0.1
Mean	1.582	7.780	0.246	0.511	0.526	12.081	2	1
Mean	1.530	6.565	0.245	0.520	0.533	11.046	2.5	0.0001
Mean	1.536	6.719	0.245	0.521	0.534	11.126	2.5	0.001
Mean	1.553	7.013	0.246	0.518	0.531	11.137	2.5	0.01
Mean	1.549	6.920	0.246	0.518	0.531	11.146	2.5	0.1
Mean	1.560	7.180	0.246	0.516	0.529	11.312	2.5	1

Table 37. Model parameter tuning results for Haarlemmermeer using the small feature selection. Best values for the parameters, Epsilon and Alpha, are in bold.

	Average metric values per coefficient value							
	MAE	MSE	MSLE	R^2	ExpVar	MaxError	Epsilon	Alpha
Mean	1.571	7.058	0.250	0.518	0.529	11.283	1	0.0001
Mean	1.572	7.064	0.250	0.518	0.530	11.275	1	0.001
Mean	1.571	7.058	0.251	0.519	0.530	11.283	**1**	**0.01**
Mean	1.572	7.062	0.250	0.518	0.529	11.281	1	0.1
Mean	1.572	7.064	0.250	0.518	0.530	11.285	1	1
Mean	1.576	7.094	0.252	0.516	0.527	11.263	1.5	0.0001
Mean	1.576	7.094	0.252	0.516	0.527	11.263	1.5	0.001
Mean	1.576	7.094	0.252	0.516	0.527	11.263	1.5	0.01
Mean	1.576	7.094	0.252	0.516	0.527	11.263	1.5	0.1
Mean	1.576	7.094	0.252	0.516	0.527	11.263	1.5	1
Mean	1.585	7.132	0.258	0.512	0.523	11.285	2	0.0001
Mean	1.585	7.132	0.258	0.512	0.523	11.285	2	0.001
Mean	1.585	7.132	0.258	0.512	0.523	11.285	2	0.01
Mean	1.585	7.132	0.258	0.512	0.523	11.285	2	0.1
Mean	1.585	7.132	0.258	0.512	0.523	11.285	2	1
Mean	1.589	7.120	0.259	0.509	0.520	11.263	2.5	0.0001
Mean	1.589	7.120	0.259	0.509	0.520	11.263	2.5	0.001
Mean	1.589	7.121	0.259	0.509	0.520	11.263	2.5	0.01
Mean	1.589	7.121	0.259	0.509	0.520	11.263	2.5	0.1
Mean	1.589	7.120	0.259	0.509	0.520	11.263	2.5	1

9.7.5 Alkmaar

Table 38. Model parameter tuning results for Alkmaar using the full feature selection. Best values for the parameters, Epsilon and Alpha, are in bold.

	Average metric values per coefficient value							
	MAE	MSE	MSLE	R^2	ExpVar	MaxError	Epsilon	Alpha
Mean	1.477	5.368	0.250	0.555	0.564	10.088	1	0.0001
Mean	1.473	5.320	0.249	0.555	0.564	10.075	1	0.001
Mean	1.477	5.317	0.250	0.554	0.563	10.033	1	0.01
Mean	1.471	5.270	0.249	0.556	0.565	10.056	**1**	**0.1**
Mean	1.489	5.584	0.250	0.552	0.562	9.863	1	1
Mean	1.493	5.675	0.250	0.550	0.559	9.965	1.5	0.0001
Mean	1.492	5.649	0.250	0.551	0.560	9.947	1.5	0.001
Mean	1.479	5.427	0.249	0.553	0.562	9.958	1.5	0.01
Mean	1.480	5.415	0.250	0.552	0.561	9.867	1.5	0.1
Mean	1.490	5.644	0.250	0.551	0.560	10.015	1.5	1
Mean	1.475	5.384	0.250	0.553	0.561	9.893	2	0.0001
Mean	1.475	5.336	0.250	0.553	0.562	9.845	2	0.001
Mean	1.481	5.499	0.250	0.552	0.560	9.957	2	0.01
Mean	1.472	5.319	0.250	0.552	0.560	10.083	2	0.1
Mean	1.483	5.568	0.250	0.552	0.560	9.926	2	1
Mean	1.467	5.212	0.250	0.552	0.560	9.998	2.5	0.0001

Mean	1.476	5.406	0.250	0.551	0.559	9.968	2.5	0.001
Mean	1.469	5.221	0.250	0.552	0.560	9.956	2.5	0.01
Mean	1.479	5.461	0.250	0.550	0.558	10.012	2.5	0.1
Mean	1.479	5.433	0.250	0.549	0.557	9.777	2.5	1

Table 39. Model parameter tuning results for Alkmaar using the small feature selection. Best values for the parameters, Epsilon and Alpha, are in bold.

	Average metric values per coefficient value							
	MAE	**MSE**	**MSLE**	**R^2**	**ExpVar**	**MaxError**	**Epsilon**	**Alpha**
Mean	1.542	6.208	0.255	0.539	0.549	11.179	1	0.0001
Mean	1.539	6.178	0.253	0.540	0.549	11.169	1	0.001
Mean	1.538	6.168	0.254	0.540	0.551	11.142	**1**	**0.01**
Mean	1.540	6.177	0.254	0.539	0.549	11.167	1	0.1
Mean	1.546	6.299	0.256	0.538	0.548	11.163	1	1
Mean	1.546	6.288	0.256	0.536	0.546	11.013	1.5	0.0001
Mean	1.546	6.288	0.256	0.536	0.546	11.013	1.5	0.001
Mean	1.546	6.288	0.256	0.536	0.546	11.013	1.5	0.01
Mean	1.546	6.288	0.256	0.536	0.546	11.013	1.5	0.1
Mean	1.546	6.288	0.256	0.536	0.546	11.013	1.5	1
Mean	1.548	6.160	0.259	0.534	0.543	10.945	2	0.0001
Mean	1.548	6.160	0.259	0.534	0.543	10.945	2	0.001
Mean	1.547	6.156	0.259	0.534	0.543	10.938	2	0.01
Mean	1.548	6.157	0.259	0.534	0.544	10.939	2	0.1
Mean	1.547	6.156	0.259	0.534	0.543	10.939	2	1
Mean	1.552	6.194	0.260	0.531	0.540	10.956	2.5	0.0001
Mean	1.552	6.194	0.260	0.531	0.540	10.956	2.5	0.001
Mean	1.552	6.194	0.260	0.531	0.540	10.956	2.5	0.01
Mean	1.552	6.194	0.260	0.531	0.540	10.956	2.5	0.1
Mean	1.552	6.194	0.260	0.531	0.540	10.956	2.5	1

9.8 KDE bandwidths

Table 40. KDE bandwidths used per municipality, year, and method.

Mun	Year excluded	Bandwidths		
		Bootstrap	Likelihood	Least-squares
Amsterdam	2010	712	284	79
Alkmaar	2010	591	328	157
Haarlem	2010	537	226	163
Haarlemmermeer	2010	1035	402	182
Zaanstad	2010	653	330	139
Amsterdam	2011	709	235	63
Alkmaar	2011	556	319	122
Haarlem	2011	542	187	147
Haarlemmermeer	2011	1030	410	189
Zaanstad	2011	652	308	167
Amsterdam	2012	714	286	79
Alkmaar	2012	573	310	113
Haarlem	2012	541	194	172
Haarlemmermeer	2012	1026	417	205
Zaanstad	2012	654	277	173
Amsterdam	2013	702	283	79
Alkmaar	2013	578	317	90
Haarlem	2013	538	206	141
Haarlemmermeer	2013	1023	436	185
Zaanstad	2013	658	279	136
Amsterdam	2014	716	294	79
Alkmaar	2014	551	311	69
Haarlem	2014	541	217	138
Haarlemmermeer	2014	1033	464	217
Zaanstad	2014	650	312	155
Amsterdam	2015	721	292	79
Alkmaar	2015	556	254	103
Haarlem	2015	553	182	164
Haarlemmermeer	2015	1062	436	230
Zaanstad	2015	668	321	124
Amsterdam	2016	730	307	79
Alkmaar	2016	574	292	123
Haarlem	2016	554	181	143
Haarlemmermeer	2016	1039	454	178
Zaanstad	2016	659	338	172
Amsterdam	2017	723	303	79
Alkmaar	2017	559	289	68
Haarlem	2017	554	183	143
Haarlemmermeer	2017	1049	415	167
Zaanstad	2017	659	301	147

9.9 OHCA incidence proportions per district

In this section, histograms are presented visualizing the OHCA incidence proportions per district. These proportions are calculated by dividing the incidence of each district by the total (predicted) incidence in the municipality. Results are shown for the predictions using the full or small feature selection and for the real OHCA incidence, for each year.

9.9.1 OHCA incidence proportions Amsterdam

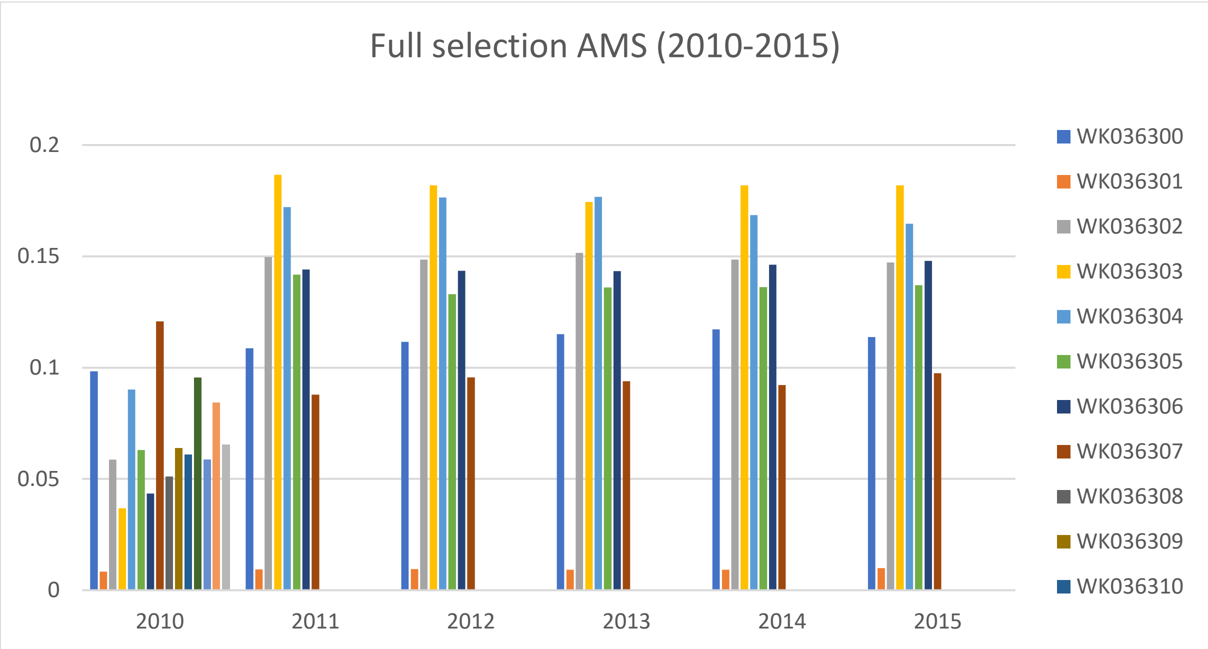

Figure 14. Histogram visualizing the proportional estimated OHCA incidence of each district of Amsterdam per year (2010-2015) using the full feature selection.

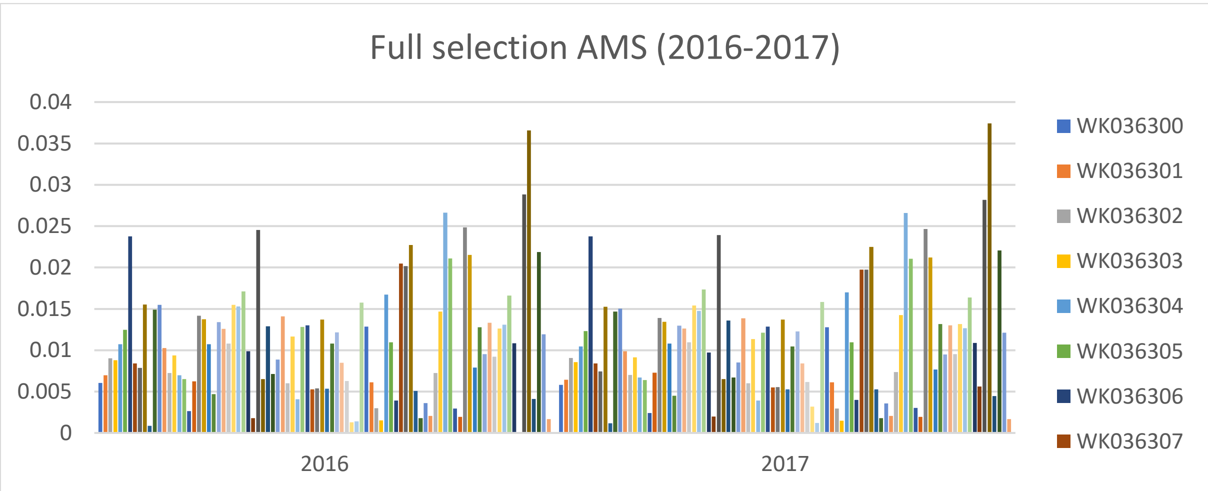

Figure 15. Histogram visualizing the proportional estimated OHCA incidence of each district of Amsterdam per year (2016-2017) using the full feature selection.

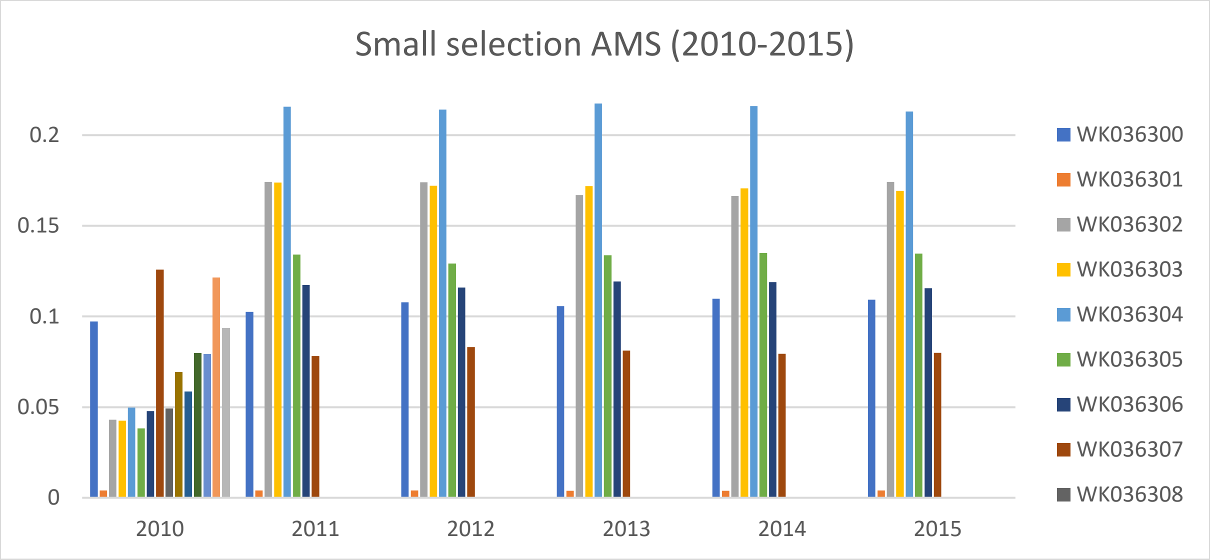

Figure 16. Histogram visualizing the proportional estimated OHCA incidence of each district of Amsterdam per year (2010-2015) using the small feature selection.

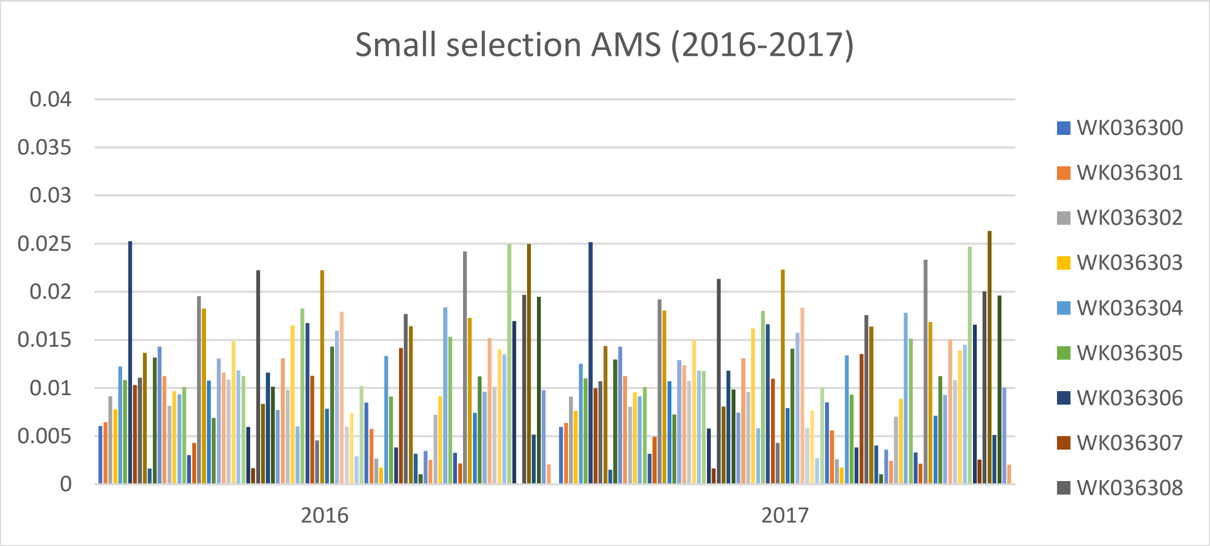

Figure 17. Histogram visualizing the proportional estimated OHCA incidence of each district of Amsterdam per year (2016-2017) using the small feature selection.

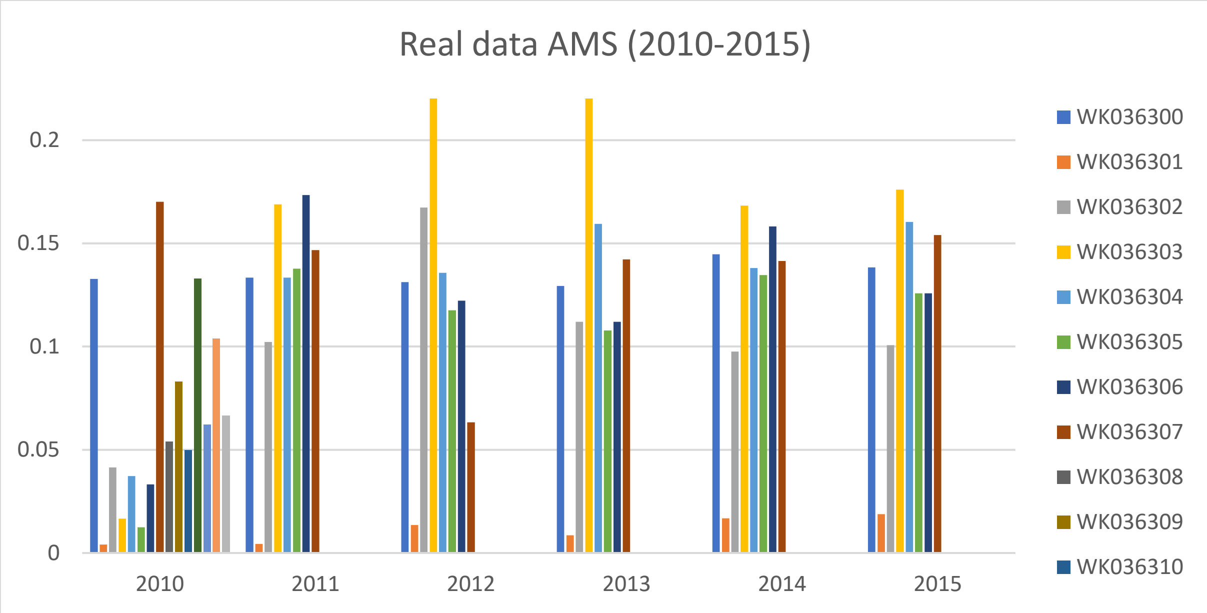

Figure 18. Histogram visualizing the proportional true OHCA incidence of each district of Amsterdam per year (2010-2015).

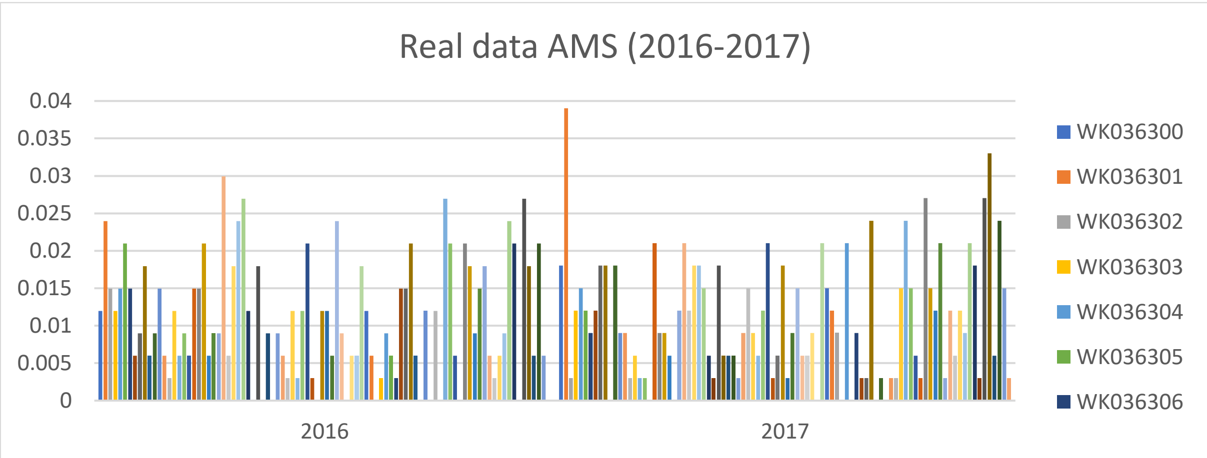

Figure 19. Histogram visualizing the proportional true OHCA incidence of each district of Amsterdam per year (2016-2017).

9.9.2 OHCA incidence proportions Zaanstad

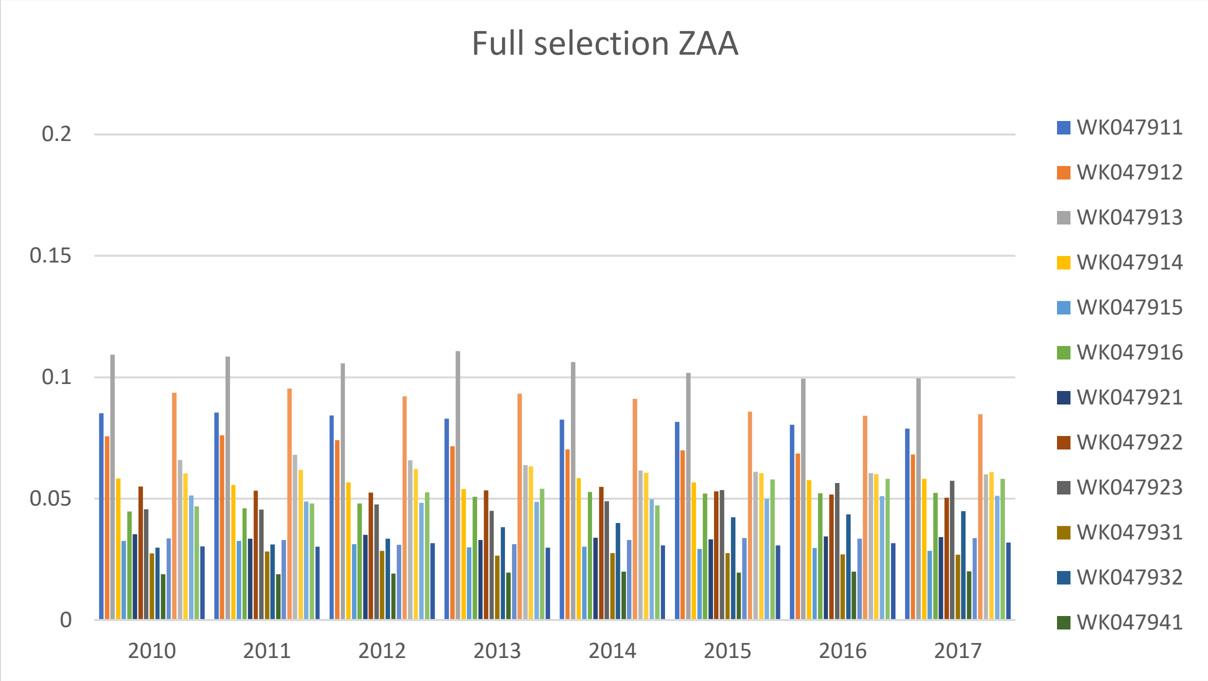

Figure 20. Histogram visualizing the proportional estimated OHCA incidence of each district of Zaanstad per year using the full feature selection.

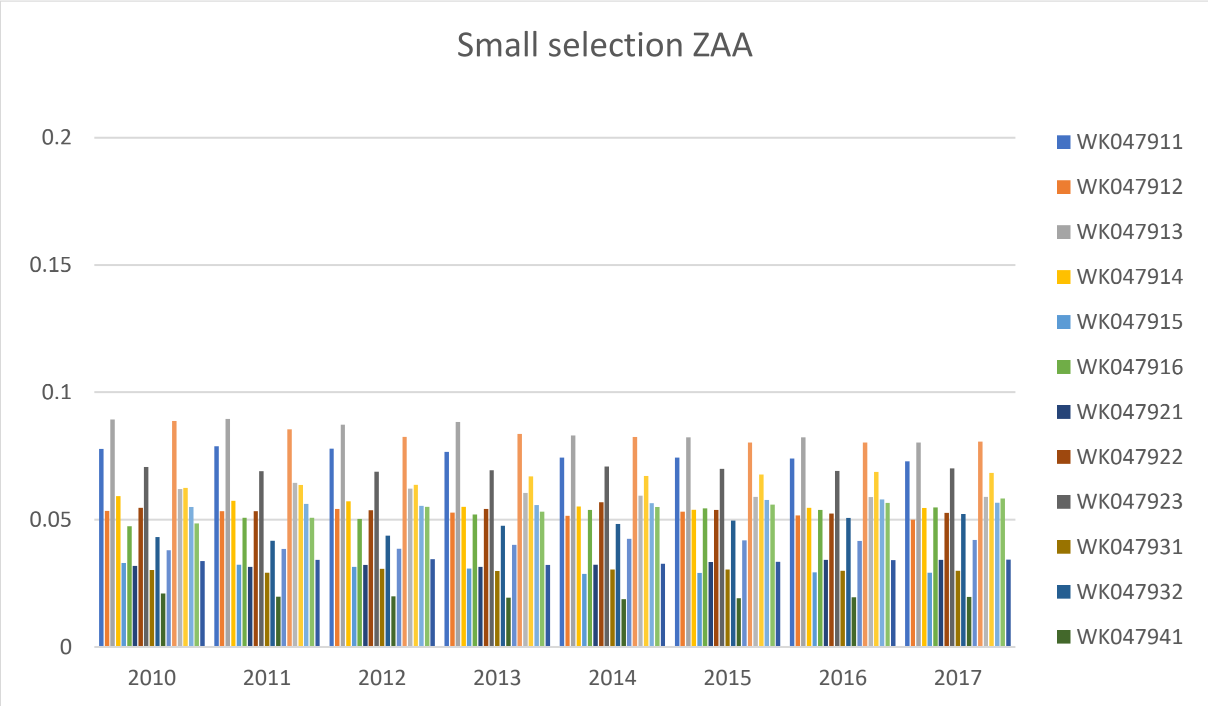

Figure 21. Histogram visualizing the proportional estimated OHCA incidence of each district of Zaanstad per year using the small feature selection.

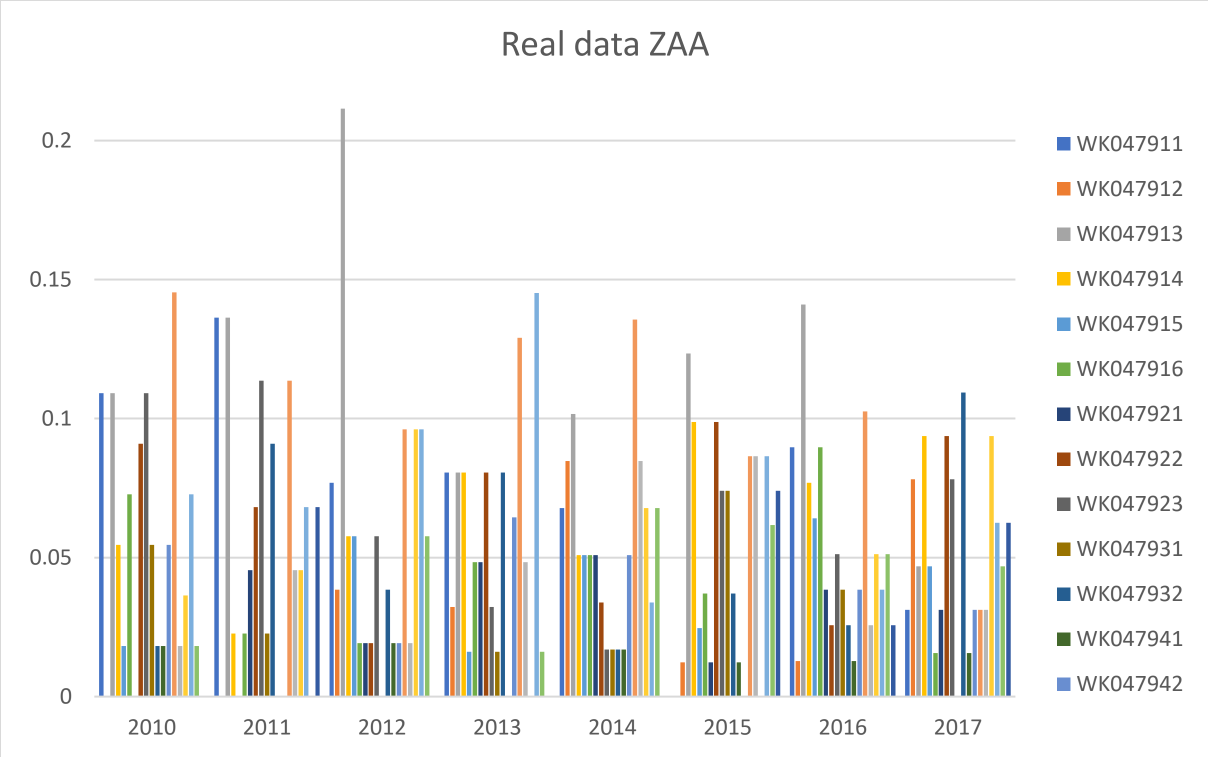

Figure 22. Histogram visualizing the proportional true OHCA incidence of each district of Zaanstad per year.

9.9.3 OHCA risk proportions Haarlem

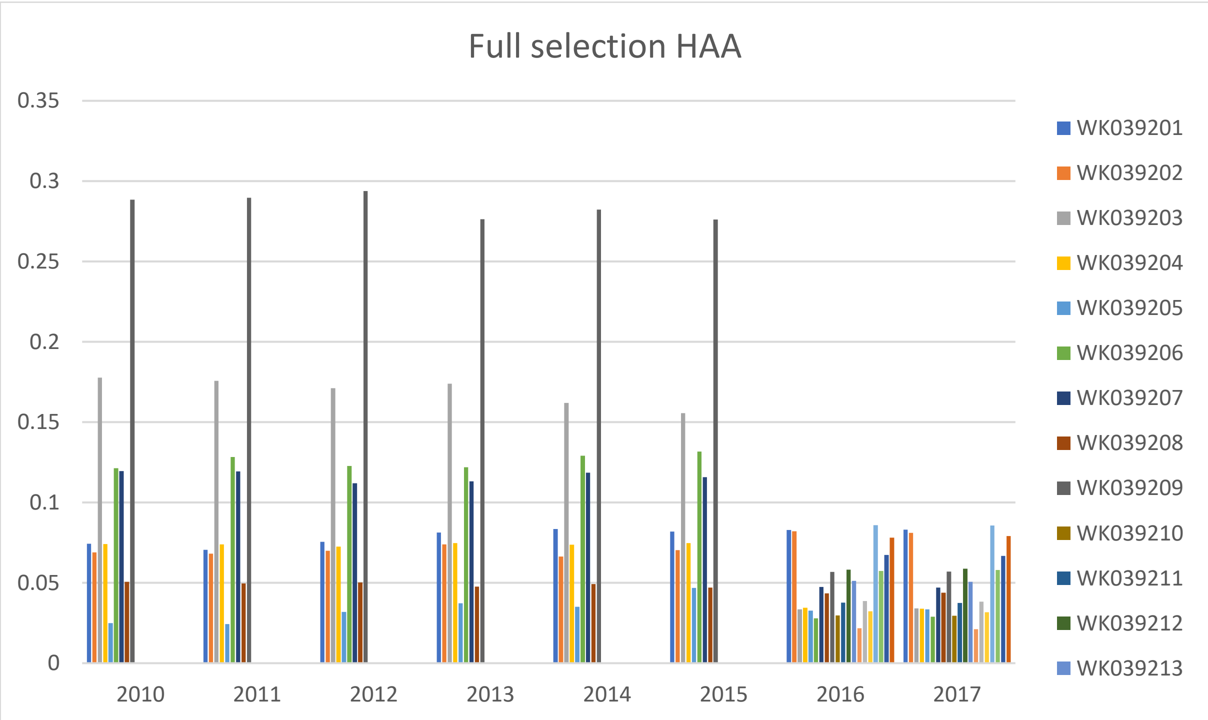

Figure 23. Histogram visualizing the proportional estimated OHCA incidence of each district of Haarlem per year using the full feature selection.

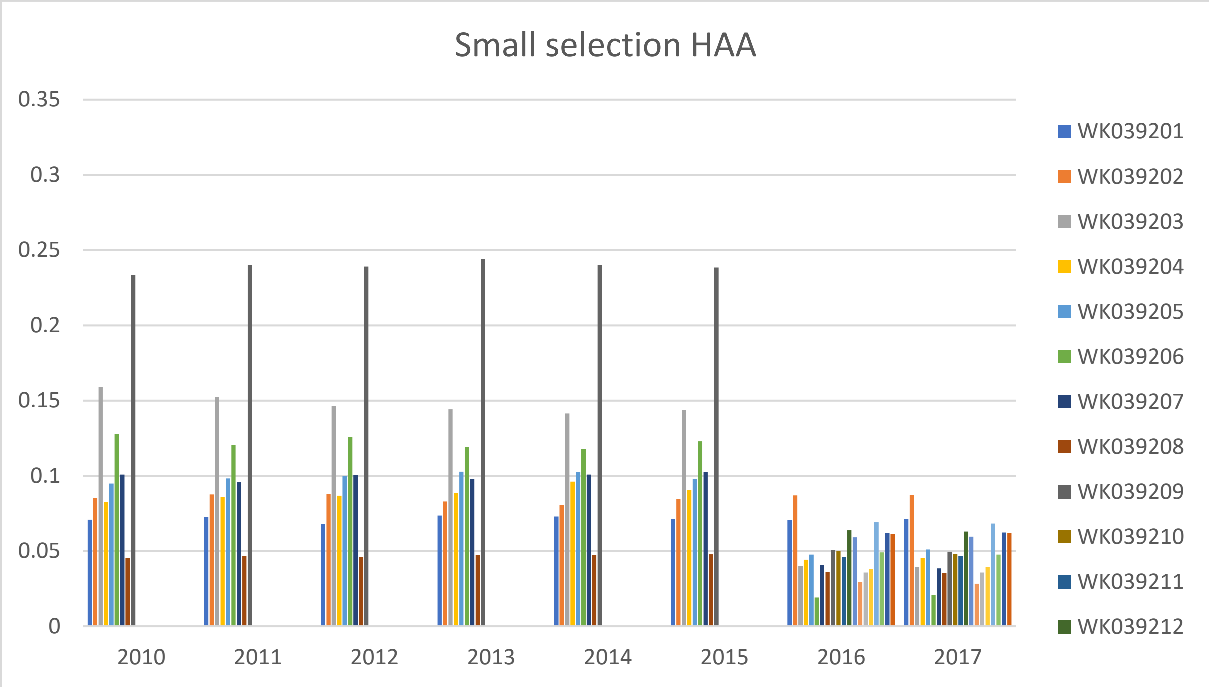

Figure 24. Histogram visualizing the proportional estimated OHCA incidence of each district of Haarlem per year using the small feature selection.

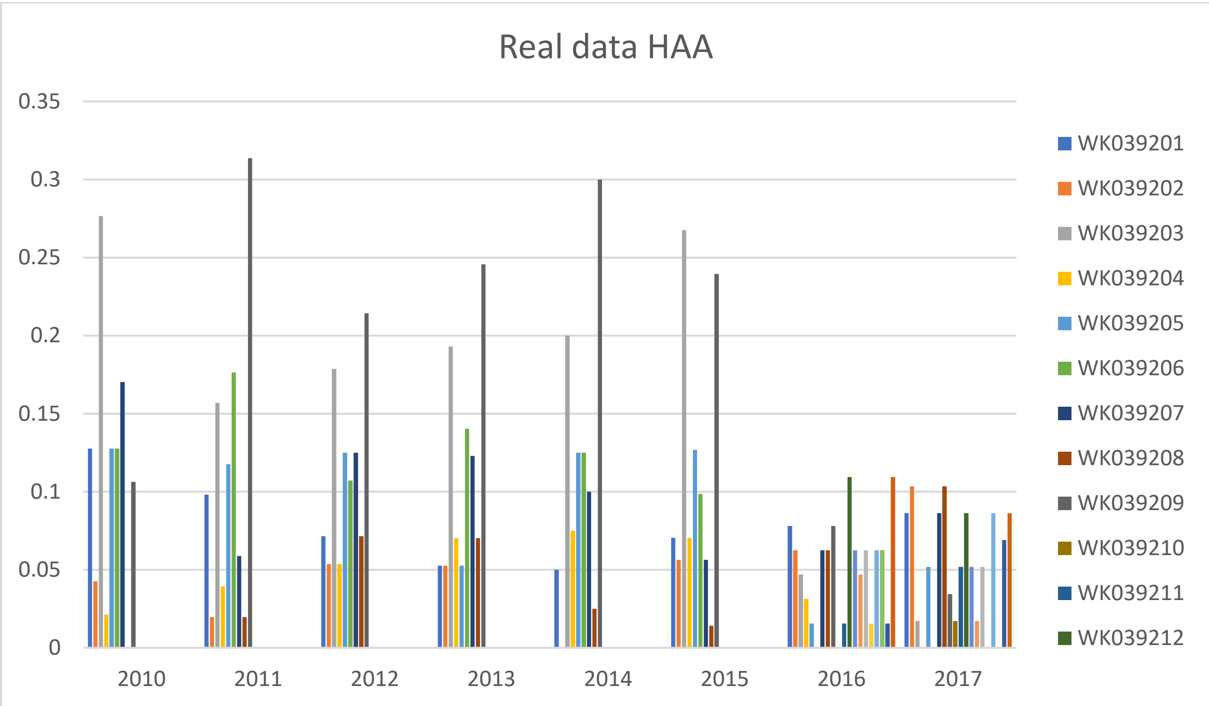

Figure 25. Histogram visualizing the proportional true OHCA incidence of each district of Haarlem per year.

9.9.4 OHCA incidence proportions Haarlemmermeer

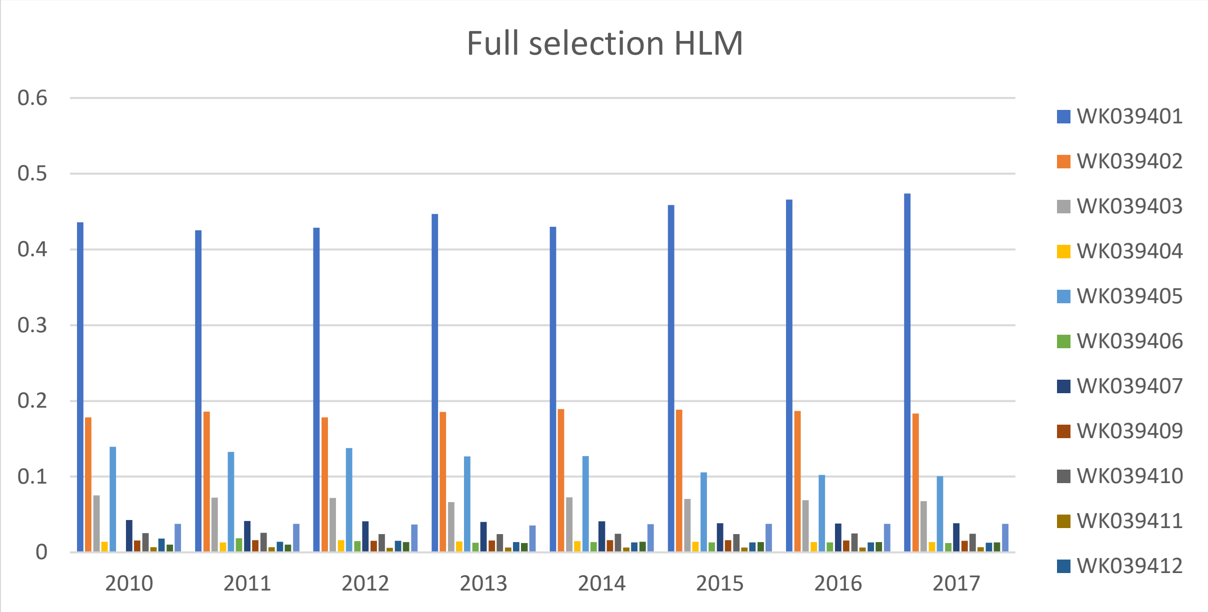

Figure 26. Histogram visualizing the proportional estimated OHCA incidence of each district of Haarlemmermeer per year using the full feature selection.

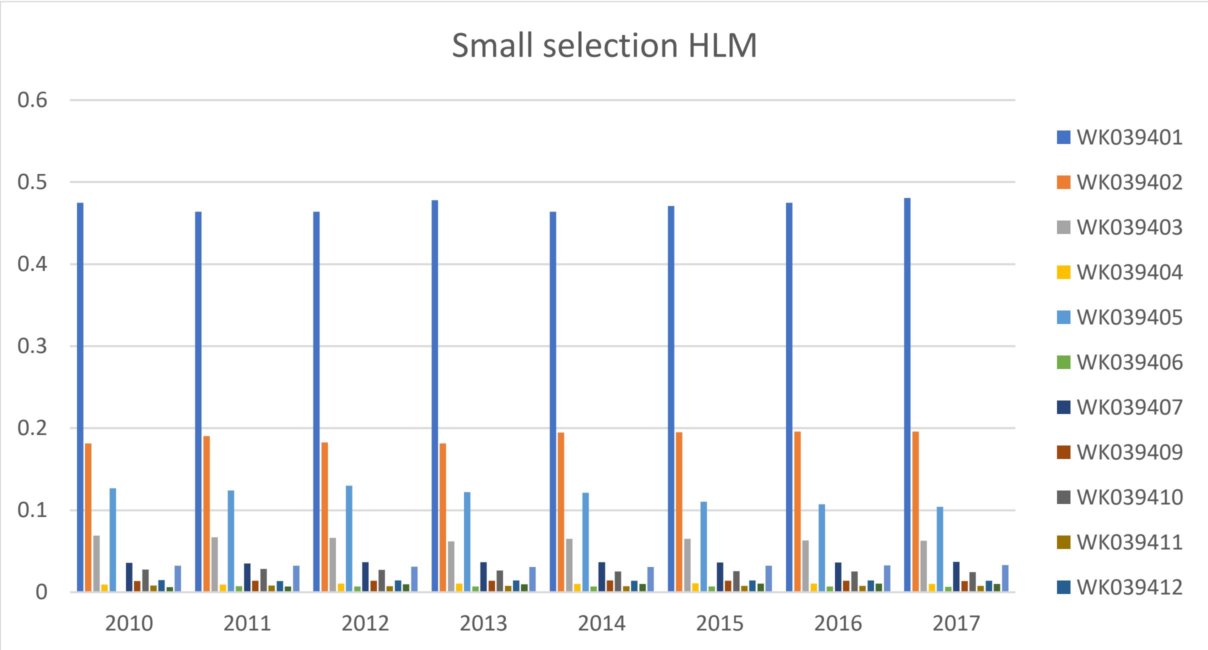

Figure 27. Histogram visualizing the proportional estimated OHCA incidence of each district of Haarlemmermeer per year using the small feature selection.

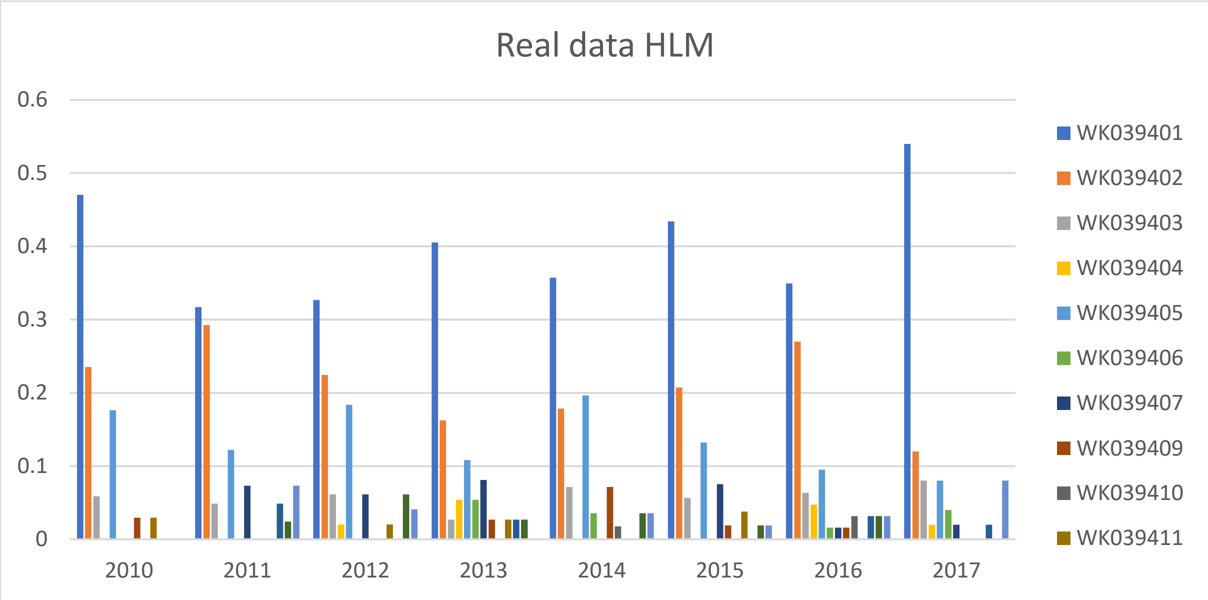

Figure 28. Histogram visualizing the proportional true OHCA incidence of each district of Haarlemmermeer per year.

9.9.5 OHCA incidence proportions Alkmaar

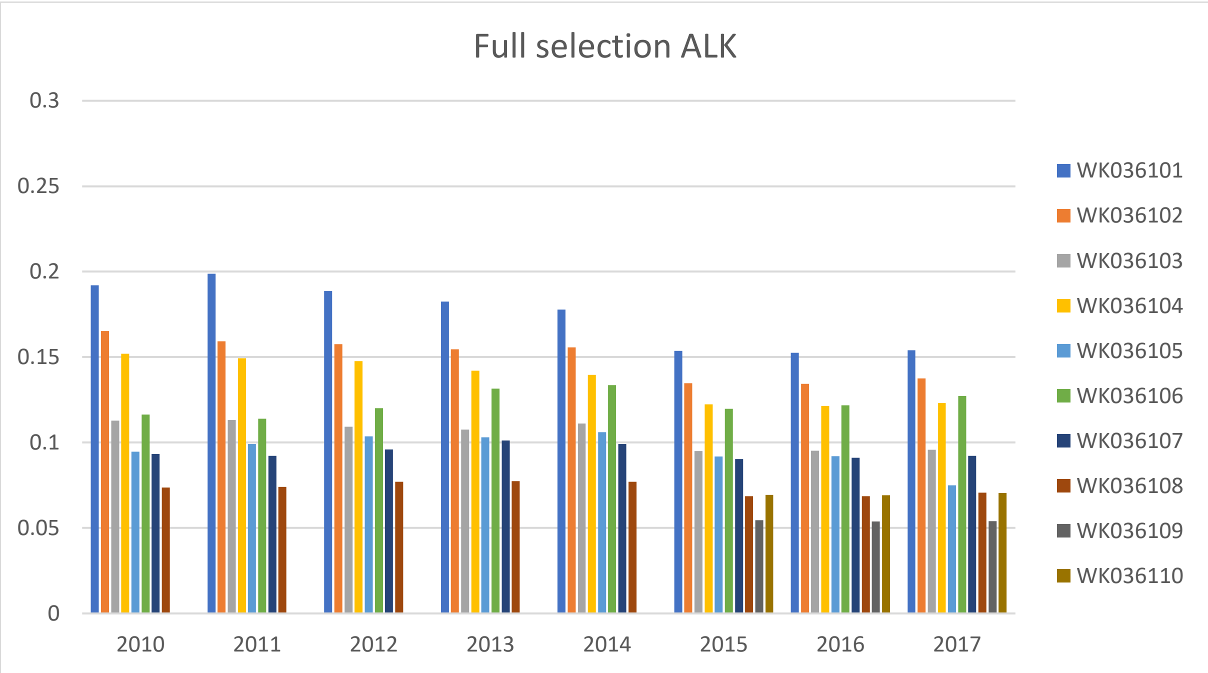

Figure 29. Histogram visualizing the proportional estimated OHCA incidence of each district of Alkmaar per year using the full feature selection.

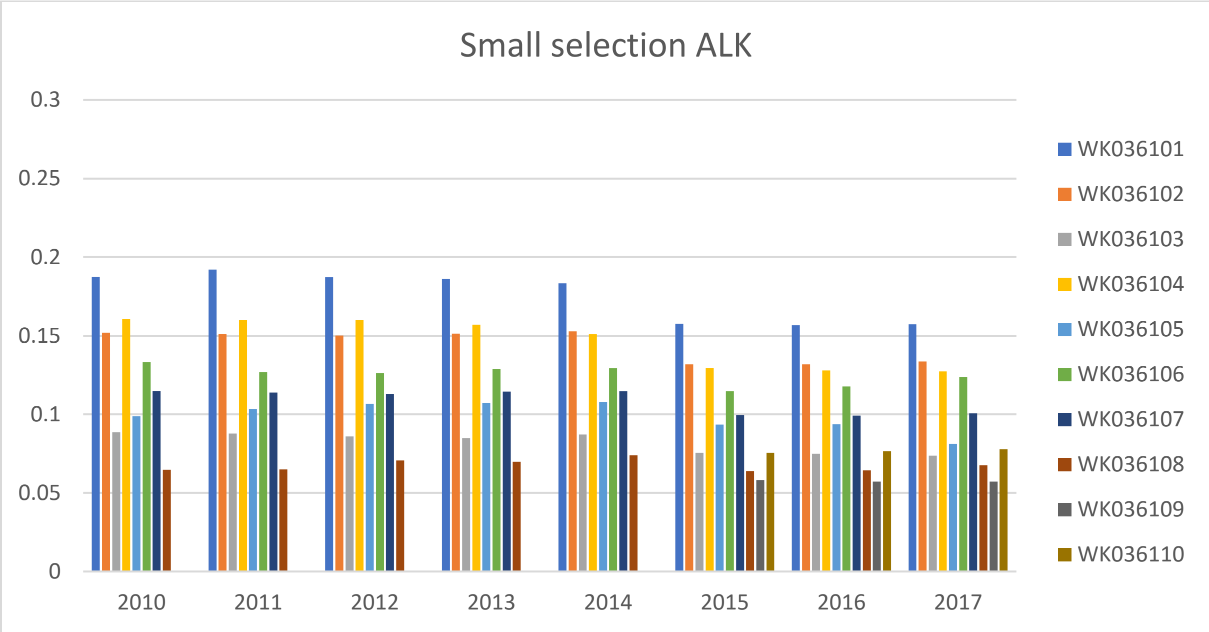

Figure 30. Histogram visualizing the proportional estimated OHCA incidence of each district of Alkmaar per year using the small feature selection.

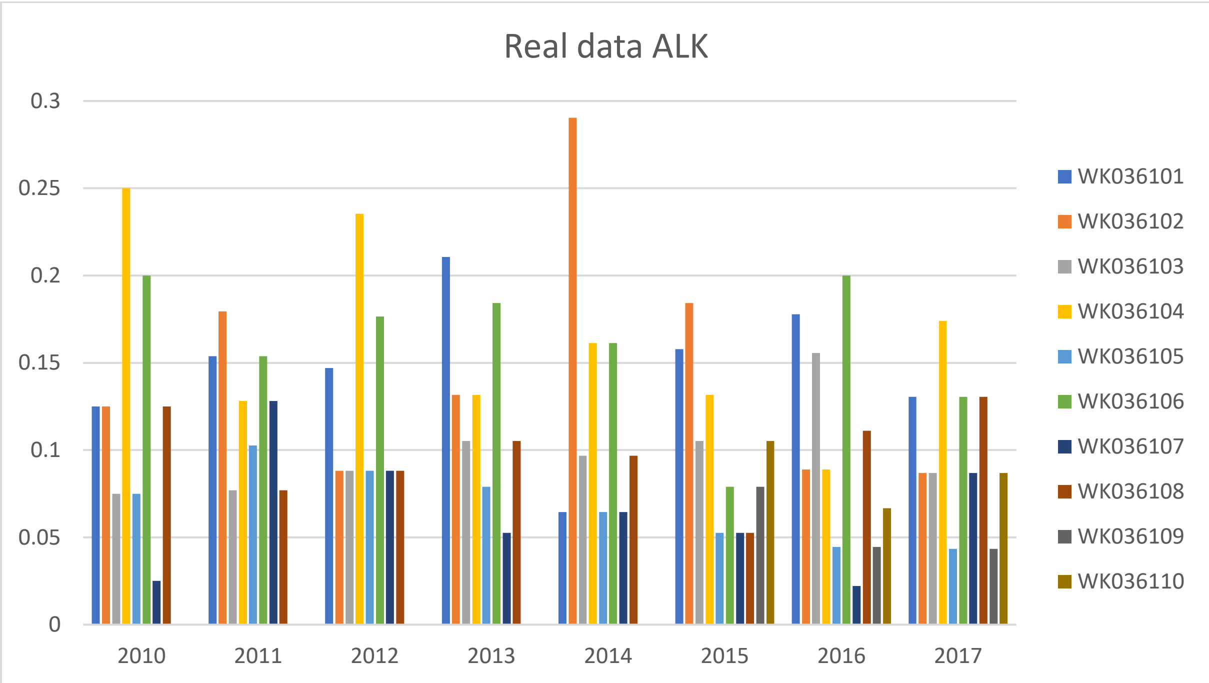

Figure 31. Histogram visualizing the proportional true OHCA incidence of each district of Alkmaar per year.